Robust predictive control by zonotopic set-membership estimation.

Vu Tuan Hieu Le

N° d'ordre : 2012-16-TH

THÈSE DE DOCTORAT

DOMAINE : STIC
Spécialité : Automatique

Ecole Doctorale « Sciences et Technologies de l'Information des Télécommunications et des Systèmes »

Présentée par :

Vu Tuan Hieu LE

Sujet :

Commande prédictive robuste par des techniques d'observateurs à base d'ensembles zonotopiques

Soutenue le 22 Octobre 2012 devant les membres du jury :

M. Teodoro ALAMO	Universidad de Sevilla, Espagne	Co-encadrant, invité
M. Eduardo CAMACHO	Universidad de Sevilla, Espagne	Co-encadrant
M. Christophe COMBASTEL	ENSEA, Cergy-Pontoise	Examinateur
Mme Estelle COURTIAL	Université d'Orléans PRISME, Orléans	Examinatrice
M. José Adrian DE DONÁ	University of Newcastle, Australie	Rapporteur
M. Didier DUMUR	SUPELEC, Gif sur Yvette	Directeur de thèse
Mme Françoise LAMNABHI-LAGARRIGUE	LSS, CNRS, Gif sur Yvette	Présidente du jury
M. Vicenç PUIG	Universitat Politècnica de Catalunya, Espagne	Rapporteur
Mme Cristina STOICA	SUPELEC, Gif sur Yvette	Co-encadrante

To my father
To my mother
To my wife
and my family

Acknowledgement

I would like first to thank my supervisors Didier Dumur, Cristina Stoica, Teodoro Alamo and Eduardo Camacho who have encouraged and supported me since the beginning of my thesis. I am grateful for their help, their availability to correct my last minute papers.

I am grateful to As. Prof. José De Dona and Prof. Vincenç Puig for reviewing my thesis and to Prof. Françoise Lamnabhi-Lagarrigue, Dr. Estelle Courtial, and Dr. Christophe Combastel for being part of the examination committee of my thesis.

I also would like to thank all professors and personnel of the Automatic Control Department of Supélec, especially to Ms. Josiane Dartron and Mr. Léon Marquet for their help during my three years at Supélec. It is also a pleasure to thank the personnel of the Automatic Control Department of University of Seville for their support during my trips in Seville. I will not forget my colleagues who supported me with their pleasant presence during coffee breaks and badminton sessions, specially: Bien, Dung, Nam and Vy.

Special thank to my professors at ENSEA, Prof. Jean-Pierre Barbot and Dr. Malek Ghanes who encouraged me to continue on the research direction.

Finally, I am grateful to my wife, my parents, my sister and my family for their support and their encouragements.

Contents

List of Figures

List of Tables

List of symbols

$\mathbb{R}$	Set of real numbers
$\mathbb{R}^+$	Set of strictly positive real numbers
$\mathbb{R}^n$	Set of n-dimensional real vector
$\mathbf{B}^n$	Unitary box in $\mathbb{R}^n$
A	General notation for a matrix
I_n	Identity matrix in $\mathbb{R}^{n\times n}$
$[A]$	General notation for an interval matrix
$vert([A])$	Vertices of interval matrix A
$mid([A])$	Center of interval matrix A
$rad([A])$	Radius of interval matrix A
A^T	Transpose of matrix A
A^{-1}	Inverse of matrix A
$det(A)$	Determinant of matrix A
$tr(A)$	Trace of matrix A
$Im(A)$	Image of matrix A
$diag(\sigma_1, \ldots, \sigma_n)$	Diagonal matrix of dimension n
$Z = Z(p; H) = p \oplus H\mathbf{B}^m$	General notation of a m-zonotope
$rs(H)$	Round-sum of matrix H
$box(Z)$	Approximation of zonotope Z by a box
$Par(Z)$	Approximation of zonotope Z by a parallelotope
$\Diamond(Z)$	Zonotope inclusion
$A \succ 0$	General notation for strictly positive definite matrix A
$A \succeq 0$	General notation for positive definite matrix A
$A \prec 0$	General notation for strictly negative definite matrix A
$A \preceq 0$	General notation for negative definite matrix A
$\lvert \cdot \rvert$	Absolute value
$\lVert \cdot \rVert_\infty$	Infinity norm
$\lVert \cdot \rVert_P$	P-norm
$\lVert \cdot \rVert_F$	Frobenius norm

$\in$	It belongs to
$\subset$	Subset
$\cap$	Intersection
$\oplus$	Minkowski sum
$\ominus$	Pontryagin difference
$M(S)$	Image of a set S
$d(X, Y)$	Distance between X and Y (also called "normal" distance)
$d_H(X, Y)$	Hausdorff distance between X and Y
$\binom{n}{m}$	n combination of m elements
$n!$	Factorial of n
$y_{k/i}$	i-th row of vector y_k
$conv(\cdot)$	Convex hull
$\omega \sim N(0, Q)$	Random variable ω having zero means, normal distribution and covariance matrix Q

Acronyms

BMI	Bilinear Matrix Inequality
CARIMA	Controlled Auto-Regressive Integrated Moving Average
CRHPC	Constrained Receding Horizon Predictive Control
DMC	Dynamic Matrix Control
EHAC	Extended Horizon Adaptive Control
EPSAC	Extended Prediction Self-Adaptive Control
ESO	Equivalent Single-Output
ESOCE	Equivalent Single-Output with Coupling Effect
EVP	Eigenvalue problem
GPC	Generalized Predictive Control
LMI	Linear Matrix Inequality
LQ	Linear Quadratic control
LQR	Linear Quadratic Regulator
LTI	Linear Time Invariant
MAC	Model Algorithmic Control
MHRC	Model predictive heuristic control
MIMO	Multi Input Multi Output
MPC	Model Predictive Control
MPT	Multi-Parametric Toolbox
MURHAC	Multi-predictor Receding Horizon Adaptive Control
MUSMAR	Multi-step Multivariable Adaptive Control
PAZI	Polytope and Zonotope Intersection
PFC	Predictive Functional Control
PMI	Polynomial Matrix Inequality
QP	Quadratic Programming
SISO	Single Input Single Output
SOS	Sum of Squares
SVD	Singular Value Decomposition

TMPC	Tube-based Model Predictive Control
UFC	Unified Predictive Control

Chapitre 1

Résumé

Dans la majorité des applications réelles, la dynamique du système est souvent affectée par des variations de paramètres, des perturbations agissant sur l'état et des bruits de mesure. De plus, certains paramètres physiques ne sont pas connus avec exactitude, seules les bornes (inférieure et supérieure) de variation étant disponibles. Ainsi, ces incertitudes peuvent avoir des influences importantes sur le comportement du système considéré. Dans ce contexte, le but principal de cette thèse est de prendre en compte les différentes incertitudes dans la modélisation des systèmes. Dans cet esprit, deux problèmes seront résolus dans ces travaux de thèse :

- Des méthodes d'estimation d'état pour des systèmes incertains fondées sur des méthodes ensemblistes, plus précisément des ensembles zonotopiques, sont tout d'abord développées. Ces méthodes conduisent à résoudre de problèmes via un formalisme d'Inégalité Matricielle Linéaire (LMI), Inégalité Matricielle Bilinéaire (BMI) ou Inégalité Matricielle Polynomiale (PMI) selon le cas envisagé.

- En utilisant le résultat de l'estimation zonotopique, une commande prédictive robuste fondée sur des tubes d'incertitudes est ensuite proposée.

Cette thèse est structurée comme suit : le Chapitre 2 propose une introduction portant sur le contexte, les motivations, les contributions et les publications issues des résultats obtenus pendant les travaux. Le Chapitre 3 propose une introduction détaillée des méthodes de représentation d'incertitudes (intervalle, ellipsoïde, polytope ou zonotope). Ensuite le Chapitre 4 présente une nouvelle technique d'estimation ensembliste fondée sur des zonotopes pour des systèmes affectés par des perturbations, des bruits de mesure et des incertitudes paramétriques. Utilisant les résultats de l'estimation zonotopique, le Chapitre 5 formule la mise en oeuvre de la commande

prédictive robuste par retour de sortie pour le même type de système. Dans le Chapitre 5, les résultats théoriques développés sont implantés sur un système de suspension magnétique. Le résumé de chaque chapitre est proposé ci-dessous.

1.1 Chapitre 3 : Représentation des incertitudes par des ensembles convexes

Le Chapitre 3 traite des différentes approches existant dans la littérature pour représenter des incertitudes : l'approche stochastique ou probabiliste et l'approche déterministe ou ensembliste. L'approche probabiliste [99], [12] est fondée sur l'hypothèse que les lois de probabilité sur des perturbations et des bruits de mesure sont connues. Pourtant, dans plusieurs applications, ces lois de probabilité ne sont pas toujours connues, seules les bornes de ces perturbations pouvant être déterminées. Dans ce contexte, l'approche déterministe s'avère plus adaptée à la modélisation de perturbations. Dans cette approche, une variable incertaine est représentée par un ensemble convexe qui caractérise le domaine de valeurs possibles de cette variable. Dans la littérature, plusieurs façons de représenter un ensemble en fonction de la complexité et la précision existent, par exemple les représentations par : intervalle, ellipsoïde, polytope, parallélotope et zonotope. Les ensembles les plus représentatifs sont exposés par la suite.

1.1.1 Intervalle

La manière la plus simple pour caractériser un domaine de variation d'un paramètre est l'intervalle.

***Définition* 1.1.** Un *intervalle* $I = [a, b]$ est défini par un ensemble borné $\{x : a \leq x \leq b\}$.

***Définition* 1.2.** Le *centre* et le *rayon* d'un intervalle $I = [a, b]$ sont représentés par $mid(I) = \frac{a+b}{2}$ et $rad(I) = \frac{b-a}{2}$, respectivement.

***Définition* 1.3.** Un *matrice intervalle* $[M] \in \mathbb{I}^{n\times m}$ est une matrice qui a des intervalles comme éléments. Cela permet d'aboutir aux calculs simples fondés sur l'analyse par intervalles. En revanche, la précision d'estimation est parfois dégradée du fait d'occurrences multiples (voir Exemple 3.1) et de l'effet d'enveloppement (voir Exemple 3.2)[68].

1.1.2 Ellipsoïde

Un autre famille d'ensembles utilisée dans la littérature du fait de son avantage de faible complexité est représentée par l'ellipsoïde.

***Définition* 1.4.** Soit un vecteur $c \in \mathbb{R}^n$ et une matrice symétrique définie positive $P = P^T \succ 0$, *l'ellipsoïde* E est défini par l'expression suivante :

$$E = \{x \in \mathbb{R}^n : (x-c)^T P^{-1}(x-c) \leq 1\} \tag{1.1}$$

Le vecteur $c \in \mathbb{R}^n$ est nommé le *centre* de l'ellipsoïde E et la matrice P est appelée la *matrice de forme* de l'ellipsoïde E.

L'avantage de la représentation d'un ensemble de paramètres incertains par ellipsoïdes est que la complexité est fixée par la dimension de l'espace (quadratique) [78]. Malgré cet avantage, la précision d'estimation dans le contexte d'ellipsoïdes reste parfois conservative [66].

1.1.3 Polytope

Dans le domaine de l'automatique, une représentation très utilisée pour décrire des ensembles est le polytope. L'avantage du polytope est qu'il peut conduire à une approximation très précise de tout ensemble convexe [81], [26], [127]. Un polytope peut être défini de deux façons équivalentes qui permettent de choisir une représentation adaptée au problème particulier considéré.

***Définition* 1.5.** (*H-représentation*) Un polyèdre $P \in \mathbb{R}^n$ est défini comme l'intersection d'un nombre fini de demi-espaces :

$$P = \{x \in \mathbb{R}^n : H \cdot x \leq K\} \tag{1.2}$$

avec $H \in \mathbb{R}^{m \times n}$ et $K \in \mathbb{R}^m$. Si P est borné, alors P devient un polytope.

***Définition* 1.6.** (*V-représentation*) Soit un ensemble fini de points $V = \{v_1, v_2, \ldots, v_m\} \in \mathbb{R}^n$, un polytope P est défini par l'enveloppe convexe de l'ensemble V :

$$P = conv(V) = \{\alpha_1 v_1 + \alpha_2 v_2 + \ldots + \alpha_m v_m : \alpha_i \in \mathbb{R}^+, \sum_{i=1}^{m} \alpha_i = 1\} \tag{1.3}$$

Les deux représentations définies par les définitions 1.5 et 1.6 sont équivalentes [151]. L'inconvénient principal du polytope est lié à sa complexité qui augmente exponentiellement avec le nombre de sommets. Cette propriété du polytope rend souvent le calcul très coûteux au niveau du temps de calcul.

1.1.4 Zonotope

Le zonotope est un cas particulier de polytope, plus précisément un polytope symétrique (d'où une diminution de complexité en comparaison avec le polytope quelconque). Comme un zonotope est un polytope, le zonotope peut être mis sous forme d'une H-représentation ou d'une V-représentation. Cependant l'avantage du zonotope vient de ses propres définitions exposées ci-dessous.

***Définition* 1.7.** (*G-représentation*) Soit un vecteur $p \in \mathbb{R}^n$ et un ensemble de vecteurs $G = \{g_1, g_2, ..., g_m\} \subset \mathbb{R}^n$, $m \geq n$. Un *zonotope* Z d'ordre m est défini par :

$$Z = (p; g_1, g_2, ..., g_m) = \{x \in \mathbb{R}^n : x = p + \sum_{i=1}^{m} \alpha_i g_i; -1 \leq \alpha_i \leq 1\} \quad (1.4)$$

Le vecteur p est appelé le *centre* du zonotope Z. Les vecteurs g_1, ..., g_m sont appelés les *générateurs* du zonotope Z. L'*ordre* d'un zonotope est défini par le nombre de générateurs (m dans ce cas). Cette définition est équivalente à la définition d'un zonotope par la somme de Minkowski d'un nombre fini de segments définis par $g_i\mathbf{B}^1$, avec $i = 1, \ldots, m$:

$$Z = (p; g_1, g_2, ..., g_m) = p \oplus g_1\mathbf{B}^1 \oplus \ldots \oplus g_m\mathbf{B}^1 \quad (1.5)$$

Un exemple de zonotope construit par 3 générateurs est présenté Figure 1.1.

L'avantage principal du zonotope, qui facilite la résolution du problème d'estimation d'état considéré dans cette thèse, vient de la définition suivante.

***Définition* 1.8.** (*Projection linéaire d'un hypercube*) Un zonotope d'ordre m dans $\mathbb{R}^n$ ($m \geq n$) est la translation de centre $p \in \mathbb{R}^n$ de l'image d'un hypercube de dimension m dans $\mathbb{R}^n$ par une application linéaire. Soit une matrice $H \in \mathbb{R}^{n \times m}$ représentant l'application linéaire, le zonotope Z est défini par :

$$Z = (p; H) = p \oplus H\mathbf{B}^m \quad (1.6)$$

Grâce à cette définition, les opérations comme la somme de Minkowski ou l'image linéaire du zonotope peuvent être effectuées facilement. Différentes propriétés intéressantes du zonotope sont regroupées dans [82]. Comme le zonotope propose un bon compromis entre la complexité du calcul et la précision de la représentation, il a été privilégié dans cette thèse pour représenter des incertitudes.

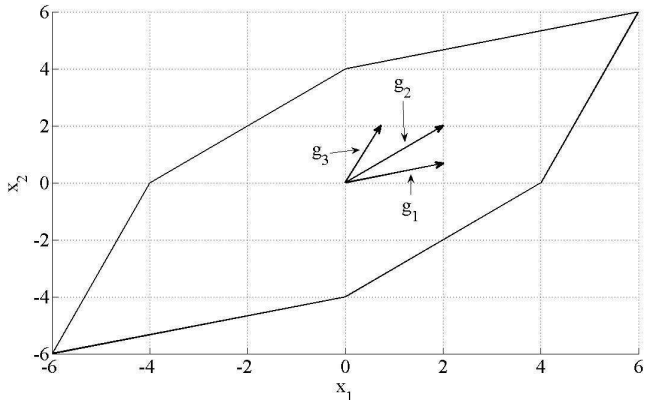

FIGURE 1.1 – 3-zonotope et ses générateurs en $2D$

1.2 Chapitre 4 : Estimation d'état par approche ensembliste fondée sur des zonotopes

Ce chapitre examine le problème d'estimation d'état du système affecté par des incertitudes paramétriques, perturbations et bruits de mesure. Si les incertitudes sont modélisées par une approche stochastique, le filtre de Kalman fondé sur deux étapes (prédiction et mise à jour) est susceptible de résoudre ce problème. Quand l'approche déterministe est utilisée, le choix des méthodes d'estimation ensemblistes est une solution appropriée. Cette technique d'estimation est développée depuis 35 ans par plusieurs auteurs [147], [126], [145], [144], [68], [2], [82] etc. Avec la présence d'incertitudes, l'état du système ne peut pas être exactement estimé, l'estimation ensembliste propose donc de calculer à chaque instant un ensemble contenant l'état du système, cohérent avec les incertitudes du modèle, les perturbations éventuelles et les mesures bruitées. Différentes représentations d'ensembles peuvent être utilisées : intervalles, ellipsoïdes, polytopes, zonotopes. Grâce à ses avantages présentés au Chapitre 3, le zonotope a été privilégié dans cette thèse pour résoudre le problème d'estimation ensembliste. Le problème d'estimation à résoudre dans ce chapitre est formulé comme suit.

Considérons un système linéaire discret et invariant dans le temps :

$$\begin{cases} x_{k+1} = Ax_k + \omega_k \\ y_k = Cx_k + v_k \end{cases} \tag{1.7}$$

où $x_k \in \mathbb{R}^{n_x}$ est le vecteur d'état du système, $y_k \in \mathbb{R}^{n_y}$ est le vecteur de mesures à l'instant k, les matrices A et C ont les dimensions appropriées

avec la paire (C, A) détectable. Les notations $\omega_k \in \mathbb{R}^{n_x}$, $v_k \in \mathbb{R}^{n_y}$ sont utilisées pour les perturbations sur l'état et le bruit de mesure, respectivement. Les perturbations et les bruits de mesure sont supposés bornés par des zonotopes $\omega_k \in W, v_k \in V$. On suppose également que l'état initial appartient à un zonotope X_0. Pour simplifier le calcul, les centres du zonotope V et du n_x-zonotope W sont supposés être à l'origine. Si cette hypothèse n'est pas satisfaite, un changement de coordonnées peut être utilisé pour ramener les centres des zonotopes à l'origine. Avec ces hypothèses et à partir de la définition du zonotope, les ensembles W et V peuvent être réécrits sous la forme : $W = F\mathbf{B}^{n_x}$ et $V = \Sigma\mathbf{B}^{n_y}$, où $\Sigma \in \mathbb{R}^{n_y \times n_y}$ une matrice diagonale. Avec ce modèle, l'estimation ensembliste fondée sur des zonotopes calcule un ensemble zonotopique contenant de manière garantie l'état du système affecté par des incertitudes. Avant de détailler cette approche, quelques notions utiles sont définies.

***Définition* 1.9.** Soit le système (1.7), *l'ensemble des états cohérents avec les mesures ("consistent state set")* à l'instant k est défini par $X_{y_k} = \{x \in \mathbb{R}^n : |c^T x - y_k| \leq \sigma\}$.

***Définition* 1.10.** Pour le système (1.7), *l'ensemble exact des états incertains ("exact uncertain state set")* X_k est l'ensemble contenant les états cohérents avec la sortie mesurée et l'ensemble des états initiaux possibles X_0 : $X_k = (AX_{k-1} \oplus W) \cap X_{y_k}$, pour $k \geq 1$.

Similaire au filtre de Kalman, l'estimation ensembliste se décompose en trois étapes :

1. *Prédiction* : calculer un domaine prédit $\bar{X}_k$ contenant l'état du système en tenant compte des perturbations ;
2. *Mesure* : calculer l'ensemble des états cohérents X_{y_k} en utilisant la mesure y_k ;
3. *Mise à jour* : calculer l'intersection de l'ensemble des états cohérents et du domaine prédit afin de trouver l'ensemble contenant l'état du système.

L'algorithme de l'estimation ensembliste est illustré Figure 1.2. A l'instant k, l'ensemble prédit $\bar{X}_k$ (bleu) est déterminé à partir de l'ensemble contenant l'état $\hat{X}_{k-1}$ (rouge) à l'instant $k-1$. Ensuite, on considère l'intersection de cet ensemble avec l'ensemble des états cohérents X_{y_k} (vert) qui est calculé à partir de la mesure y_k. Enfin, l'ensemble contenant l'état $\hat{X}_k$ à l'instant k est l'approximation extérieure de cette intersection.

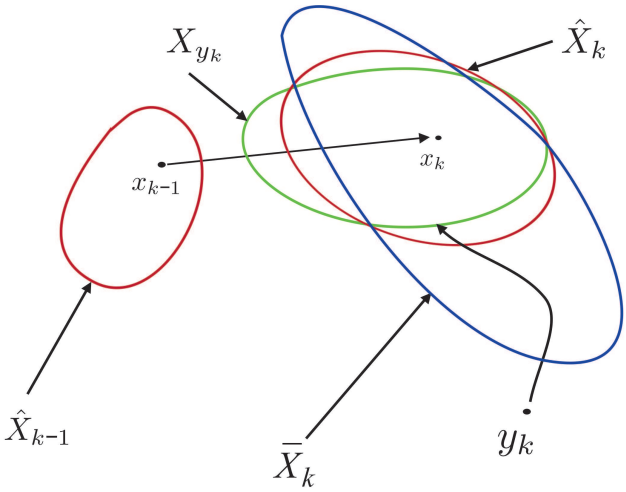

FIGURE 1.2 – Illustration de l'estimation ensembliste

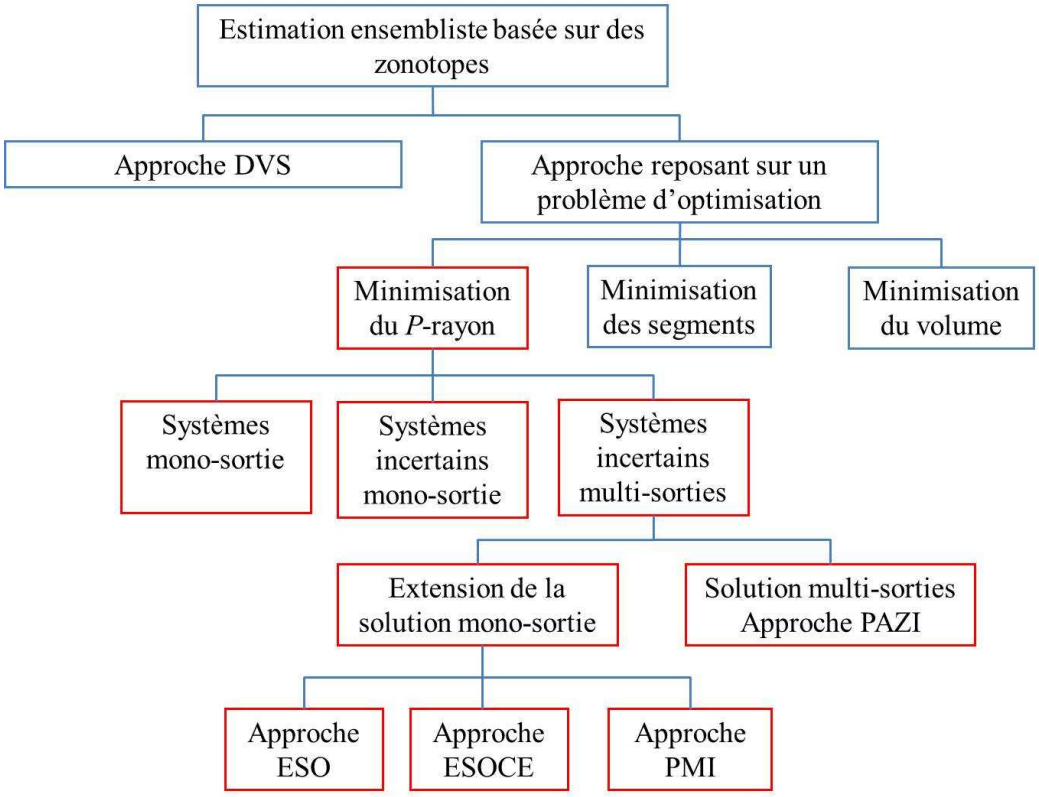

FIGURE 1.3 – Estimation ensembliste fondée sur des zonotopes

En pratique le calcul exact de l'intersection de l'ensemble des états cohérents et du domaine prédit est difficile, donc on cherche souvent à majorer cette intersection par une approximation extérieure (zonotopique dans cette thèse) de cet ensemble. Quelques méthodes pour résoudre ce problème sont regroupées dans le schéma Figure 1.3. Les méthodes existant dans la littérature sont encadrées en bleu. L'approche fondée sur la minimisation des segments d'un zonotope présentée dans [2] permet d'avoir un calcul simple mais la précision d'estimation est limitée. L'approche DVS présentée par [37] et l'approche reposant sur la minimisation du volume d'un zonotope [2] ont des bonnes précisions d'estimation mais les calculs sont complexes. Les contributions de ce chapitre encadrées en rouge permettent d'avoir un bon compromis entre la précision et la complexité. Ces méthodes seront ensuite détaillées dans les sections suivantes.

1.2.1 Système mono-sortie

Considérons tout d'abord un système linéaire mono-sortie invariant à temps discret :

$$\begin{cases} x_{k+1} = Ax_k + \omega_k \\ y_k = c^T x_k + v_k \end{cases} \tag{1.8}$$

La perturbation et le bruit de mesure sont bornés par $\omega_k \in W = F\mathbf{B}^{n_x}$, $v_k \in V = \sigma\mathbf{B}^1 \subset \mathbb{R}$, avec $\sigma \in \mathbb{R}^+$. Soit $\hat{X}_{k-1}$ une approximation extérieure zonotopique de l'ensemble contenant l'état du système $\hat{X}_{k-1} = \hat{p}_{k-1} \oplus \hat{H}_{k-1}\mathbf{B}^r$ à l'instant $k-1$ et la mesure de la sortie y_k à l'instant k, l'ensemble prédit $\bar{X}_k$ peut être obtenu par la relation :

$$\bar{X}_k = A\hat{p}_{k-1} \oplus \begin{bmatrix} A\hat{H}_{k-1} & F \end{bmatrix} \mathbf{B}^{r+n_x} = \bar{p}_k \oplus \bar{H}_k \mathbf{B}^{r+n_x} \tag{1.9}$$

Avec la définition de l'ensemble V, l'ensemble des états cohérents X_{y_k} à l'instant k est une bande de contraintes : $X_{y_k} = \{x \in \mathbb{R}^n : |c^T x - y_k| \leq \sigma\}$. Pour déterminer l'ensemble contenant l'état du système à l'instant k, il faut rechercher une approximation extérieure de l'intersection du zonotope $\bar{X}_k$ et de la bande de contraintes X_{y_k}. Ce problème peut être résolu en utilisant la propriété suivante :

Propriété 1. Soit un zonotope $Z = p \oplus H\mathbf{B}^r \subset \mathbb{R}^n$, une bande de contraintes $S = \{x \in \mathbb{R}^n : |c^T x - d| \leq \sigma\}$ et un vecteur $\lambda \in \mathbb{R}^n$. Définissons une famille de vecteurs $\hat{p}(\lambda) = p + \lambda(d - c^T p) \in \mathbb{R}^n$ et une famille de matrices $\hat{H}(\lambda) = \begin{bmatrix} (I - \lambda c^T)H & \sigma\lambda \end{bmatrix} \in \mathbb{R}^{n \times (m+1)}$. Alors l'expression suivante est satisfaite $Z \cap S \subseteq \hat{X}(\lambda) = \hat{p}(\lambda) \oplus \hat{H}(\lambda)B^{r+1}$.

En utilisant cette propriété, on obtient l'approximation extérieure de l'ensemble contenant l'état à l'instant k :

$$\hat{X}_k(\lambda) = \hat{p}_k(\lambda) \oplus \hat{H}_k(\lambda)\mathbf{B}^{r+n_x+1} \tag{1.10}$$

avec les notations suivantes :

$$\begin{cases} \hat{p}_k(\lambda) = A\hat{p}_{k-1} + \lambda(y_k - c^T A\hat{p}_{k-1}) \\ \hat{H}_k(\lambda) = \begin{bmatrix}(I - \lambda c^T)A\hat{H}_{k-1} & (I - \lambda c^T)F & \sigma\lambda\end{bmatrix} \end{cases} \tag{1.11}$$

Comme λ est un vecteur libre, (1.11) représente une famille de zonotopes contenant l'état à l'instant k. Donc la valeur du vecteur λ doit permettre d'obtenir une meilleur précision de l'approximation. Les auteurs de [2] proposent deux méthodes basées sur différents critères pour calculer le vecteur λ. La première méthode minimise les segments du zonotope $\hat{X}(\lambda)$. Cette méthode aboutit à un calcul simple, mais le résultat est parfois conservatif. La deuxième méthode minimise le volume du zonotope en résolvant un problème d'optimisation coûteux en temps de calcul avec un résultat plus performant. Dans ce chapitre, un nouveau critère d'optimisation est proposé permettant de gérer le compromis entre la complexité du calcul et la précision de l'estimation. Cette méthode est fondée sur la définition du P-rayon d'un zonotope comme suit.

***Définition* 1.11.** Soit un zonotope $Z = p \oplus H\mathbf{B}^m$, le P-rayon de ce zonotope est défini par l'expression suivante :

$$L = \max_{z \in Z}(\|z - p\|_P^2) \tag{1.12}$$

avec $P = P^T \succeq 0$ une matrice symétrique définie positive.

Cette définition est illustrée Figure 1.4 où le zonotope est illustré en bleu et l'ellipsoide associé au zonotope est illustré en rouge.

Pour trouver le vecteur optimal λ, un critère d'optimisation du P-rayon du zonotope est utilisé. Une matrice symétrique définie positive $P = P^T \succ 0$ et le vecteur λ seront déterminés tel que le P-rayon de l'ensemble zonotopique des états estimés n'augmente pas. Cette condition est illustrée Figure 1.5 qui propose le zonotope (bleu) représentant l'ensemble contenant l'état du système et l'ellipsoïde (rouge) associé au P-rayon de ce zonotope. [1]

Cette condition peut être exprimée par l'expression mathématique (condition nécessaire et suffisante) suivante qui caractérise la non-croissance du P-rayon :

$$L_k \leq \beta L_{k-1} + \max_s \|Fs\|_2^2 + \sigma^2 \tag{1.13}$$

[1] Le zonotope n'inclut pas l'ellipsoïde associé (Figure 1.4) car l'ellipsoïde est seulement un critère pour caractériser la taille du zonotope.

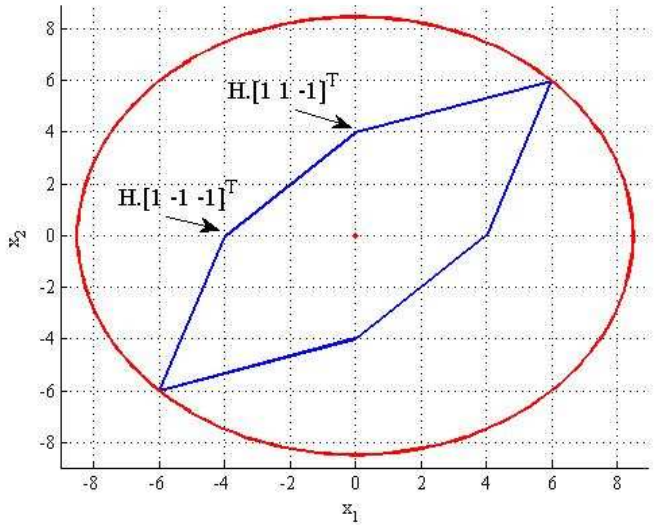

FIGURE 1.4 – Zonotope et ellipsoide associé au P-rayon du zonotope

avec $\beta \in (0,1)$ afin d'assurer la non-croissance du P-rayon et $\max_s \|Fs\|_2^2 + \sigma^2 > 0$ est ajouté afin de borner l'influence des perturbations et des bruits de mesure. Suivant la démarche proposée Chapitre 4 (équations (4.43)-(4.58)), l'optimisation suivante doit être résolue afin de trouver la valeur de λ :

$$\max_{\tau,\beta,P,Y} \tau$$

sous les contraintes BMI :

$$\begin{cases} \frac{(1-\beta)P}{\sigma^2+const} \succeq \tau I \\ \begin{bmatrix} \beta P & 0 & 0 & A^TP - A^TcY^T \\ * & F^TF & 0 & F^TP - F^TcY^T \\ * & * & \sigma^2 & Y^T\sigma \\ * & * & * & P \end{bmatrix} \succeq 0 \\ \tau > 0 \end{cases} \tag{1.14}$$

avec les variables de décision P, $Y = P\lambda$, $\beta \in (0,1)$ et τ.

Comme β est une variable scalaire, ce problème d'optimisation peut être facilement résolu en utilisant un solveur de BMI [2](par exemple $PenBMI$ [74]) ou une boucle de recherche sur la valeur de β.

Pour éviter le problème BMI, une modification du problème d'optimisation (1.14) est ensuite présentée. Au lieu d'optimiser la valeur du P-rayon, la

[2]Cette BMI est un cas particulier du produit entre un scalaire et une matrice.

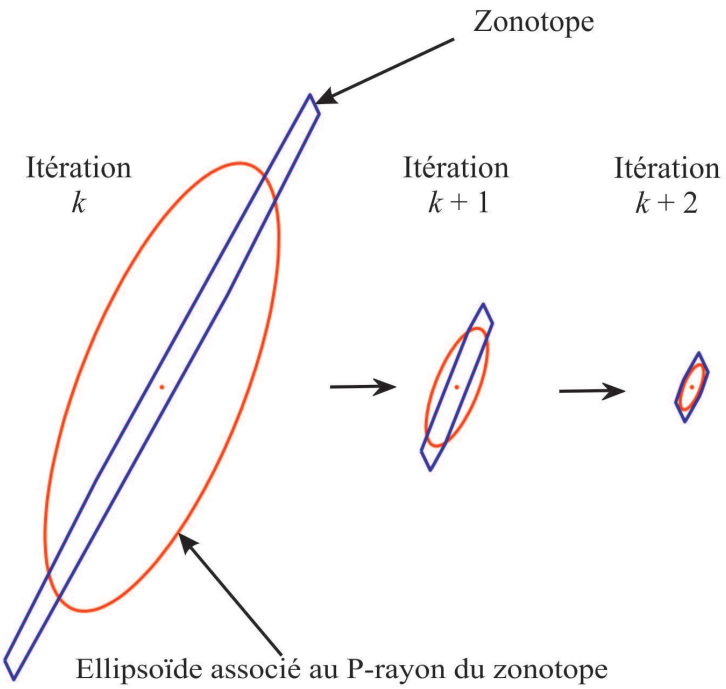

FIGURE 1.5 – Evolution de l'estimation d'état garantie

valeur minimale de β est cherchée permettant d'avoir une vitesse décroissante maximale du P-rayon. Ce critère conduit à un problème d'optimisation de type LMI fondé sur l'algorithme de bissection sur β :

$\min_{\beta\in(0,1)} \beta$ en utilisant l'algorithme de bissection sur β

tel que le problème suivant soit faisable

$\max_{\tau,P,Y} \tau$

sous les contraintes LMI :

$$\begin{cases} \frac{(1-\beta)P}{\sigma^2+const} \succeq \tau I \\ \begin{bmatrix} \beta P & 0 & 0 & A^TP - A^TcY^T \\ * & F^TF & 0 & F^TP - F^TcY^T \\ * & * & \sigma^2 & Y^T\sigma \\ * & * & * & P \end{bmatrix} \succeq 0 \\ \tau > 0 \end{cases} \tag{1.15}$$

Dans le cas des systèmes incertains (la matrice A est inconnue mais appartient à une matrice intervalle $[A]$), la solution est similaire avec une hypothèse

supplémentaire (la matrice A est Schur stable). Comme (1.15) est convexe en A et $[\![A]\!]$ est un ensemble convexe, si (1.15) est vraie pour chaque sommet de $[\![A]\!]$, elle sera respectée pour tous les éléments A appartenant à la matrice intervalle $[\![A]\!]$ [122]. Donc la matrice P et le vecteur λ sont la solution du problème d'optimisation suivant :

$$\max_{\tau,\beta,P,Y} \tau$$

sous les contraintes BMI :

$$\begin{cases} \frac{(1-\beta)P}{\sigma^2+const} \succeq \tau I \\ \begin{bmatrix} \beta P & 0 & 0 & \tilde{A}_i^T P - \tilde{A}_i^T c Y^T \\ * & F^T F & 0 & F^T P - F^T c Y^T \\ * & * & \sigma^2 & Y^T \sigma \\ * & * & * & P \end{bmatrix} \succeq 0 \\ \tau > 0 \end{cases} \tag{1.16}$$

pour $i = 1, ..., 2^q$, où $\tilde{A}_i$ sont les sommets de la matrice intervalle $[\![A]\!]$, q est le nombre des éléments intervalles de $[\![A]\!]$ et $Y = P\lambda$.

1.2.2 Système multi-sorties

Comme indiqué dans le schéma Figure 1.3, le problème d'estimation pour des systèmes multi-sorties peut être résolu par deux familles de solutions. La première famille regroupe les solutions qui sont des extensions directes de la solution pour des systèmes mono-sorties.

Considérons le système multi-sorties (1.7) ; l'ensemble contenant l'état du système $\hat{X}_k$ peut être déterminé en répétant successivement l'intersection entre l'ensemble prédit $\bar{X}_{y_k}$ avec chaque élément du vecteur de mesure y_k, noté $y_{k/i}$:

$$y_{k/i} = c_i^T x_k + v_{k/i}, i = 1, \ldots, n_y \tag{1.17}$$

où c_i^T est la ligne i de la matrice C et le bruit $v_{k/i}$ est borné par l'intervalle $V_i = \sigma_i \mathbf{B}^1$, avec $\sigma_i = \Sigma_{ii}$ (avec Σ_{ii} élément de la matrice Σ).

Supposons l'ensemble contenant l'état du système $\hat{X}_{k-1} = \hat{p}_{k-1} \oplus \hat{H}_{k-1}\mathbf{B}^r$ à l'instant $k-1$, alors l'ensemble prédit à l'instant suivant $\bar{X}_k$ est calculé comme (1.9). L'ensemble contenant l'état du système est déterminé comme suit.

De façon similaire à (1.10), une approximation extérieure de l'intersection entre la bande de contraintes obtenue par le premier élément du vecteur de mesure $(y_{k/1})$ et l'ensemble prédit $(\bar{X}_k)$ est calculée par :

$$\hat{X}_{k/1}(\lambda_1) = \hat{p}_{k/1}(\lambda_1) \oplus \hat{H}_{k/1}(\lambda_1)\mathbf{B}^{r+n_x+1} \tag{1.18}$$

avec $\hat{p}_{k/1}(\lambda_1) = A\hat{p}_{k-1} + \lambda_1(y_{k/1} - c_1^T A\hat{p}_{k-1})$
et $\hat{H}_{k/1}(\lambda_1) = \begin{bmatrix}(I - \lambda_1 c_1^T)A\hat{H}_{k-1} & (I - \lambda_1 c_1^T)F & \sigma_1\lambda_1\end{bmatrix}$.
Ensuite, on détermine l'intersection de cet ensemble $\hat{X}_{k/1}(\lambda_1)$ avec la bande de contraintes obtenue par le deuxième élément du vecteur de mesure $(y_{k/2})$:

$$\hat{X}_{k/2}(\lambda_1, \lambda_2) = \hat{p}_{k/2}(\lambda_1, \lambda_2) \oplus \hat{H}_{k/2}(\lambda_1, \lambda_2)\mathbf{B}^{r+n_x+2} \tag{1.19}$$

avec $\hat{p}_{k/2}(\lambda_1, \lambda_2) = \hat{p}_{k/1}(\lambda_1) + \lambda_2(y_{k/2} - c_2^T\hat{p}_{k/1}(\lambda_1))$
et $\hat{H}_{k/2}(\lambda_1, \lambda_2) = \begin{bmatrix}(I - \lambda_2 c_2^T)\hat{H}_{k/1}(\lambda_1) & \sigma_2\lambda_2\end{bmatrix}$.

Cette procédure est répétée jusqu'au dernier élément du vecteur de mesure (y_{k/n_y}) conduisant à :

$$\begin{aligned}\hat{X}_{k/n_y}(\lambda_1, ..., \lambda_{n_y}) = \hat{p}_{k/n_y}(\lambda_1, ..., \lambda_{n_y})\oplus \\ \oplus\hat{H}_{k/n_y}(\lambda_1, ..., \lambda_{n_y})\mathbf{B}^{r+n_x+n_y}\end{aligned} \tag{1.20}$$

avec

$$\begin{aligned}\hat{p}_{k/n_y}(\lambda_1, ..., \lambda_{n_y}) = \hat{p}_{k/n_y-1}(\lambda_1, ..., \lambda_{n_y-1})+ \\ + \lambda_{n_y}(y_{k/n_y} - c_{n_y}^T\hat{p}_{k/n_y-1}(\lambda_1, ..., \lambda_{n_y-1}))\end{aligned} \tag{1.21}$$

et

$$\hat{H}_{k/n_y}(\lambda_1, ..., \lambda_{n_y}) = \begin{bmatrix}(I - \lambda_{n_y} c_{n_y}^T)\hat{H}_{k/n_y-1}(\lambda_1, ..., \lambda_{n_y-1}) & \sigma_{n_y}\lambda_{n_y}\end{bmatrix} \tag{1.22}$$

En conclusion, l'ensemble contenant l'état à l'instant k est le suivant :

$$\hat{X}_k(\lambda_1, ..., \lambda_{n_y}) = \hat{p}_k(\lambda_1, ..., \lambda_{n_y}) \oplus \hat{H}_k(\lambda_1, ..., \lambda_{n_y})\mathbf{B}^{r+n_x+n_y} \tag{1.23}$$

avec $\hat{p}_k(\lambda_1, ..., \lambda_{n_y}) = \hat{p}_{k/n_y}(\lambda_1, ..., \lambda_{n_y})$
et $\hat{H}_k(\lambda_1, ..., \lambda_{n_y}) = \hat{H}_{k/n_y}(\lambda_1, ..., \lambda_{n_y})$.

Pour déterminer les vecteurs λ_i, $i = 1, \ldots, n_y$, trois approches sont proposées dans ce chapitre et sont détaillées ci-dessous.

1.2.2.1 Approche ESO ("Equivalent Single-Output")

Dans cette approche, le système multi-sorties (1.7) est considéré comme un ensemble de n_y systèmes mono-sortie indépendants. Donc, les vecteurs λ_y sont indépendamment calculés en résolvant n_y problèmes d'optimisation (1.14) séparés. L'algorithme suivant décrit la procédure proposée.

***Algorithme* 1.1.**

1. Pour $j = 1, ..., n_y$
   Etape j : Calculer λ_j en utilisant la mesure $y_{k/j}$;

   Fin.

2. L'ensemble contenant l'état est calculé par l'équation (1.23) avec les vecteurs $\lambda_1,\ldots,\lambda_{n_y}$ connus.

1.2.2.2 Approche ESOCE ("Equivalent Single-Output with Coupling Effect")

Pour réduire le conservatisme de la première approche, issu du couplage possible entre les différentes sorties du système, une deuxième approche est formulée par l'algorithme suivant.

***Algorithme* 1.2.**

1. Etape 1 : Calculer λ_1 en utilisant la mesure $y_{k/1}$ et (1.14) ;

2. Pour $j = 2, ..., n_y$
   Etape j : En utilisant la mesure $y_{k/j}$ et les vecteurs $\lambda_1, ..., \lambda_{j-1}$ calculés aux étapes précédentes, calculer λ_j en résolvant :

   $\max\limits_{\tau,\beta,P,Y_j} \tau$
   sous les contraintes

$$\begin{cases} \frac{(1-\beta)P}{\sigma_1^2+...+\sigma_j^2+const} \succeq \tau I \\ \begin{bmatrix} \beta P & 0 & 0 & ... & 0 & B_1 \\ * & F^TF & 0 & ... & 0 & B_2 \\ * & * & \sigma_1^2 & ... & 0 & B_3 \\ ... & ... & ... & ... & ... & ... \\ * & * & * & ... & \sigma_j^2 & B_{j+2} \\ * & * & * & ... & * & P \end{bmatrix} \succeq 0 \\ \tau > 0 \end{cases} \tag{1.24}$$

avec

$$\begin{aligned}
B_1 &= ((\prod_{i=1}^{j}(I-\lambda_{j+1-i}c_{j+1-i}^T))A)^T P \\
B_2 &= ((\prod_{i=1}^{j}(I-\lambda_{j+1-i}c_{j+1-i}^T))F)^T P \\
B_3 &= (\prod_{i=1}^{j-1}(I-\lambda_{j+1-i}c_{j+1-i}^T)\sigma_1\lambda_1)^T P \\
&\vdots \\
B_j &= ((I-\lambda_j c_j^T)(I-\lambda_{j-1}c_{j-1}^T)\sigma_{j-2}\lambda_{j-2})^T P \\
B_{j+1} &= ((I-\lambda_j c_j^T)\sigma_{j-1}\lambda_{j-1})^T P \\
B_{j+2} &= (\sigma_j\lambda_j)^T P
\end{aligned} \tag{1.25}$$

et $Y_j = P\lambda_j$.

Fin.

1.2.2.3 Approche PMI (Inégalité matricielle polynomiale)

Dans les solutions pour les systèmes multi-sorties proposées dans les paragraphes précédents, les vecteurs $\lambda_1, \ldots, \lambda_{n_y}$ sont successivement calculés, les résultats obtenus pouvant ainsi être conservatifs. Pour surmonter ce problème, une troisième solution qui calcule tous ces vecteurs en même temps est proposée. Cette nouvelle solution conduit à résoudre une Inégalité Matricielle Polynomiale (PMI) :

$$\max_{\tau,\beta,P,\lambda_1,\ldots,\lambda_{n_y}} \tau$$

sous les contraintes

$$\begin{cases}
\frac{(1-\beta)P}{\sigma_1^2+\ldots+\sigma_{n_y}^2+const} \succeq \tau I \\
\begin{bmatrix}
\beta P & 0 & 0 & \ldots & 0 & B_1 \\
* & F^TF & 0 & \ldots & 0 & B_2 \\
* & * & \sigma_1^2 & \ldots & 0 & B_3 \\
\ldots & \ldots & \ldots & \ldots & \ldots & \ldots \\
* & * & * & \ldots & \sigma_{n_y}^2 & B_{n_y+2} \\
* & * & * & \ldots & * & P
\end{bmatrix} \succeq 0 \\
\tau > 0
\end{cases} \tag{1.26}$$

avec les notations (1.25) ($j = n_y$).

Ce problème d'optimisation est difficile à résoudre, mais une solution sous-optimale peut être trouvée en utilisant des techniques de relaxation. Dans cette thèse, ce problème est résolu en utilisant la technique proposée par [62]

qui ajoute des variables supplémentaires pour transformer le problème PMI en un problème sous-optimal de type LMI.

1.2.3 Approche par intersection entre un polytope et un zonotope (PAZI)

Dans les paragraphes précédents, l'ensemble contenant l'état pour des systèmes multi-sorties est obtenu en utilisant les algorithmes étape par étape (approche ESO, approche ESOCE et approche PMI). Ces algorithmes ne calculent pas directement l'ensemble des états cohérents avec les mesures, de plus l'ordre choisi pour la prise en compte des différentes mesures peut influencer la précision de l'estimation. Ce paragraphe propose de calculer l'intersection de l'ensemble des états cohérents avec les mesures (un polytope) avec l'ensemble prédit (un zonotope). Ce problème peut être résolu en utilisant la proposition suivante.

***Proposition* 1.1.** Soit un zonotope $Z = p \oplus H\mathbf{B}^r \subset \mathbb{R}^n$, un polytope $Po = \{x \in \mathbb{R}^n : |Cx - d| \leq \begin{bmatrix} \sigma_1 \\ \vdots \\ \sigma_m \end{bmatrix} d \in \mathbb{R}^m,\ \sigma_i \in \mathbb{R}^+,\ i = 1, \ldots, m\}$ et une matrice $\Lambda \in \mathbb{R}^{n \times m}$, on définit le vecteur $\hat{p}(\Lambda) = p + \Lambda(d - Cp) \in \mathbb{R}^{n_x}$ et la matrice $\hat{H}(\Lambda) = \begin{bmatrix}(I - \Lambda C)H & \Lambda\Sigma\end{bmatrix}$, avec $\Sigma = diag(\sigma_1, \ldots, \sigma_m) \in \mathbb{R}^{m \times m}$ une matrice diagonale. Une famille de zonotopes (paramétrisée par la matrice Λ) contenant l'intersection du zonotope Z et du polytope Po est obtenu sous la forme $Z \cap Po \subseteq \hat{Z}(\Lambda) = \hat{p}(\Lambda) \oplus \hat{H}(\Lambda)B^{r+m}$.

De façon similaire aux développements précédentes, l'ensemble prédit est calculé par (1.9). Avec la définition de l'ensemble V, l'ensemble des états cohérents X_{y_k} est un polytope décrit par :

$$X_{y_k} = \{x \in \mathbb{R}^n : |Cx - y_k| \leq \begin{bmatrix} \sigma_1 \\ \vdots \\ \sigma_{n_y} \end{bmatrix}\} \tag{1.27}$$

Alors, l'ensemble exact des états incertains est l'intersection entre le zonotope $\bar{X}_k$ et le polytope X_{y_k}. En utilisation la Proposition 1.1, l'ensemble contenant l'état du système multi-sorties (1.7) à l'instant k est une famille de zonotopes paramétrisée par la matrice Λ comme suit :

$$\hat{X}_k(\Lambda) = \hat{p}_k(\Lambda) \oplus \hat{H}_k(\Lambda)\mathbf{B}^{r+n_x+n_y} \tag{1.28}$$

avec $\hat{p}_k(\Lambda) = A\hat{p}_{k-1} + \Lambda(y_k - CA\hat{p}_{k-1})$
et $\hat{H}_k(\Lambda) = \begin{bmatrix}(I - \Lambda C)A\hat{H}_{k-1} & (I - \Lambda C)F & \Lambda\Sigma\end{bmatrix}$.

La matrice Λ est calculée telle que le P-rayon de l'ensemble contenant l'état soit non-croissant. Cette condition conduit à résoudre le problème d'optimisation suivant :

$$\max_{\tau,\beta,P,Y} \tau$$

sous contraintes BMI :

$$\begin{cases} \frac{(1-\beta)P}{\sigma_1^2+\ldots+\sigma_{n_y}^2+const} \succeq \tau I \\ \begin{bmatrix} \beta P & 0 & 0 & A^TP - A^TC^TY^T \\ * & F^TF & 0 & F^TP - F^TC^TY^T \\ * & * & \Sigma^T\Sigma & Y^T\Sigma \\ * & * & * & P \end{bmatrix} \succeq 0 \\ \tau > 0 \end{cases} \tag{1.29}$$

avec le changement de variable $Y = P\Lambda$.

Pour illustrer l'avantage de l'approche proposée, l'exemple suivant est traité. Considérons le système linéaire multi-sorties suivant :

$$\begin{cases} x_{k+1} = \begin{bmatrix} 0 & -0.5 \\ 1 & 1+0.3\delta_k \end{bmatrix} x_k + \begin{bmatrix} 0.1 & 0 \\ 0 & 0.1 \end{bmatrix} \omega_k \\ \\ y_k = \begin{bmatrix} -2 & 1 \\ 1 & 1 \end{bmatrix} x_k + \begin{bmatrix} 0.2 & 0 \\ 0 & 0.2 \end{bmatrix} v_k \end{cases} \tag{1.30}$$

La perturbation et le bruit de mesure sont bornés par w_k, $v_k \in \mathbf{B}^2$. L'état initial est inconnu mais appartient à l'ensemlbe $3\mathbf{B}^2$. L'approche PAZI est comparée avec l'approche fondée sur la décomposition de valeur singulière (SVD) [37] et l'approche ESOCE. La Figure 1.6 montre que la taille de l'ensemble contenant l'état est diminuée à chaque instant en raison de la condition sur le P-rayon. De plus, la comparaison de l'approche proposée dans cette thèse avec l'approche SVD montre une amélioration du temps de calcul tout en gardant la même précision d'estimation (Figures 1.7, 1.8, Tableau 1.1).

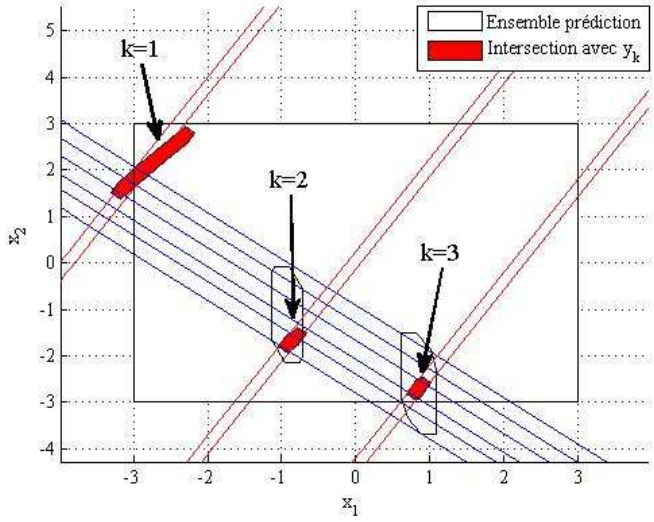

FIGURE 1.6 – Evolution de l'ensemble contenant l'état obtenue par approche PAZI

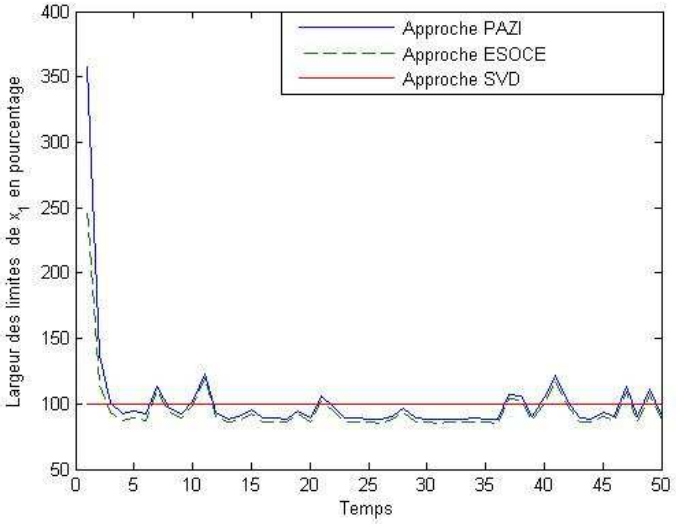

FIGURE 1.7 – Comparaison des limites de x_1 obtenues par plusieurs approches

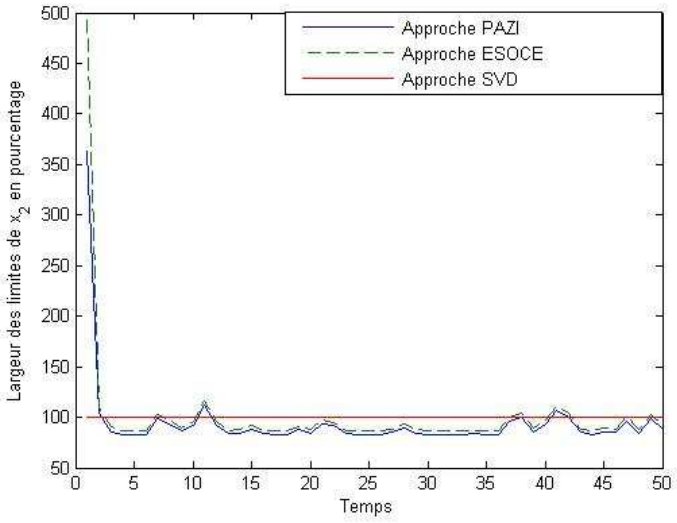

FIGURE 1.8 – Comparaison des limites de x_2 obtenues par plusieurs approches

TABLE 1.1 – Temps de calcul pour 50 périodes d'échantillonnage

Approche	Temps(seconde)
Approche PAZI (sans inclure l'optimisation hors-ligne BMI)	0.0468
Approche (avec l'optimisation hors-ligne BMI incluse)	0.2808
Approche SVD [37]	1.5444

1.3 Chapitre 4 : Commande prédictive robuste fondée sur l'estimation ensembliste pour des systèmes incertains

La commande prédictive fondée sur l'estimation ensembliste construite au chapitre précédent est présentée dans ce chapitre. La commande prédictive est choisie en raison de ses avantages, en particulier sa facilité de mise en oeuvre et sa capacité à traiter des contraintes. Cette commande est basée sur un problème d'optimisation résolu à chaque instant, sur un horizon fini de prédiction, afin de déterminer une séquence de commandes dont seul le premier élément sera appliqué au système. Fondée sur l'horizon glissant, la procédure est reprise à l'instant suivant. Deux techniques de commande prédictive robuste développées dans ce chapitre pour des systèmes affectés par

des perturbations et des bruits de mesure sont présentées plus spécifiquement. La commande robuste pour des systèmes qui ont des paramètres incertains reste un problème ouvert à cause du problème d'optimisation non convexe et du manque de garantie de stabilité du système et de faisabilité de la loi de commande.

Considérons le système incertain suivant :

$$\begin{cases} x_{k+1} = Ax_k + Bu_k + F\omega_k \\ y_k = Cx_k + v_k \end{cases} \tag{1.31}$$

où $x_k \in \mathbb{R}^{n_x}$ est l'état du système, $y_k \in \mathbb{R}^{n_y}$ est la mesure à l'instant k. $\omega_k \in \mathbb{R}^{n_x}$ et $v_k \in \mathbb{R}^{n_y}$ représentent la perturbation et le bruit de mesure. Les incertitudes et l'état initial sont supposés bornés par des ensembles convexes : $\omega_k \in W$, $v_k \in V$ and $x_0 \in X_0$, avec W un zonotope contenant l'origine, V un pavé et X_0 un zonotope.

Le system (1.31) subit des contraintes sur l'état et l'entrée : $x_k \in X$, $u_k \in U$, où X et U sont des ensembles compacts, convexes et contenant l'origine. Dans la suite, deux techniques de commande pour ce système sont considérées.

1.3.1 Commande prédictive "boucle-ouverte"

Comme le système (1.31) est influencé par des incertitudes (ω_k, v_k), l'état du système est estimé en utilisant l'estimation ensembliste par zonotopes présentée au Chapitre 4. Grâce à la propriété de non-croissance de l'estimation ensembliste présentée (1.13), la borne de l'erreur d'estimation n'augmente pas dans le temps. Donc, la solution la plus simple est de négliger l'erreur d'estimation et de considérer l'état estimé comme l'état réel du système. Si l'état estimé est dirigé vers le point de référence, l'état réel converge vers un ensemble contenant ce point. Ainsi, la fonction de coût suivante de type quadratique est choisie pour déterminer l'entrée du système :

$$J_k = \sum_{i=1}^{N} \|\hat{y}_{k+i} - y_{k+i}^{ref}\|_Q^2 + \sum_{i=0}^{N-1} \|u_{k+i} - u_{k+i}^{ref}\|_R^2 \tag{1.32}$$

avec $\hat{y}_{k+i} = C\hat{x}_{k+i}$ et $\hat{x}_{k+i}$ le centre de l'ensemble zonotopique contenant l'état à l'instant $k+i$. Les notations suivantes ont été également utilisées : N l'horizon de prédiction, y_{k+i}^{ref} la sortie future souhaitée, u_{k+i}^{ref} l'entrée future souhaitée. La matrice de pondération Q est une matrice symétrique définie positive et la matrice de pondération R est définie positive. Le problème

d'optimisation doit inclure les contraintes suivantes sur l'entrée et l'état :

$$\begin{cases} u_{k+i} \in U, i = 0, \ldots, N-1 \\ x_{k+i} \in X, i = 1, \ldots, N \end{cases} \tag{1.33}$$

Minimiser le critère (1.32) sous les contraintes (1.33) est un problème d'optimisation convexe qui permet de déterminer la commande appliquée au système (1.31).

1.3.2 Commande prédictive robuste à base de tubes d'incertitudes

La commande prédictive "boucle-ouverte" est simple, mais elle ne garantie ni la stabilité du système, ni la faisabilité du problème d'optimisation. Pour cette raison, une deuxième technique de commande prédictive à base de tubes d'incertitudes est présentée dans ce chapitre. Dans cette approche, le problème d'optimisation de l'état réel du système est remplacé par le problème d'optimisation de l'état nominal (l'état du système nominal qui n'est pas affecté par des incertitudes). De plus, l'erreur d'estimation est prise en compte dans la loi de commande afin de garantir la stabilité du système commandé et la faisabilité de la loi de commande.

Si l'on note $\hat{x}_k$ le centre de l'ensemble zonotopique des états estimés à l'instant k, alors on peut déduire l'équation suivante :

$$\begin{aligned} \hat{x}_{k+1} &= A\hat{x}_k + Bu_k + \Lambda(y_{k+1} - \hat{y}_{k+1}) \\ &= A\hat{x}_k + Bu_k + \Lambda(y_{k+1} - C(A\hat{x}_k + Bu_k)) \end{aligned} \tag{1.34}$$

avec Λ calculé par (1.29).[3]

Soit l'erreur d'estimation de l'observateur $\tilde{x}_k = x_k - \hat{x}_k$. L'erreur d'estimation à l'instant suivant $\tilde{x}_{k+1}$ est calculée à partir des équations (1.31) et (1.34).

$$\tilde{x}_{k+1} = (I - \Lambda C)A\tilde{x}_k + \omega_k^e \tag{1.35}$$

avec $\omega_k^e \in W^e = (I - \Lambda C)W \oplus (-\Lambda V)$. En considérant que l'erreur d'estimation initiale appartient à un ensemble initial $\tilde{x}_0 \in S_0^e$, l'équation récursive suivante $S_{k+1}^e = (A - \Lambda CA)S_k^e \oplus W^e$ peut être déduite à partir de la relation (1.35). Comme la matrice Λ est calculée de sorte que l'ensemble des états

[3]La différence entre l'approche proposée dans cette thèse et celle dans [100] est l'utilisation de l'estimation ensembliste à la place de l'observateur de Luenberger [100] afin d'améliorer la vitesse de convergence de l'erreur d'estimation, donc la performance de la commande.

estimés soit non croissant, la séquence d'ensembles $\{S_k^e\}$ est monotone non croissante.

L'équation de l'observateur peut maintenant être réécrite comme suit :

$$\hat{x}_{k+1} = A\hat{x}_k + Bu_k + \omega_k^{co} \tag{1.36}$$

avec $\omega_k^{co} = \Lambda(CA\tilde{x}_k + C\omega_k + v_{k+1})$. Comme $\tilde{x}_k \in S_k^e$, on obtient l'équation suivante :

$$\omega_k^{co} \in W_k^{co} = \Lambda CAS_k^e \oplus \Lambda CW \oplus \Lambda V \tag{1.37}$$

Comme la séquence des ensembles S_k^e est monotone non croissante et W_k^{co} dépend linéairement de S_k^e, alors la séquence de l'ensemble W_k^{co} est aussi monotone non croissante.

Considérons maintenant le système nominal qui n'est pas affecté par des perturbations :

$$\underline{x}_{k+1} = A\underline{x}_k + B\underline{u}_k \tag{1.38}$$

où $\underline{u}_k$ est la commande appliquée au système nominal. Pour réduire l'effet des perturbations, on souhaite que la trajectoire du système perturbé soit la plus proche possible de la trajectoire du système nominal (i.e. soit située à l'intérieur du tube des trajectoires possibles de rayon minimal). En appliquant la commande prédictive robuste décrite ici, on peut montrer que la trajectoire du système nominal converge vers l'origine et le centre de l'ensemble des états estimés converge vers un ensemble compact contenant l'origine et donc les états réels convergent aussi vers un ensemble compact contenant l'origine, ce qui prouve la stabilité entrée-état. En appliquant la commande suivante $u_k = \underline{u}_k + K(\hat{x}_k - \underline{x}_k)$ au système, on peut déduire que la déviation entre l'état nominal $\underline{x}_k$ et l'état estimé $\hat{x}_k$ (notée $e_k = \hat{x}_k - \underline{x}_k$) satisfait la relation :

$$e_{k+1} = (A + BK)e_k + \omega_k^{co} \tag{1.39}$$

La matrice de retour d'état nominal K est choisie telle que $A + BK$ soit stable. Si à l'instant k la déviation $e_k \in S_k^{co}$, alors à l'instant $k+1$ on a $e_{k+1} \in S_{k+1}^{co}$, avec $S_{k+1}^{co} = (A + BK)S_k^{co} \oplus W_k^{co}$.

De façon similaire à [100], la fonction de coût suivante correspondant à une stratégie prédictive robuste est minimisée afin d'obtenir la séquence de commande :

$$V_N(\underline{x}_k, \underline{u}) = \frac{1}{2}V_f(\underline{x}_{k+N}) + \sum_{i=0}^{N-1} \frac{1}{2}l(\underline{x}_{k+i}, \underline{u}_{k+i}) \tag{1.40}$$

où N est l'horizon de prédiction et $\underline{u}$ est la séquence de commandes :

$$\underline{u} = \{\underline{u}_k, \underline{u}_{k+1}, \ldots, \underline{u}_{k+N-1}\} \tag{1.41}$$

La fonction de coût d'état $l(\underline{x}_k, \underline{u}_k)$ et la fonction de coût terminale $V_f(\underline{x}_{k+N})$ sont définies par :

$$\begin{cases} l(\underline{x}_k, \underline{u}_k) = \frac{1}{2}(\underline{x}_k^T Q \underline{x}_k + \underline{u}_k^T R \underline{u}_k) \\ V_f(\underline{x}_{k+N}) = \frac{1}{2}\underline{x}_{k+N}^T P_f \underline{x}_{k+N} \end{cases} \tag{1.42}$$

où P_f, Q, R sont des matrices définies positives. Avec ces notations, les contraintes variant dans le temps à l'instant k sont :

$$\begin{cases} \underline{u}_{k+i} \in \underline{U}_{k+i},\ i = 0, \ldots, N-1 \\ \underline{x}_{k+i} \in \underline{X}_{k+i},\ i = 0, \ldots, N-1 \\ \underline{x}_{k+N} \in \underline{X}_f \end{cases} \tag{1.43}$$

avec $\underline{U}_{k+i} = U \ominus K S_{k+i}^{co}$ et $\underline{X}_{k+i} = X \ominus S_{k+i}$.

Considérons maintenant l'ensemble admissible de commande à l'instant k avec l'état nominal $\underline{x}$:

$$\mathcal{U}_N(\underline{x}_k) = \{\underline{u} : \underline{u}_{k+i} \in \underline{U}_{k+i}, \underline{x}_{k+i} \in \underline{X}_{k+i}, \underline{x}_{k+N} \in \underline{X}_f, \\ i = 0, \ldots, N-1\} \tag{1.44}$$

Pour déduire la commande du système, le problème d'optimisation suivant est résolu en ligne :

$$V_N^*(\hat{x}_k) = \min_{\underline{x}_k, \underline{u}} \{V_N(\underline{x}_k, \underline{u}) : \underline{u} \in \mathcal{U}_N(\underline{x}_k), \hat{x}_k \in \underline{x}_k \oplus S_k^{co}\} \tag{1.45}$$

La solution de ce problème d'optimisation est donnée par la paire $(\bar{x}^*, \bar{u}^*)$:

$$\underline{x}_k^*(\hat{x}_k), \underline{u}^*(\hat{x}_k) = arg \min_{\underline{x}_k, \underline{u}} \{V_N(\underline{x}_k, \underline{u}) : \underline{u} \in \mathcal{U}_N(\underline{x}_k), \hat{x}_k \in \underline{x}_k \oplus S_k^{co}\} \tag{1.46}$$

Ainsi la commande prédictive appliquée au système (1.31) à l'instant k est :

$$\kappa_N(\hat{x}_k) = \hat{u}_k^*(\hat{x}_k) + K(\hat{x}_k - \underline{x}_k^*(\hat{x}_k)) \tag{1.47}$$

où $\hat{u}_k^*(\hat{x}_k)$ est le premier élément de la séquence $\underline{u}^*(\hat{x}_k)$.

Avec ces hypothèses et en utilisant cette loi de commande, nous pouvons montrer que la paire $(x, \hat{x})$ est pilotée de façon robuste vers $(S_\infty, S_\infty^{co})$, en satisfaisant toutes les contraintes. Malgré des résultats positifs de la commande prédictive robuste à base de tubes d'incertitudes, son application dans le cas de systèmes avec incertitudes paramétriques (la matrice A a des incertitudes par intervalle) reste un problème ouvert à cause du manque de garantie de la stabilité du système et de la faisabilité de la loi de commande.

1.4 Chapitre 5 : Application

Dans ce chapitre, les techniques d'estimation et de commande prédictive développées aux chapitres précédents sont appliquées à un système de suspension magnétique (Figure 1.9). Le système se compose d'un électro-aimant fixe, pour lequel un courant d'alimentation variable permet de modifier la force magnétique résultante, et d'un pendule mobile, aimanté, attiré plus ou moins fortement par la partie fixe. Le système est supposé avoir une symétrie radiale parfaite et on s'intéressera ici uniquement à la commande sur l'axe vertical de façon à stabiliser le pendule autour de l'origine. La première par-

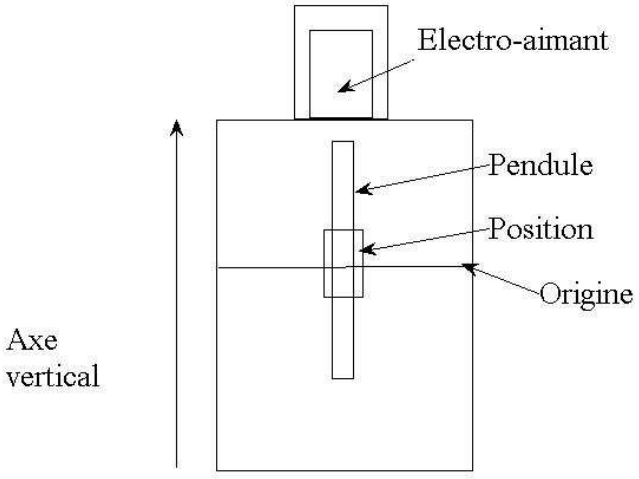

FIGURE 1.9 – Maquette de la suspension magnétique

tie de ce chapitre consiste à modéliser ce système. Pour simplifier le calcul et faciliter la visualisation, le système est modélisé sans la partie de puissance. Le modèle non-linéaire du système de suspension magnétique est élaboré sous forme d'équation différentielle. L'état x se compose de la position et de la vitesse du pendule et la sortie mesurée est la position du pendule. Après avoir établi ce modèle, le système est linéarisé autour de l'origine et discrétisé afin d'obtenir un modèle linéaire discret. L'analyse de stabilité de ce modèle montre que le système est instable en boucle ouverte ce qui correspond bien au comportement physique du système. De plus, le système est soumis à des contraintes sur l'état (la position et la vitesse du pendule) et l'entrée (le courant d'alimentation).

La deuxième partie développe l'implantation de la loi de commande prédictive robuste fondée sur l'estimation ensembliste zonotopique. Comme le système est affecté par des perturbations et de bruit de mesure, l'estimation ensembliste zonotopique est implantée afin d'estimer l'état du système. Ensuite la loi de commande prédictive à base de tubes d'incertitudes est utilisée afin de stabiliser le pendule autour de l'origine. Les résultats de simulations sont montrés Figures 1.10, 1.11, 1.12. Ces figures montrent que le pendule est stabilisé autour de l'origine, de plus les contraintes sur la commande et l'état sont respectées.

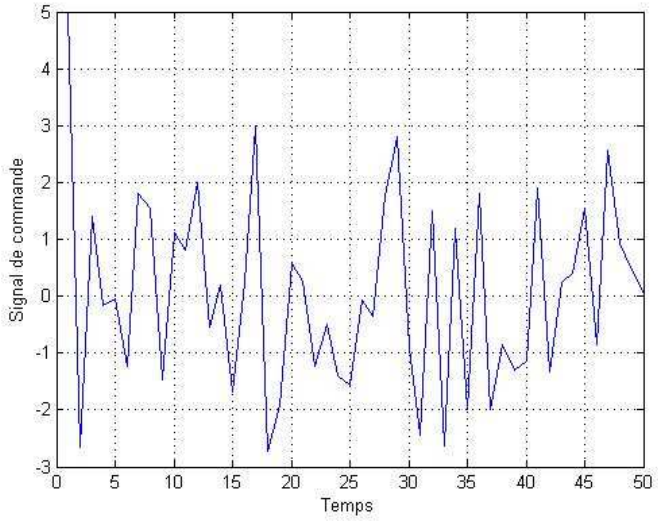

FIGURE 1.10 – Signal de commande appliqué au système de suspension magnetique

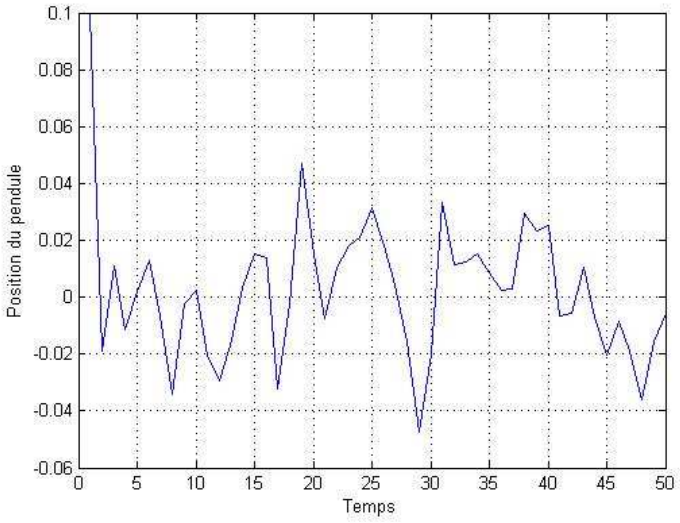

FIGURE 1.11 – Position du pendule obtenue par la commande prédictive à base de tubes d'incertitudes

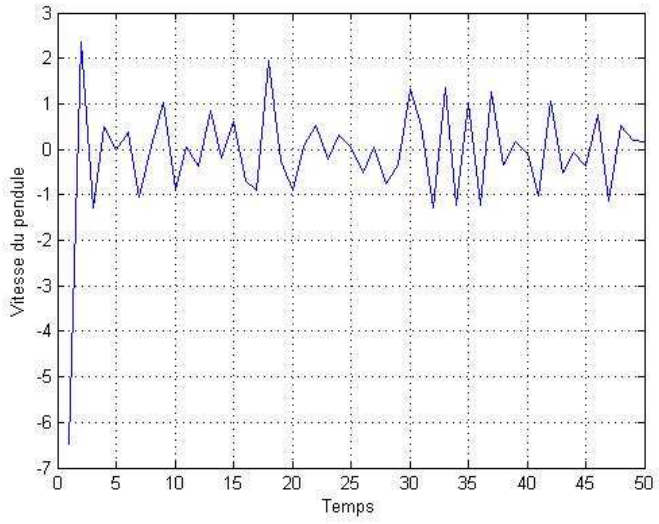

FIGURE 1.12 – Vitesse du pendule obtenue par la commande prédictive à base de tubes d'incertitudes

1.5 Conclusion

Cette thèse vise deux domaines fondamentaux de l'Automatique : l'estimation et la commande. Dans ce but, les contributions principales de la thèse sont les suivantes. Premièrement développer une estimation ensembliste zonotopique fondée sur la minimisation d'un nouveau critère : le P-rayon de cet ensemble zonotopique. Fondé sur l'approximation de l'intersection d'un zonotope avec une bande de mesures, ce nouveau critère permet d'obtenir un bon compromis entre la précision de l'estimation et la complexité du calcul. Cette technique d'estimation est développée non seulement pour des systèmes mono-sortie, mais également pour des systèmes multi-sorties. Plusieurs contributions visent l'estimation des systèmes multi-sorties (approche ESO, approche ESOCE, approche PMI), une contribution majeure étant le résultat de l'approximation de l'intersection d'un zonotope et d'un polytope (approche PAZI). La deuxième contribution principale de la thèse est le développement d'une loi de commande prédictive robuste (sous contraintes, avec des perturbations et bruit de mesure inconnus, mais bornés) par retour de sortie fondée sur l'estimation ensembliste zonotopique.

Ce travail peut être étendu en considérant l'estimation ensembliste zonotopique pour des systèmes avec retard. De plus, les résultats développés peuvent être appliqués pour résoudre le problème du diagnostic et de la commande tolérante aux défauts. Un problème intéressant à traiter dans le futur reste de trouver une loi de commande prédictive à base de tubes de trajectoire pour des systèmes affectés par des incertitudes par intervalles.

Chapter 2

Introduction

2.1 Context and motivations

The work of this thesis is found at the intersection of two major problems in automatic control: state estimation and robust constrained control for discrete-time uncertain systems subject to disturbances and measurement noises. The goal of this thesis is to take into account uncertainties, disturbances, measurement noises and constraints to build a state estimation and an output feedback control law which can guarantee the feasibility and the stability of the closed-loop system in this specific context.

In the literature, when an uncertain system is subjected to disturbances, there are two main ways to describe parameter uncertainties, disturbances and noises acting on a dynamic system:

- *Stochastic approach*, which assumes that the disturbances, noises and parameter uncertainties are unknown but its probability distributions are known.

- *Deterministic approach*, which assumes that disturbances, noises and parameter uncertainties are unknown but bounded by some convex sets. The main advantage of the deterministic approach is that disturbances and noises are supposed to be bounded and this is often simpler to verify than the criterion on the probability distribution. This is the main reason why many authors [147], [126], [20] etc. have chosen the deterministic approach to model the disturbances and the noises affecting the system behavior. Based on this remark, the deterministic approach has been chosen in this thesis to model the parameter uncertainties, the disturbances and the measurement noises.

Due to the presence of measurement noises, the system state, which is necessary to build the control law, is not available. In this case the implementation of a state estimator is necessary. This state estimation problem can be solved by different methods such as Luenberger observer [94], functionnal observer [109], moving-horizon estimation [57], set-membership estimation [147], [126], [20] etc. In this thesis the set-membership estimation method is chosen because of its ability to deal with uncertainties and disturbances. The set-membership estimation has been applied to the problem of state estimation of uncertain systems since 1960s [147], [126], [37], [2] etc. This approach permits to obtain a set containing the real system state consistent with the disturbances and measurement noises. With the development of robust control theory, the set-membership estimation technique is shown to be suitable to deal with unknown but bounded uncertainties, disturbances and measurement noises. If constraints are added to the previous problem, then a predictive control feature should be added. This results in using robust predictive control strategies based on set-membership estimation in order to answer to the proposed problem. In particular, zonotopic sets will be used due to its flexibility and low-complexity.

This thesis builds upon previous results on the zonotopic set-membership state estimation [37], [2] and the output feedback Tube-based Model Predictive Control [100]. The aim of the state estimation problem is to obtain a small estimation set which contains the real state. The proposed method in [37] computes a zonotopic outer approximation of the set of states based on a Singular Value Decomposition of a matrix [140], which offers good performance of the estimation. In [2], the authors proposed a method to compute the zonotopic guaranteed state estimation based on two optimization problems. The first solution is based on the minimization of the volume of a zonotope and offers a high accuracy estimation with a complex computation, while the second solution considers the minimization of the segments of the zonotope and proposes a simple computation but with a deterioration of the estimation accuracy. For these reasons, the goal of this PhD thesis is to propose a new method permitting to improve the estimation performance, while keeping a low complexity level. Moreover, this zonotopic set-membership estimation is proposed to replace the Luenberger observer in the output feedback Tube-based Model Predictive Control [100]. This association permits us to improve the performance of the closed-loop system as it will be shown in the future sections.

2.2 Outline and contributions of the thesis

In this section, the description of the main chapters (excluding this introductive chapter) is given with highlights on the main contributions.

- **Chapter 1**: This chapter offers a synthesis in French of the main results presented in this thesis.

- **Chapter 3**: The goal of this chapter is to answer the question on how to represent the uncertainties, the disturbances and the noises in the deterministic approach. The chapter starts with a short description of the deterministic approach in which the disturbances and noises are assumed to be bounded by known convex sets. After that, some basic definitions and operations necessary to manipulate sets and matrix computations are presented. As the disturbances are bounded by a convex set, the next part consists in presenting a list of the most popular families of sets which are used in the literature, with its advantages and weak points. Due to the advantages of zonotope, the family of zonotopic sets is further chosen to bound the disturbances and measurement noises.

- **Chapter 4**: In this chapter, a zonotopic set-membership estimation is proposed to solve the problem of state estimation for interval uncertain systems subject to unknown but bounded disturbances and measurement noises. This chapter proposes a new optimization criterion based on the minimization of the P-radius of a zonotope (that will be defined later on in this thesis) in order to obtain a zonotopic guaranteed state estimation as a trade-off between the low computation complexity and the performance of the state estimation. Moreover, this criterion permits to guarantee the non-increasing property of the guaranteed state estimation at each time instant; to the best of the authors knowledge, this can not be found in the other approaches proposed in the literature. The chapter proposes a pedagogical structure in three steps. It starts with the state estimation solution based on matrix inequalities optimization and zonotopic outer approximation of the intersection between a zonotope and a strip for single-output linear discrete time invariant systems subject to disturbances and measurement noises. Based on this solution, in a second step the state estimation problem is extended to the case of single-output linear discrete-time variant systems (i.e. it considers the case of systems with interval parametric uncertainties). To solve this new problem, the maximum principle [122] is

used. The case of multi-output systems leads to two different classes of solutions:

  - The first class is the direct application proposed for the single-output systems for each output of the multi-output system leading to a conservative result. Several approaches belonging to this first class will be developed and compared (Equivalent Single-Output approach, Equivalent Single-Output with Coupling Effect and Polynomial Matrix Inequality approach).
  - The second class based on an original result on the zonotopic approximation of the intersection between a polytope and a zonotope permits to improve the performance of the estimation while considering all the output measurements in the same time.

- **Chapter 5**: The problem of robust predictive control is discussed in this chapter, in the context of zonotopic set-membership estimation. The performance of model predictive control is illustrated by many industrial applications. This large application is explained by its ability to deal with disturbances and constraints acting on the system. Based on the zonotopic set-membership estimation built in Chapter 4, two predictive control laws are presented. The first control law is an open-loop predictive control which has a simple implementation/structure but does not guarantee the stability of the closed-loop system. To offer a stability proof, a second controller which is a feedback predictive control based on a tube of trajectories is proposed for the case of linear discrete-time invariant systems with bounded disturbances and measurement noises, subject to constraints. Moreover, when interval parametric uncertainties are added, the optimization problem in the first control law becomes non convex and the recursive feasibility in the tube-based predictive control is lost. For these reasons, in this thesis we have chosen to apply a modified open-loop predictive control for uncertain systems, the output feedback predictive control based on the zonotopic set-membership estimation still remaining an open problem.

- **Chapter 6**: This chapter proposes an application of the proposed approaches to control a magnetic levitation system. The first step consists in describing and modeling this non-linear unstable continuous-time system subject to bounded disturbances, measurement noises and constraints. The proposed model is linearized around an equilibrium point and discretized for a given sampling time. Based on this model, the open-loop Model Predictive Control and the Tube-based Model Pre-

dictive Control associated to the zonotopic set-membership estimation are used to stabilize this system around the equilibrium point.

- **Chapter 7**: The last chapter resumes the developed work in this PhD thesis and proposes some future directions both on theoretical developments and on real applications.

The work in this thesis has resulted in several accepted/submitted publications to prestigious international conferences and journals:

Published journal paper:

- **V. T. H. Le**, C. Stoica, D. Dumur, T. Alamo, E. F. Camacho, Commande prédictive robuste par des techniques d'observateurs basées sur des ensembles zonotopiques, *Journal Européen des Systèmes Automatisés (JESA)*, no. 2-3/2012, pp. 235-250, DOI 10.3166/JESA.46.235-250, ISSN 1269-6935, ISBN 978-2-7462-3957-9, 2012.

Submitted journal paper:

- **V. T. H. Le**, C. Stoica, T. Alamo, E. F. Camacho, D. Dumur, Zonotopic guaranteed state estimation for uncertain systems, *submitted to Automatica* (second review round), 2012.

Published conference papers:

- **V. T. H. Le**, T. Alamo, E. F. Camacho, C. Stoica, D. Dumur, A new approach for guaranteed state estimation by zonotopes, *Proceedings of the 18th IFAC World Congress*, Milan, Italy, pp. 9242-9247, 28 August - 2 September 2011.

- **V. T. H. Le**, C. Stoica, D. Dumur, T. Alamo, E. F. Camacho, Robust tube-based constrained predictive control via zonotopic set-membership estimation, *Proceedings of the 50th IEEE Conference on Decision and Control and European Control Conference*, Orlando, Florida, U.S.A., pp. 4580-4585, 12-15 December 2011.

- **V. T. H. Le**, T. Alamo, E. F. Camacho, C. Stoica, D. Dumur, Zonotopic set-membership estimation for interval dynamic systems, Proceedings of the 2012 IEEE American Control Conference, Montréal, Canada, pp. 6787-6792, 27-29 June 2012.

- **V. T. H. Le**, C. Stoica, D. Dumur, T. Alamo, E. F. Camacho, A Polynomial Matrix Inequality approach for zonotopic set-membership

estimation of multivariable systems, *Proceedings of the 20th Mediterranean Conference on Control and Automation*, Barcelona, Spain, pp. 18-23, 3-6 July 2012.

Submitted conference paper:

- **V. T. H. Le**, C. Stoica, T. Alamo, E. F. Camacho, D. Dumur Zonotopic set-membership estimation for multi-output uncertain systems, *submitted to Europeen Control Conference 2013*.

Workshop (oral presentation):

- **V. T. H. Le**, C. Stoica, T. Alamo, E. F. Camacho, D. Dumur, Guaranteed state estimation by zonotopes for systems with interval uncertainties, Small Workshop on Interval Methods (SWIM), Oldenburg, Germany, 4-6 June 2012.

Chapter 3

Set theory for uncertainty representation

In the control systems context, a mathematical model is frequently used to describe the system behavior, offering the possibility to analyze and to design control strategies for the considered system. The quality of the control depends on the model accuracy, i.e. on how well the mathematical model developed on the theoretical side agrees with results of repeated experiments. But the mathematical model can not exactly represent the real system due to a lack of knowledge or unreliable information of the system. To validate this model some uncertainties can be added to the mathematical model. Moreover perturbations influencing the real system have to be taken into account in the mathematical model in order to ensure a similar behavior of the real system and the mathematical model. The importance of uncertainties in system design can be seen in [99], [9], [10] and the references therein. In the literature, there are two ways to represent uncertainties: the statistical (or stochastic) approach and the deterministic approach.

Stochastic approach: The uncertainty is modeled by a random process with a known statistical property. This approach is widely used in different scientific domains (e.g. economy [12], biology [143], engineering [99]), especially when estimates of the probability distribution of the uncertain parameters are available. But in many applications, this probability distribution of the uncertain parameters is not known; only bounds of this uncertainty can be fixed. In this case the probabilistic assumption on the uncertainty is not anymore validated, making this method not suitable for modeling the uncertainties.

Deterministic approach: The uncertainty is supposed belonging to a set: a classical (crisp) set (a set, wherein the degree of membership of any object in the set is either 0 or 1) or a fuzzy set (a set, wherein the degree of

membership of any object in the set is between 0 and 1). In the literature, different families of classical sets are used depending on their accuracy and their complexity. Usually, the accuracy and the complexity of the uncertainties representation are inversely proportional, depending on the particular problem related to the choice of a suitable geometric form. In the following parts, some popular families of sets are presented with their advantages and their weaknesses. Note that in this thesis only convex (classical) sets are considered because of the role of convexity in the theory of optimization [19].

3.1 Basic set definitions

Before presenting the most known families of sets, some basic set definitions and operations are introduced. These definitions are used along this thesis.

***Definition* 3.1.** A set $S \subset \mathbb{R}^n$ is called *convex set* if for any $x_1, x_2, \ldots, x_k \in S$ and any $\alpha_1, \alpha_2, \ldots, \alpha_k \in \mathbb{R}^+$ such that $\sum_{i=1}^{k} \alpha_i = 1$, then the element $\sum_{i=1}^{k} \alpha_i x_i$ is in S.

***Definition* 3.2.** A *convex hull* of a given set S, denoted $conv(S)$ is the smallest convex set containing S.

***Definition* 3.3.** A set $S \subset \mathbb{R}^n$ is called a *C-set* if S is compact, convex and contains the origin. This is a *proper set* if its interior is not empty.

***Definition* 3.4.** *Inclusion* operator : $X \subseteq Y$, if and only if $\forall x \in X$, then $x \in Y$.

***Definition* 3.5.** *Intersection* operator : $X \cap Y = \{z : z \in X \text{ and } z \in Y\}$.

***Definition* 3.6.** The *image of a set S under a map (projection) M* is the set $M(S) = \{y : y = M(x), x \in S\}$.

***Definition* 3.7.** The *Minkowski sum* of two sets X and Y is defined by $X \oplus Y = \{x + y : x \in X, y \in Y\}$.

***Definition* 3.8.** The *Pontryagin difference* of two sets X and Y is defined by $X \ominus Y = \{z : z + y \in X, \forall y \in Y\}$.

***Definition* 3.9.** Let X and Y be two non-empty sets, the distance of two sets X and Y is defined as $d(X, Y) = min\{d(x, y) : x \in X, y \in Y\}$.

***Definition* 3.10.** Let X and Y be two non-empty sets. The *Hausdorff distance* of these two sets X and Y is defined by the following expression $d_H(X, Y) = max\{\bar{d}_H(X, Y), \bar{d}_H(Y, X)\}$, with $\bar{d}_H(X, Y) = \max_{x \in X} \min_{y \in Y} d(x, y)$.

The Hausdorff distance permits to characterize the quality of the approximation of X by Y [65]. If X and Y have the same closure, then the Haursdoff distance is equal to 0.

The following figure illustrates the difference between the "normal" distance (Definition 3.9) which is equal to 0 and the Hausdorff distance which is different to 0 between the two sets X and Y.

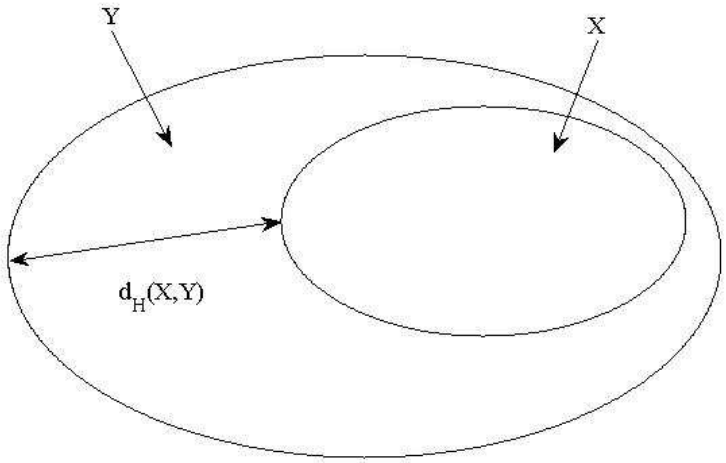

Figure 3.1: Difference between the "normal" distance and the Hausdorff distance between two sets X and Y

3.2 Basic matrix operation definitions

In this section, some matrix operations which are used in this thesis are introduced.

***Definition* 3.11.** A matrix $M = M^T \in \mathbb{R}^{n\times n}$ is called a *semi positive-definite matrix* (respectively *semi negative-definite matrix*), denoted $M \succeq 0$ ($M \preceq 0$), if $z^T Mz \geq 0$ ($z^T Mz \leq 0$) for all non-zero vectors z with real entries ($z \in \mathbb{R}^n$).

***Definition* 3.12.** A matrix $M = M^T \in \mathbb{R}^{n\times n}$ is called a *strictly positive-definite matrix* (respectively *strictly negative-definite matrix*), denoted $M \succ 0$ ($M \prec 0$), if $z^T Mz > 0$ ($z^T Mz < 0$) for all non-zero vectors z with real entries ($z \in \mathbb{R}^n$).

***Definition* 3.13.** A mathematical expression of the following form is called *Linear Matrix Inequality* (LMI):

$$F(x) = F_0 + \sum_{i=1}^{n} x_i F_i \succ 0 \tag{3.1}$$

where $x = \begin{bmatrix} x_1 & x_2 & \dots & x_n \end{bmatrix}^T \in \mathbb{R}^n$ is the vector of decision variables and F_i, $i = 0, \dots, n$ are given symmetric matrices.

The two following problems related to LMI are considered in this thesis:

1. *Feasibility problem*: Does it exist a solution $x \in \mathbb{R}^n$ such that the LMI $F(x) \succ 0$ is feasible?

2. *Optimization problem*: Minimize a linear cost function $b^T x$ subjected to the LMI constraint $F(x) \succ 0$.

***Definition* 3.14.** (*Schur complement* [24], [124]) Consider the following LMI:

$$\begin{bmatrix} Q(x) & S(x) \\ S^T(x) & R(x) \end{bmatrix} \succeq 0 \tag{3.2}$$

where $Q(x)$, $R(x)$ are symmetric matrices and $Q(x)$, $R(x)$, $S(x)$ are affine on x, then this LMI is equivalent to:

$$\begin{cases} Q(x) \succeq 0 \\ Q(x) - S(x)R(x)^{-1}S^T(x) \succeq 0 \end{cases} \tag{3.3}$$

or

$$\begin{cases} R(x) \succeq 0 \\ R(x) - S^T(x)Q(x)^{-1}S(x) \succeq 0 \end{cases} \tag{3.4}$$

***Definition* 3.15.** A *Bilinear Matrix Inequality* (BMI) is defined by the following expression:

$$F(x) = F_0 + \sum_{i=1}^{n} x_i F_i + \sum_{i=1}^{n} \sum_{j=1}^{m} x_i x_j F_{ij} \succ 0 \tag{3.5}$$

where $x = \begin{bmatrix} x_1 & x_2 & \dots & x_n \end{bmatrix}^T \in \mathbb{R}^n$ if $n \geq m$ or $x = \begin{bmatrix} x_1 & x_2 & \dots & x_m \end{bmatrix}^T \in \mathbb{R}^m$ if not, is the vector of decision variables and F_0, F_i, F_{ij} $i, j = 1, \dots, n$ are given symmetric matrices.

***Definition* 3.16.** A *Polynomial Matrix Inequality* (PMI) is defined by the following expression:

$$F(x) = xF \succ 0 \tag{3.6}$$

where $x = \begin{bmatrix} 1 & x_1 & ... & x_n & x_1^2 & x_1x_2 & ... & x_1x_n & ... & x_n^n \end{bmatrix}^T \in \mathbb{R}^n$ is the vector of decision variables and $F = \begin{bmatrix} F_0 & F_1 & ... & F_n & F_{11} & F_{12} & ... & F_{1n} & ... & F_{n...n} \end{bmatrix}$, with F_* given symmetric matrices.

Note that LMI and BMI are just a particular case of PMI.

3.3 Interval set

A very simple way to define uncertainties is using the *interval* notion. This is based on the idea of enclosing numerical errors into an interval. In many cases obtaining the probability of occurrence of different uncertainties is not possible. Therefore, it can be easier and thus suitable to bound the uncertainties by intervals. Moreover, the interval analysis permits to simplify most of the standard operations [107], [60], [68]. This approach is developed in many domains such as identification, diagnosis, estimation etc. especially when a short computation time is required.

***Definition* 3.17.** An *interval* $I = [a, b]$ is defined as the set $\{x : a \leq x \leq b\}$.

***Definition* 3.18.** The *center* and the *radius* of an interval $I = [a, b]$ are respectively defined as $mid(I) = \frac{a+b}{2}$ and $rad(I) = \frac{b-a}{2}$.

***Definition* 3.19.** An *interval matrix* $[\![M]\!] \in \mathbb{I}^{n\times m}$ is a matrix whose elements are intervals.

It means that each element M_{ij}, with $i = 1, ..., n$, $j = 1, ..., m$ of this matrix is defined as the set $M_{ij} = \{m_{ij} : a_{ij} \leq m_{ij} \leq b_{ij}\}$. In the matrix space, the interval matrix is a hyper-rectangle and hence a convex set. Let $vert([\![M]\!])$ denote the set of all matrices $\tilde{A} = [\tilde{a}_{ij}]$, with $i = 1, ..., n$, $j = 1, ..., m$ such that $\tilde{a}_{ij} = a_{ij}$ or $s_{ij} = b_{ij}$. Thus $vert([\![M]\!])$ contains all the vertices of the interval matrix $[\![M]\!]$. The notations $mid([\![M]\!])_{ij} = \frac{a_{ij}+b_{ij}}{2}$ and $rad([\![M]\!])_{ij} = \frac{b_{ij}-a_{ij}}{2}$ define the coefficient of the center and the radius of an interval matrix $[\![M]\!]$, respectively.

***Definition* 3.20.** The *unitary interval* is denoted $\mathbf{B}$ = [-1,1].

***Definition* 3.21.** The *set of real compact intervals* $[a, b]$, where $a, b \in \mathbb{R}$ and $a \leq b$ is denoted $\mathbb{I}$.

***Definition* 3.22.** A *box* $([a_1, b_1], ..., [a_n, b_n])^T$ is an interval vector.

***Definition* 3.23.** A *unitary box* in $\mathbb{R}^n$, denoted $\mathbf{B}^n$, is a box composed by n unitary intervals.

Consider two given intervals $[x] = [\underline{x}, \bar{x}]$, $[y] = [\underline{y}, \bar{y}]$. If $\circ$ denotes an operation between the two intervals $[x]$ and $[y]$, then this can be formalized as:

$$[x] \circ [y] = \{x \circ y : x \in [x], y \in [y]\} \tag{3.7}$$

The four basic operations of interval analysis are defined as follows:

1. $[x] + [y] = [\underline{x} + \underline{y}, \bar{x} + \bar{y}]$
2. $[x] - [y] = [\underline{x} - \bar{y}, \bar{x} - \underline{y}]$
3. $[x] * [y] = [min(\underline{x}.\underline{y}, \underline{x}.\bar{y}, \bar{x}.\underline{y}, \bar{x}.\bar{y}), max(\underline{x}.\underline{y}, \underline{x}.\bar{y}, \bar{x}.\underline{y}, \bar{x}.\bar{y})]$
4. $[x]/[y] = [x] * [1/\bar{y}, 1/\underline{y}]$, if $0 \notin [y]$

Despite the simplicity of the interval analysis, a drawback of this approach is that the computation results are sometimes conservative due to the dependency effect (when a variable appears more than one time in a function) and the wrapping effect (the growth of the domain representation due to over-estimation at each sampling time) [107], [76], [68]. These two effects are further analyzed via two examples.

***Example* 3.1.** (*Dependency effect*) Consider a function $f_1(x, y) = x - y$, and a function $f_2(x) = x - x$ with $x, y \in [-1, 1]$. Using the interval analysis we can find that the value domain of f_1 and f_2 is the same $[-2, 2]$, even if the real value domain of f_2 is 0. This problem, called the dependency effect, lies in the fact that the occurrence of the same variable x in the function f_2 is independently considered. This can lead to a an important over approximation of the result.

***Example* 3.2.** (*Wrapping effect*) Consider two variables x and y belonging to the unitary interval $[-1, 1]$, and a function $f(x, y) = \begin{bmatrix} 0 & -0.5 \\ 1 & 1 \end{bmatrix} . \begin{bmatrix} x \\ y \end{bmatrix}$. Figure 3.2 shows the exact solution (in red) of the function f and the result obtained using the interval analysis (blue). Comparing these solutions, an important over-approximation of the interval analysis solution can be noticed. If this operation is repeated several times, the difference between the exact solution and the solution of the interval analysis is more and more important. This problem is called the wrapping effect.

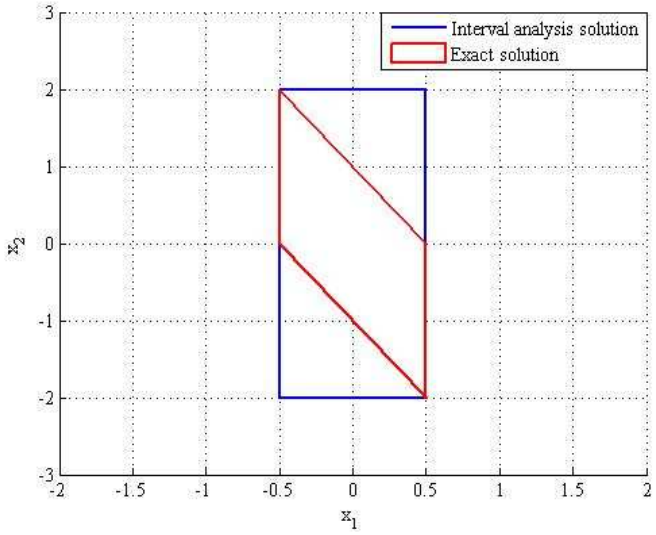

Figure 3.2: Wrapping effect in the interval analysis

3.4 Ellipsoidal set

A popular set which is used in a large class of applications in automatic control due to its low complexity is the *ellipsoidal* set [126].

***Definition* 3.24.** Given a vector $c \in \mathbb{R}^n$ and a symmetric positive definite matrix P, the *ellipsoid* E is defined as follows:

$$E = \{x \in \mathbb{R}^n : (x-c)^T P^{-1}(x-c) \leq 1\} \tag{3.8}$$

The vector $c \in \mathbb{R}^n$ is called the *center* of the ellipsoid E and the matrix P is called the *shape matrix* of the ellipsoid E. From this definition, the complexity of an ellipsoidal representation is quadratic in the dimension of the space [78] (expression $(x-c)^T P^{-1}(x-c)$).

Figure 4.3 proposes an example of ellipsoid with $c = \begin{bmatrix} 0 \\ 0 \end{bmatrix}$ and $P = \begin{bmatrix} 1 & 1 \\ 1 & 4 \end{bmatrix}$.

Concrete studies on ellipsoids and their operations can be found in [24], [78]. Despite the simple representation of ellipsoids, there are still some drawbacks which lead to a conservative result, such as the ellipsoidal set is not closed under some operations (sum, intersection etc.) and its low flexibility in the shape form in comparison with polyhedral set which will be presented in the next section.

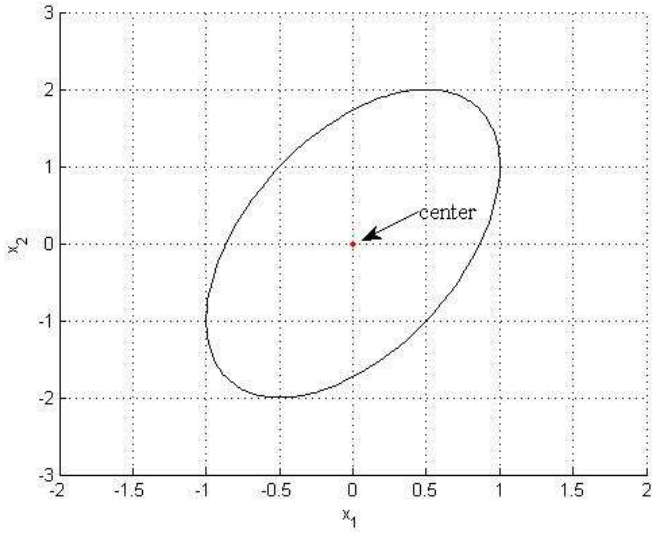

Figure 3.3: Ellipsoid

3.5 Polyhedral set

The *polyhedral* set is one of the most popular geometrical form used in many fields such as control and optimization. A polyhedral set in a finite-dimensional Euclidean space is the intersection of finitely many closed half-spaces [151]. A bounded polyhedral is denoted as a *polytope*. Due to its flexibility, polytopes offer a good approximation of any convex set [81], [26], [127]. Another advantage of polytopes in comparison with ellipsoids is that it is closed under the mentioned operations. Moreover, its dual representation (half-space representation and vertex representation) permits to choose the suitable form for a particular problem. The main disadvantage of polytopes is related to its complexity depending on the number of vertices, which is not fixed by the space dimension. Therefore, even if a polytope can well approximate any convex set, the complexity can quickly increase with the number of vertices even in a low space dimension. Despite this weak point, polytopes are one of the most popular convex sets used in automatic control. In order to formalize the notations, the main definitions of polytopes are summarized below.

***Definition* 3.25.** (*Half-space representation*) A polyhedral $P \in \mathbb{R}^n$ can be defined as the intersection of a finite number of half-spaces:

$$P = \{x \in \mathbb{R}^n : H \cdot x \leq K\} \tag{3.9}$$

with $H \in \mathbb{R}^{m\times n}$, $K \in \mathbb{R}^m$. If P is bounded, then P is a polytope.

Figure 3.4 shows the half-space representation of a polytope with $H = \begin{bmatrix} -0.9996 & 0.0001 & 0.9728 & 0.5492 \\ -0.0296 & 1 & 0.2318 & -0.8357 \end{bmatrix}^T$, $K = \begin{bmatrix} 0.0233 & 1.7775 & 1.9766 & 0.7572 \end{bmatrix}^T$ (H_i, K_i are the i^{th}-column of matrix H and K respectively).

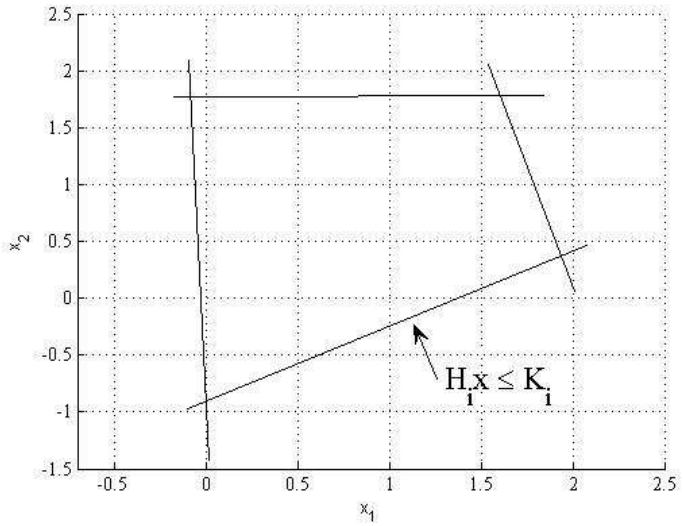

Figure 3.4: H-representation of polytope

***Definition* 3.26.** (*Vertex representation*) For a finite set of points $V = \{v_1, v_2, \ldots, v_m\} \in \mathbb{R}^n$, a polytope P can be defined as the convex hull of the set V:

$$P = conv(V) = \{\alpha_1 v_1 + \alpha_2 v_2 + \ldots + \alpha_m v_m : \alpha_i \in \mathbb{R}^+, \sum_{i=1}^{m} \alpha_i = 1\} \quad (3.10)$$

Figure 3.5 shows the vertex representation of a polytope with $V = \{\begin{bmatrix} -0.0760 \\ 1.7775 \end{bmatrix}, \begin{bmatrix} 1.6085 \\ 1.7773 \end{bmatrix}, \begin{bmatrix} 1.9435 \\ 0.3713 \end{bmatrix}, \begin{bmatrix} 0.0034 \\ -0.9038 \end{bmatrix}\}$. The next theorem [151] shows the equivalence of these two definitions permitting to choose a suitable representation for a particular problem. For example, the proof that the polytopic set is closed under Minkowski addition is trivial when V-representation is used but not trivial with H-representation.

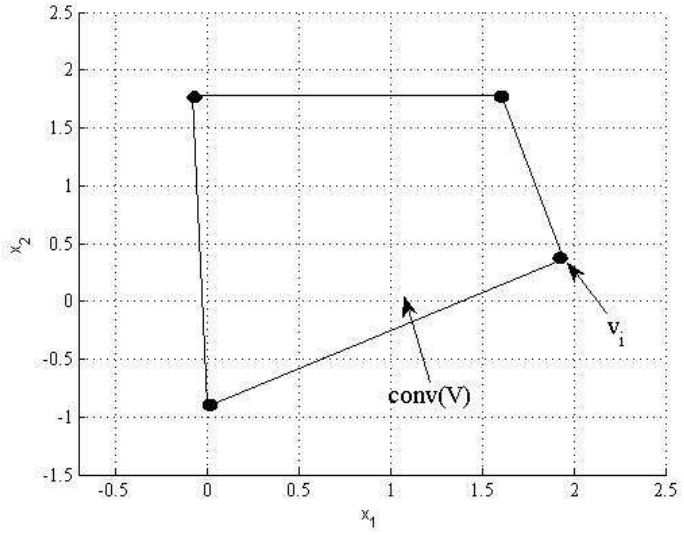

Figure 3.5: V-representation of polytope

***Theorem* 3.1.** (Equivalence of the two polytopic representations) [151] A subset $P \in \mathbb{R}^n$ is the convex hull of a finite point set (a V-polytope) if and only if it is a bounded intersection of half-spaces (a H-polytope).

This theorem shows that the H-representation can be transformed to the V-representation of a polytope and vice versa. In the literature this problem is well known as the *vertex enumeration problem* for the transformation of a V-polytope to an H-polytope and the *facet enumeration problem* for the transformation of a H-polytope to V-polytope. There exist algorithms to solve these transformation problems, but they are time consuming (e.g. [42], [47]). More details on polytopes can be found in [151], [23].

An example of the same polytope defined by H-representation and V-representation is given in Figures 3.4 and 3.5.

Even if polytopes can well approximate any convex set, their applications are limited due to their complexity. In the next section, another geometrical form which offers a good compromise between complexity and flexibility is presented.

3.6 Zonotopic set

In this thesis, zonotopes will be used to represent uncertainties due to the flexibility, the reduced complexity and specially the efficient computation of

linear transformation and Minkowski sum. *Zonotopes* are a special class of convex polytopes, more precisely symmetric polytopes. Similar to polytopes, zonotopes can be represented by the half-space representation and the vertex representation. In addition, zonotopes can be represented by another forms which will be detailed in the next sub-section.

3.6.1 Zonotope definition

***Definition* 3.27.** (Generator representation) Given a vector $p \in \mathbb{R}^n$ and a set of vectors $G = \{g_1, g_2, ..., g_m\} \subset \mathbb{R}^n$, $m \geq n$, a *zonotope* Z of order m is defined as following:

$$Z = (p; g_1, g_2, ..., g_m) = \{x \in \mathbb{R}^n : x = p + \sum_{i=1}^{m} \alpha_i g_i; -1 \leq \alpha_i \leq 1\} \quad (3.11)$$

The vector p is called the *center* of the zonotope Z. These vectors $g_1, \ldots, g_m$ are called generators of Z. The *order* of a zonotope is defined by the number of its generators (m in this case). The case of $m < n$ is called degenerated zonotope.

This definition is equivalent with the definition of zonotopes by the Minskowski sum of a finite number of line segments defined by $g_i\mathbf{B}^1$.

$$Z = (p; g_1, g_2, ..., g_m) = p \oplus g_1\mathbf{B}^1 \oplus \ldots \oplus g_m\mathbf{B}^1 \quad (3.12)$$

An illustrative example of a zonotope of third order in $2D$ and its generators is given in Figure 3.6 with $p = \begin{bmatrix}0\\0\end{bmatrix}$, $g_1 = \begin{bmatrix}1\\3\end{bmatrix}$, $g_2 = \begin{bmatrix}2\\2\end{bmatrix}$, $g_3 = \begin{bmatrix}3\\1\end{bmatrix}$.

Figure 3.7 presents a 6^{th} order centered [1] zonotope in $3D$ ($p = \begin{bmatrix}0\\0\\0\end{bmatrix}$, $g_1 = \begin{bmatrix}1\\1\\0\end{bmatrix}$, $g_2 = \begin{bmatrix}1\\-1\\0\end{bmatrix}$, $g_3 = \begin{bmatrix}1\\0\\1\end{bmatrix}$, $g_4 = \begin{bmatrix}1\\0\\-1\end{bmatrix}$, $g_5 = \begin{bmatrix}0\\1\\1\end{bmatrix}$, $g_6 = \begin{bmatrix}0\\1\\-1\end{bmatrix}$).

These two examples show that the complexity of zonotopes (number of vertices in $2D$ or facets in a bigger dimension) depends on the number of generators and the dimension of the space. The complexity grows up rapidly: the number of vertices of the zonotope is 6 in Figure 3.6 and 24 in Figure 3.7, when the number of generators is increased.

[1] A centered zonotope is a zonotope whose center is the origin.

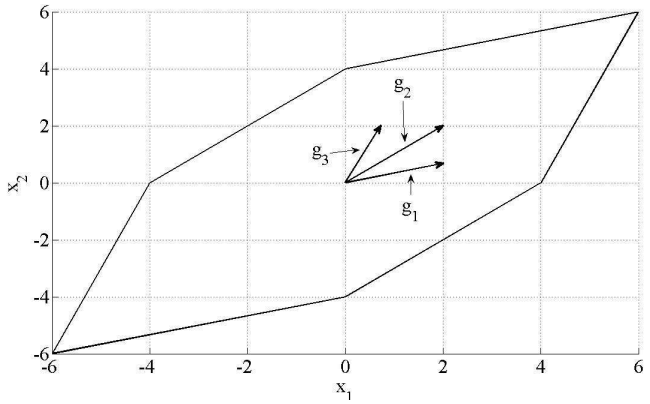

Figure 3.6: 3-zonotope and its generators in $2D$

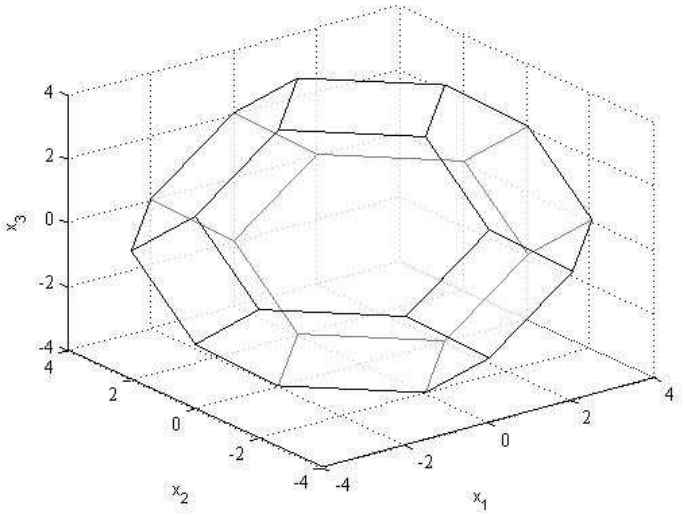

Figure 3.7: 6-zonotope in $3D$

Another definition of zonotopes that is more convenient for the approach considered in this thesis is the following.

***Definition* 3.28.** (Hypercube linear projection) A zonotope of order m in $\mathbb{R}^n$ ($m \geq n$) is the translation by the center $p \in \mathbb{R}^n$ of the image of an unitary hypercube of dimension m in $\mathbb{R}^n$ under a linear transformation. Given a matrix $H \in \mathbb{R}^{n \times m}$ representing the linear transformation, the zonotope Z is

defined by:

$$Z = (p; H) = p \oplus H\mathbf{B}^m \tag{3.13}$$

The proposed definitions of zonotopes are equivalent if we consider the matrix $H = \begin{bmatrix} g_1 & g_2 & \dots & g_m \end{bmatrix}$. From now on, to simplify the manuscript, the zonotope Z will be described by $Z(p; H)$. The same zonotope in the Figure 3.6 is constructed using the hypercube linear projection. This zonotope is the image of $3D$ hypercube (with its eight vertices $\begin{bmatrix} 1 \\ 1 \\ 1 \end{bmatrix}, \begin{bmatrix} -1 \\ 1 \\ 1 \end{bmatrix}, \begin{bmatrix} 1 \\ -1 \\ 1 \end{bmatrix}, \begin{bmatrix} 1 \\ 1 \\ -1 \end{bmatrix}, \begin{bmatrix} -1 \\ -1 \\ 1 \end{bmatrix}, \begin{bmatrix} -1 \\ 1 \\ -1 \end{bmatrix}, \begin{bmatrix} 1 \\ -1 \\ -1 \end{bmatrix}, \begin{bmatrix} -1 \\ -1 \\ -1 \end{bmatrix}$) under the projection H in $2D$ (see Figure 3.8).

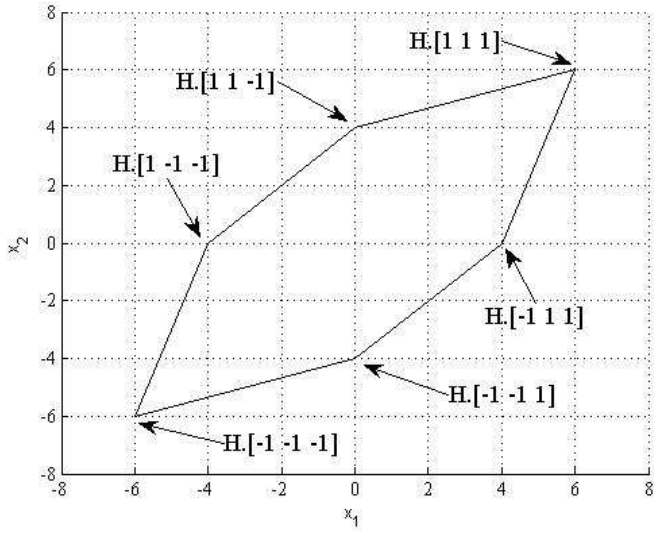

Figure 3.8: 3-zonotope and its vertices in $2D$

The generator representation of a zonotope can be converted to the V-representation and also to the H-representation. These conversions are related to the Minkowski sum of two polytopes because the generator representation is equivalent to the Minkowski sum of a finite number of line segments, which is a polytope. The conversion between the zonotopes representations is studied by many authors such as [56], [131], [48], [125], [8].

The generator representation illustrates a significant advantage of zonotopes: a complex geometrical form can be represented using a simple matrix. The zonotope from Figure 3.7 with 24 vertices in $3D$ is represented by a

3×6 matrix H. This leads to simplify the mentioned basic set operations by simple matrix computation as presented in the next part.

3.6.2 Properties of zonotopes

This part focuses on the main properties of zonotopes that will be used along this thesis.

***Property* 3.1.** (Particular forms) Given a zonotope $Z = H\mathbf{B}^m \in \mathbb{R}^n$. Due to the properties of the matrix H, some particular forms of zonotope can be obtained. If H is the identity matrix, then Z is the unit box. If H is diagonal, orthogonal or invertible, then Z is a box, a hypercube or a parallelotope [2], respectively.

***Property* 3.2.** (*Generators permutation*) The permutation of the matrix columns in the generators representation of a zonotope does not modify the zonotope.

Proof This property results from the commutativity of Minkowski sum. □

***Property* 3.3.** (*Sum of two zonotopes*) Given two centered zonotopes $Z_1 = H_1\mathbf{B}^{m_1} \in \mathbb{R}^n$ and $Z_2 = H_2\mathbf{B}^{m_2} \in \mathbb{R}^n$, the Minkowski sum of two zonotopes is also a zonotope defined by $Z = Z_1 \oplus Z_2 = \begin{bmatrix} H_1 & H_2 \end{bmatrix} \mathbf{B}^{m_1+m_2}$.

Proof From the definition of the Minkowski sum, it results in: $Z_1 \oplus Z_2 = \{H_1 z_1 + H_2 z_2 : z_1 \in \mathbf{B}^{m_1}, z_2 \in \mathbf{B}^{m_2}\}$, that can be further rewritten in a matrix formulation as $Z_1 \oplus Z_2 = \{\begin{bmatrix} H_1 & H_2 \end{bmatrix} \cdot \begin{bmatrix} z_1 \\ z_2 \end{bmatrix} : \begin{bmatrix} z_1 \\ z_2 \end{bmatrix} \in \mathbf{B}^{m_1+m_2}\} = Z$. □

***Property* 3.4.** (*Linear image of a zonotope*) The image of a centered zonotope $Z_1 = H_1\mathbf{B}^{m_1} \in \mathbb{R}^n$ by a linear mapping K can be computed by a standard matrix product $K \cdot Z_1 = (K \cdot H_1)\mathbf{B}^{m_1}$.

Proof By using matrix multiplication the proof is similar to Property 1.3. □

***Property* 3.5.** (*Zonotope inclusion or Multiplication of a zonotope by an interval matrix*) Consider a family of zonotopes represented by $Z = p \oplus [M]\mathbf{B}^m$ where $p \in \mathbb{R}^n$ is a real vector and $[M] \in \mathbb{I}^{n \times m}$ is an interval matrix.

[2] A parallelotope is a special zonotope whose number of generators is equal to the dimension of the space.

A zonotope inclusion $\Diamond(Z)$ is an outer approximation of this family defined by:

$$\Diamond(Z) = p \oplus \begin{bmatrix} mid(\llbracket M \rrbracket) & rs(rad(\llbracket M \rrbracket)) \end{bmatrix} \mathbf{B}^{m+n} \tag{3.14}$$

with $rs(rad(M))$ a diagonal matrix and $rs(rad(M))_{ii} = \sum_{j=1}^{m} |rad(M)_{ij}|$, $i = 1, ..., n$.

Proof [2] If $z \in Z$, then it is clear that there exists $b \in \mathbf{B}^m$ such that $z \in p \oplus \llbracket M \rrbracket b$. Adding and subtracting $mid(\llbracket M \rrbracket)b$ leads to:

$$z \in (p + mid(\llbracket M \rrbracket b)) \oplus (\llbracket M \rrbracket - mid(\llbracket M \rrbracket))b$$

Note that the elements of $\llbracket M \rrbracket - mid(\llbracket M \rrbracket)$ satisfy:

$$M_{ij} - mid(\llbracket M \rrbracket)_{ij} = rad(\llbracket M \rrbracket)_{ij} \mathbf{B}^1$$

and thus this leads to:

$$(\llbracket M \rrbracket - mid(\llbracket M \rrbracket)b) \subseteq rs(rad(\llbracket M \rrbracket))\mathbf{B}^n.$$

Therefore the following expression holds:

$$\begin{gathered} z \in (p + mid(\llbracket M \rrbracket)b) \oplus rs(rad(\llbracket M \rrbracket))\mathbf{B}^n \subseteq \\ \subseteq p \oplus mid(\llbracket M \rrbracket)B^m \oplus rs(rad(\llbracket M \rrbracket))\mathbf{B}^n = \Diamond(Z). \end{gathered}$$

□

3.6.3 Complexity reduction of zonotopes

This subsection discusses some techniques to reduce the complexity of a zonotope. These techniques permit to limit the number of generators of a zonotope, which is an important problem in the computation of zonotopes. For example, if the problem of reachable set [3] is addressed using zonotopes, the complexity of this zonotope increases at each sample time due to the Minkowski sum operation. The complexity reduction problem leads to approximate a high order zonotope by a lower order one. In this part, the over approximated way is presented leading to compute a reduced order zonotope enclosing the initial zonotope.

[3] This is the problem of computing all states visited by trajectories of a system starting from any $x_0 \in X_0$.

3.6.3.1 Interval hull method

***Proposition* 3.1.** Considering a zonotope $Z = p \oplus H\mathbf{B}^m \in \mathbb{R}^n$, the smallest box containing this zonotope is computed by:

$$box(Z) = p \oplus rs(H)\mathbf{B}^n \tag{3.15}$$

with $rs(H)$ a diagonal matrix such that $rs(H)_{ii} = \sum_{j=1}^{m} |H_{ij}|$, $i = 1, ..., n$.

Proof As a box is an axis aligned set, the over approximation of a zonotope by a box can be done by considering its extreme points in each direction. The extreme point in direction i can be easily computed by $p_i + \sum_{j=1}^{m} |H_{ij}|$. All extreme points in all n directions are similarly computed and the smallest box containing the zonotope Z is obtained as $box(Z) = p \oplus rs(H)\mathbf{B}^n$. □

This proposition provides a simple and fast over-approximation of a zonotope by a box. The result has a minimal complexity which is given by the dimension of the space. However, the result obtained with this proposition is conservative because the form of the zonotope is lost.

An example is proposed in the following in order to better illustrate this proposition.

***Example* 3.3.** Given a centered zonotope $Z = H\mathbf{B}^3 \in \mathbb{R}^2$, $H = \begin{bmatrix} 1 & 2 & 3 \\ 3 & 2 & 1 \end{bmatrix}$, applying the interval hull approximation leads to a box (in blue) containing the original zonotope (in red) (see Figure 3.9).

3.6.3.2 Parallelotope hull method

***Proposition* 3.2.** Given a zonotope $Z = p \oplus H\mathbf{B}^m \in \mathbb{R}^n$ $(m > n)$, an over-approximation of this zonotope by a parallelotope is computed as:

$$Par(Z) = \Gamma \cdot box(\Gamma^{-1}H) \tag{3.16}$$

where $\Gamma \in \mathbb{R}^{n \times n}$ is an invertible matrix containing n columns taken from H.

Proof [8] This approach first transforms the coordinates of Z by the linear mapping Γ^{-1} where the new coordinate axes are the column vectors of Γ. In these new coordinates, the zonotope is over approximated by a box using the interval hull. This box is transformed back to the original coordinate system, resulting in a parallelotope. The over-approximation is guaranteed by the fact that the parallelotope is over-approximated in the transformed coordinate system by the interval hull operator, such that it is also over-approximated after the transformation to the original coordinate system. □

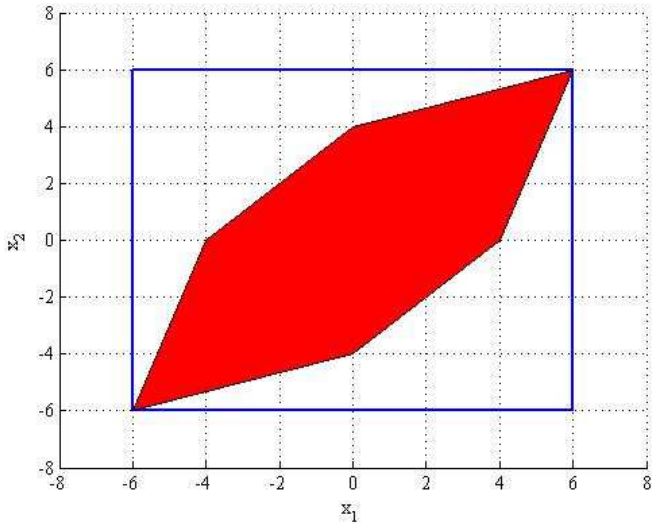

Figure 3.9: Intervall hull of a zonotope

***Example* 3.4.** The same zonotope as in Example 3.3 is taken in order to compare the two approximation methods. In Figure 3.10 this zonotope (in red) is over approximated by three different parallelotopes P_1, P_2, P_3 due to the different choice of the matrix Γ ($\Gamma_1 = \begin{bmatrix} 1 & 2 \\ 3 & 2 \end{bmatrix}$, $\Gamma_2 = \begin{bmatrix} 1 & 3 \\ 3 & 1 \end{bmatrix}$, $\Gamma_3 = \begin{bmatrix} 2 & 2 \\ 3 & 1 \end{bmatrix}$). Comparing the two examples (Figures 3.9 and 3.10), the over-approximation by the parallelotope hull is less conservative than the one by interval hull, but with a higher complexity (because n generators must be chosen among m generators to have the best approximation: the blue parallelotope). Some criteria to select the suitable generators are given in [107], [8].

3.6.3.3 Generators selection method

***Proposition* 3.3.** (*Cascade reduction*) Given a zonotope $Z = p \oplus H\mathbf{B}^{m \cdot n} \in \mathbb{R}^n$ ($m \geq n$), with H a m-block matrix of $n \times n$ matrix ($H = \begin{bmatrix} H_1 & \dots & H_m \end{bmatrix}$), let $D(l) = \begin{bmatrix} H_1 & \dots & H_l \end{bmatrix}$ be the matrix obtained by choosing l blocks of H. Choosing the biggest l ($2 \leq l \leq m$) for which $\|D(l-1)\|_\infty > \|H_l\|_\infty$ or $l = 1$ if such an integer does not exist, this norm criterion is called *fullness criterion* which imposes that the small parallelotope will be over-approximated more frequently than the big parallelotope. Then an over-approximation of Z is defined by:

$$Z \subseteq p \oplus \begin{bmatrix} rs(D(l)) & H_{l+1} & \dots & H_m \end{bmatrix} \tag{3.17}$$

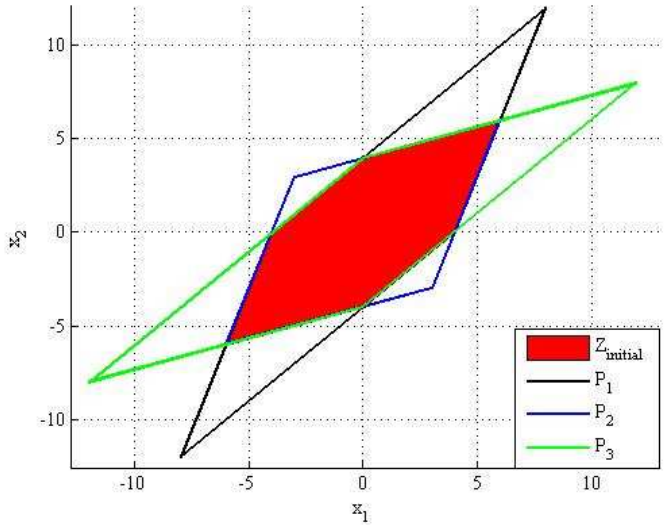

Figure 3.10: Parallelotope hull of a zonotope

This proposition is based on the representation of a zonotope by Minkowski sum of parallelotopes. More details on this proposition and its performance (a theoretical bound on quality of approximation) can be found in [75].

***Proposition* 3.4.** (*Criterion-based reduction*) Given the zonotope $Z = p \oplus H\mathbf{B}^m \in \mathbb{R}^n$ and the integer s, with $n < s < m$, denote $\hat{H}$ the matrix resulting from the reordering of the columns of the matrix H by a criterion which will be detailed in the in the following ($\hat{H} = \left[\hat{h}_1 \dots \hat{h}_i \dots \hat{h}_m\right]$). The zonotope is rewritten as: $Z = p \oplus \hat{H}_1\mathbf{B}^{s-n} \oplus \hat{H}_2\mathbf{B}^{m-s+n}$, where $\hat{H}_1$ is obtained from the first $s-n$ columns of matrix $\hat{H}$ and $\hat{H}_2$ is the remainder of $\hat{H}$. Then the initial zonotope is over-approximated by a zonotope of reduced order s as follows $Z \subseteq p \oplus \hat{H}_1\mathbf{B}^{s-n} \oplus Q\mathbf{B}^n$, where $Q\mathbf{B}^n$ is the over-approximation of the zonotope $\hat{H}_2\mathbf{B}^{m-s-n}$.

This over-approximation can be a box using Proposition 3.1 or a parallelotope using Proposition 3.2.

Proof Since a column of matrix H represents a segment of zonotope Z, then a column permutation in matrix H does not modify the zonotope Z. It means that $Z = p \oplus H\mathbf{B}^m = p \oplus \hat{H}\mathbf{B}^m$. From the definition of matrix $\hat{H}$ and

applying Property 3.3, it results in:

$$\begin{aligned} Z &= p \oplus \begin{bmatrix} \hat{H}_1 & \hat{H}_2 \end{bmatrix} \mathbf{B}^m = \\ &= p \oplus \hat{H}_1 \mathbf{B}^{s-n} \oplus \hat{H}_2 \mathbf{B}^{m-s+n} = \\ &= p \oplus \hat{H}_1 \mathbf{B}^{s-n} \oplus \begin{bmatrix} \hat{h}_{s-n+1} & \dots & \hat{h}_m \end{bmatrix} \mathbf{B}^{m-s+n} \end{aligned} \tag{3.18}$$

Propositions 3.1 and 3.2 show that the zonotope $\begin{bmatrix} \hat{h}_{s-n+1} & \dots & \hat{h}_m \end{bmatrix} \mathbf{B}^{m-s+n}$ can be approximated by $Q\mathbf{B}^n$, where Q is a diagonal matrix (if an approximation using box is used) or a full matrix (if an approximation using parallelotope is used). Therefore the following expression is true:

$$Z \subseteq p \oplus \hat{H}_1 \mathbf{B}^{s-n} \oplus Q\mathbf{B}^n = p \oplus \begin{bmatrix} \hat{H}_1 & Q \end{bmatrix} \mathbf{B}^s$$

□

The quality of the approximation depends on:

1. the value of s which limits the complexity;
2. the criterion used to split the zonotope Z;
3. the approximation method (box or parallelotope) used for the zonotope $\hat{H}_2 \mathbf{B}^{m-s-n}$.

A big value of s means a high precision of the approximation but the complexity remains high.

Two methods can be found in the literature to split the zonotope Z.

- The first approach consists in sorting the generators of the zonotope in decreasing order of the Euclidean norm [37], [2], which is equivalent to dispose the segments of zonotope from the longest to the shortest segment. Then the longest segments which have a more important role in the shape of the zonotope are kept and the contribution of the shortest segments is over-approximated by a box or a parallelotope in order to limit the complexity.
- Another criterion on sorting the generators is presented in [53] and consists in reordering the columns of matrix H in decreasing order of the term $\|h_i\|_1 - \|h_i\|_\infty$. The chosen generators (whose contribution is approximated) are close to vectors with only one non-zero component and are therefore well approximated by an interval hull.

An example is proposed in order to better illustrate the quality of different proposed methods of complexity reduction.

***Example* 3.5.** Consider a centered zonotope $Z = H\mathbf{B}^8 \in \mathbb{R}^2$, with $m = 8$, $n = 2$ and
$H = \begin{bmatrix} 0.9169 & 0.8936 & 0.3529 & 0.0099 & 0.2028 & 0.6038 & 0.1988 & 0.7468 \\ 0.4103 & 0.0579 & 0.8132 & 0.1389 & 0.1987 & 0.2722 & 0.0153 & 0.4451 \end{bmatrix}$.

This zonotope is approximated using Proposition 3.3 and Proposition 3.4 (in Proposition 3.4 the over-approximation by a box is used). Using the cascade reduction, the value of l is determined ($l = 3$). Figure 3.11 shows the approximation of the initial zonotope using the cascade reduction. Figure 3.12 shows the over-approximation of the zonotope Z ($Z_{initial}$ in red) obtained using as criterion the Euclidean norm with different values of s ($s = 4$ represented in blue line, $s = 5$ plotted in red line). This example confirms that the bigger value of s is, the better the approximation is.

Figure 3.13 compares the performance of the over-approximation of the same zonotope Z based on the two criteria of the generators reordering and selection: the Euclidean norm and the difference between the H_1 norm and the H_∞ norm. The same value $s = 6$ is chosen for both cases. In this example, the best approximation is obtained using the Euclidean norm-based criterion. In this thesis, the over-approximation based on the Euclidean norm criterion will therefore be used.

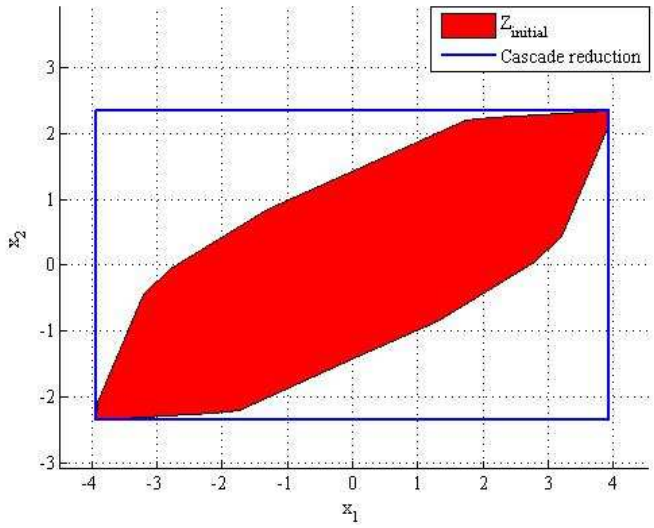

Figure 3.11: Complexity reduction of a zonotope using the cascade reduction

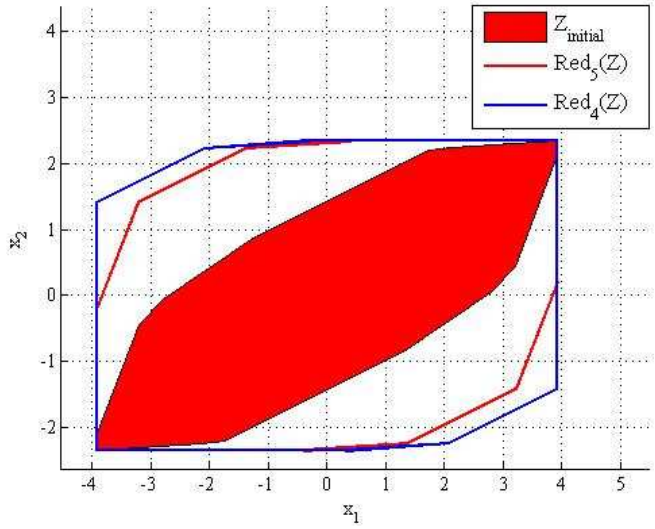

Figure 3.12: Complexity reduction of a zonotope using the Euclidean norm-based criterion

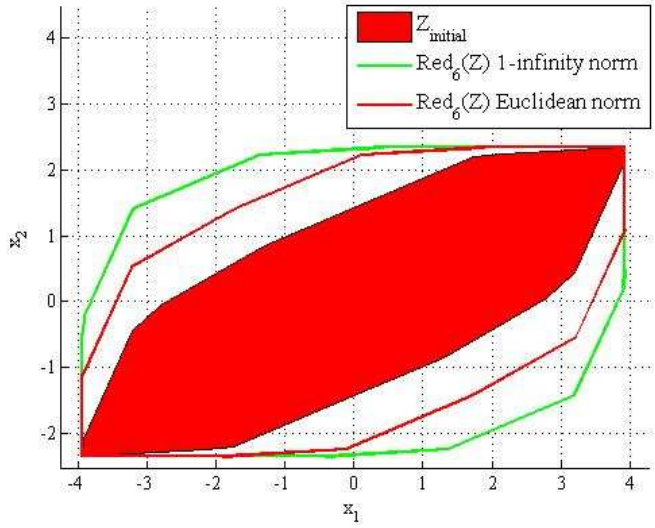

Figure 3.13: Complexity reduction of a zonotope: comparing two criteria

3.7 Conclusion

The above chapter gave a general presentation of some popular convex sets and their properties. The interval set and the interval analysis are strong tools allowing to deal with uncertainties but their application is limited due to the flexibility, the dependency effect and the wrapping effect. Even if the ellipsoidal set is used by many authors due to its simplicity, its low flexibility leads to a conservative computation result. The polytopic set can approximate whatever convex set with a high precision but polytope can not be used in fast processes due to its high complexity. The zonotopic set, a special class of polytope, offers a good compromise between complexity and flexibility (zonotope is a polytope, thus it is more flexible than an ellipsoid, and due to the symmetry property it is less complex than a polytope). Due to its interesting properties presented in this section, zonotopes will be used to represent the uncertainties in the context of set-membership estimation in the next chapters.

Chapter 4

Set-membership estimation via zonotope

4.1 Introduction

The choice of the appropriate mathematical model, which best describes the behavior of a given plant, has received increased attention in the control system literature. Mathematical models consist of several functions describing the relations between the system inputs, outputs and the (internal) states of the system at a given time instant. For example the states of the mathematical model of a motor can be the current, the velocity or the position of the motor. In different automatic control applications such as control systems, fault detection, knowledge about the system state is necessary to study the system behavior and to determine the control action. In practical applications, the measurement of the system states is not always available (due to the cost of the sensor or the harsh environnement) or can be affected by measurement noises (sometimes introducing a significant error relative to the real values of the states). For this reason, if the system is observable, a state estimator is set up to augment or replace measurement devices in the control system. This estimator uses the knowledge of the system (mathematical model, input and output signals) to produce the estimated states. The state estimator permits us to remove the sensor and thus, to reduce the cost and improve the reliability of the system with good quality estimator. Since the '60s, this problem has been studied by many authors, leading to different estimation techniques such as Kalman filter [69], Luenberger observer [94], set-membership estimation [147], [126], functionnal observer [109], [106], moving-horizon estimation [57], [104], [67], [1]. Several popular approaches discussed in the literature are listed below according to the choice of the

system model:

- **Luenberger observer**: In the context of linear systems without uncertainty, a Luenberger observer can be easily implemented [94], [95] due to its simplicity and efficiency.

  Consider a discrete-time-invariant linear system in the state-space representation: [1]

  $$\begin{cases} x_{k+1} = Ax_k + Bu_k \\ y_k = Cx_k + Du_k \end{cases} \tag{4.1}$$

  where $x_k \in \mathbb{R}^{n_x}$ is the system state, $u_k \in \mathbb{R}^{n_u}$ is the system input, $y_k \in \mathbb{R}^{n_y}$ is the output measurement. The matrices A, B, C, D have appropriate dimensions $A \in \mathbb{R}^{n_x \times n_x}$, $B \in \mathbb{R}^{n_x \times n_u}$, $C \in \mathbb{R}^{n_y \times n_x}$, $D \in \mathbb{R}^{n_y \times n_x}$. The system states can be estimated using the following observer model:

  $$\begin{cases} \hat{x}_{k+1} = A\hat{x}_k + Bu_k + L(y_k - \hat{y}_k) \\ \hat{y}_k = C\hat{x}_k + Du_k \end{cases} \tag{4.2}$$

  where $\hat{x}_k$, $\hat{y}_k$ represent the state and output estimation at time k.

  The estimation error e_k is then computed by:

  $$\begin{aligned} e_{k+1} &= x_{k+1} - \hat{x}_{k+1} \\ &= (A - LC)e_k \end{aligned} \tag{4.3}$$

  From the estimation error equation, it is proved that the estimation error tends to 0 if the gains matrix L is chosen such that the matrix $A - LC$ is Schur stable (all its eigenvalues are inside the unit circle).

- **Kalman filter**: If uncertainties are taken into account in the mathematical model in the form of stochastic process, the Kalman filter is presented as an effective solution [69]. A complete introduction of the Kalman filter can be found in [99]. Consider a linear discrete-time invariant system:

  $$\begin{cases} x_k = Ax_{k-1} + Bu_{k-1} + \omega_{k-1} \\ y_k = Cx_k + v_k \end{cases} \tag{4.4}$$

  where ω_k and v_k represent the process and the measurement noises, respectively. These disturbances and noises are assumed to be independent, zero mean, with normal distribution and covariance Q, R

[1] The discrete-model is chosen due to its facility when systems are controlled via computer.

($\omega_k \sim N(0, Q)$, $v_k \sim N(0, R)$). The Kalman filter is simply an optimal stochastic recursive estimator. At each time instant, it offers the value of the estimated state $\hat{x}_k$ and the error covariance matrix P_k which is a measure of the estimated accuracy of the estimated state. This is divided into two steps: prediction and update. The prediction step uses the estimated state at the previous time instant $\hat{x}_{k-1}$ and the knowledge of the system (the matrices A, B and the input at the previous moment u_{k-1}) to produce a priori state estimation. In the update step, this a priori state estimation is combined with the information from the measurement to obtain a posteriori estimated state. This can be summarized in the following algorithm.

***Algorithm* 4.1.**

1. Prediction step:
   - Compute the a priori state estimation $\bar{x}_k = A\hat{x}_{k-1} + Bu_{k-1}$.
   - Compute the a priori estimation error covariance: $\bar{P}_k = AP_{k-1}A^T + Q$.
2. Update step:
   - Compute the optimal Kalman gain: $K_k = \bar{P}_k C^T (C\bar{P}_k C^T + R)^{-1}$. This gain is determined by minimizing the mean square of the estimation error. The detail of computation can be seen in [99].
   - Update the state estimate $\hat{x}_k = \bar{x}_k + K_k(y_k - C\bar{x}_k)$.
   - Update the estimate error covariance $P_k = (I - K_k C)\bar{P}_k$.

For the interested reader, a toolbox dedicated to this problem is developed. footnotemark . In the parametric uncertainty context, it is well known that the performance of the proposed Kalman filter can be degraded [27]. To ensure the convergence behavior in the presence of modeling error, the robust Kalman filter is proposed, which guarantees a bound of the performance of the Kalman filter [148], [134], [110], [46].

- **Set-membership estimation**: When a system is modeled by the deterministic approach (uncertainties are bounded by some convex sets),

[1]http://www.cs.ubc.ca/ murphyk/Software/Kalman/kalman.html.

the set-membership estimation is a suitable solution for the state estimation problem. This technique has been developed in the last 35 years [147], [126], [20]. The estimator computes at each sample time a set containing all the possible system states that are consistent with the perturbations, the uncertainties and the measurement noise. Based on the prediction and correction step, the procedure of this technique is similar to the Kalman filter. While the Kalman filter deals with the average case, the set-membership estimation considers the worst case. For this reason, this approach is also called the worst-case estimation. The problem of set-membership estimation is that the complexity of this set is increased in time. To overcome this problem, the geometry of these sets has to be fixed a priori: e.g. polytopes (boxes, parallelotopes) [145], [144], [32], [17], [50], [68], [71], [116], [118], [103]; ellipsoids [126], [147], [20], [77], [51], [45], [113], [14], [13], [15]; zonotopes [115], [37], [2], [3], [82]. Polytopes which were presented in the previous chapter offer a good quality of approximation. In the linear context, polytopes can be used for an exact representation of the variation domains of the system state. However efficient results may be obtained only for a reasonable number of vertices of the polytopes [145]. Due to the low complexity, ellipsoids have been used by many authors but their limited flexibility can lead to a conservative result of estimation. As presented in the previous chapter, zonotopes which are used in many automatic control applications such as reachability analysis [7], collision detection [59], identification [25], state estimation [115], [37], [2], [3], fault detection [58], [66], [137] and fault diagnosis [40] offer a good compromise between the complexity and the flexibility. Moreover, the author of [75] shows that, by using zonotopes, the wrapping effect is reduced leading to a more precise result of the estimation. As the deterministic approach is chosen to describe the modeling of the system, the set-membership estimation is considered as a suitable solution. In the next section, zonotopes are chosen to represent the set of all the possible system states in the context of set-membership estimation due to their advantages in comparison with other geometrical forms.

4.2 Problem formulation

To simplify the manuscript, the following linear discrete-time autonomous system is considered (this system can be easily generalized to controlled sys-

tem):

$$\begin{cases} x_{k+1} = Ax_k + \omega_k \\ y_k = Cx_k + v_k \end{cases} \tag{4.5}$$

where $x_k \in \mathbb{R}^{n_x}$ is the state of the system, $y_k \in \mathbb{R}^{n_y}$ is the measured output at sample time k, the matrices A and C have appropriate dimensions $A \in \mathbb{R}^{n_x \times n_x}$, $C \in \mathbb{R}^{n_y \times n_x}$ and this couple (C,A) is detectable. The vector $\omega_k \in \mathbb{R}^{n_x}$ represents the state perturbation vector and $v_k \in \mathbb{R}^{n_y}$ is the measurement perturbation (noise, offset, etc.). It is assumed that the uncertainties and the initial state are bounded by zonotopes: $\omega_k \in W, v_k \in V$ and the initial state belongs to a zonotope $x_0 \in X_0$ which can be large due to the lack of knowledge on the system. The two zonotopes W and V are supposed to be centered at the origin; if this assumption is not satisfied an appropriate change of coordinates can be used to bring the center of the zonotopes to the origin.

Consider the mathematical model (4.5) and these assumptions, the set-membership estimation technique leads to compute at each sample time k a domain of all the possible values of the unknown state x_k. Similar to the Kalman filter, the set-membership estimation algorithm is based on 3 steps: prediction, measurement and correction [2]. The guaranteed state estimation is obtained in the correction step which is the combination of the state information from the prediction and the information from the measurement. Before detailing this algorithm, some useful notations will be defined.

***Definition* 4.1.** Given the system (4.5) and a measured output y_k, the *measurement consistent state set* at time instant k (the state set which is consistent with the measured output y_k) is defined as $X_{y_k} = \{x \in \mathbb{R}^n : (y_k - Cx) \in V\}$.

***Definition* 4.2.** Consider the system (4.5). The *exact uncertain state set* $X_k = (AX_{k-1} \oplus W) \cap X_{y_k}$, $k \geq 1$ is equal to the set of states that are consistent with the measured output and the initial state set X_0.

Thus, the exact uncertain state set X_k contains all the possible values of the system state consistent with the measurement. In practice, the computation of the exact uncertain state set is difficult. Even if X_{k-1} is assumed to have a particular geometrical form (for example: zonotope, ellipsoid etc.), it is not sure that at time instant k the exact uncertain state set X_k has the same form. For this reason, in practice this set is approximated by an outer bound (the zonotopic set will be used along this PhD thesis). The following hypotheses are considered at the time instant k:

[2] In the Kalman filter, the measurement step is included in the correction step, in the set-membership algorithm it is clear-cut for a better understanding.

- An outer bound of the exact uncertain state set, denoted $\hat{X}_{k-1}$, is available.
- An output measurement y_k is obtained.

Under these assumptions, a zonotopic outer bound $\hat{X}_k$ of the exact uncertain state set X_k can be estimated using the following algorithm.

***Algorithm* 4.2.**

1. *Prediction step*: Given the system (4.5), compute a zonotope $\bar{X}_k = A\hat{X}_{k-1} \oplus W$ (denoted *predicted state set*) that offers a bound for the uncertain trajectory of the system.
2. *Measurement step*: Compute the *measurement consistent state set* X_{y_k} using the measurement y_k.
3. *Correction step*: Compute an outer approximation $\hat{X}_k$ (denoted *guaranteed state estimation set*) of the intersection between X_{y_k} and $\bar{X}_k$.

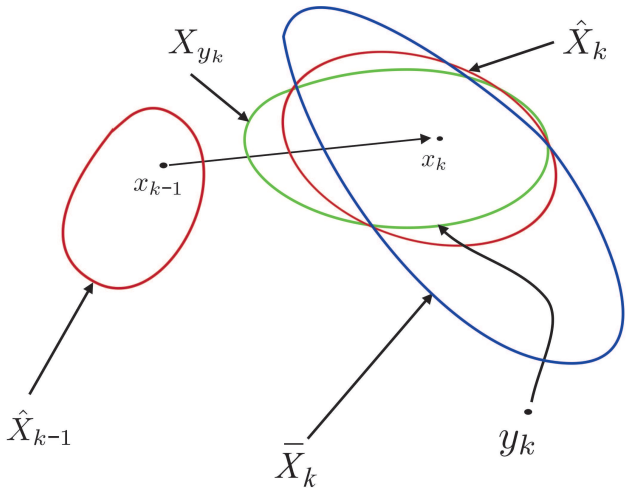

Figure 4.1: Set-membership estimation algorithm

The general case of the proposed algorithm is illustrated in Figure 4.1. At the time instant k, from the known guaranteed state estimation $\hat{X}_{k-1}$ (the

red set), the predicted state set $\bar{X}_k$ (the blue set) is determined. This set is intersected with the measurement consistent state set X_{y_k} (the green set) which is induced by the output measurement y_k. Thus, at time instant k the guaranteed state estimation $\hat{X}_k$ (the red set) is the outer approximation of this intersection.

To obtain a zonotope bounding the uncertain trajectory of the system in step 1 of Algorithm 4.2, Properties 1.1 and 1.2 are used. The predicted state set computation using zonotopes relies on a simple matrix computation and is not subject to any approximation. However, this computation increases the order of the zonotope at each step. In order to control the domain complexity, a reduction step is implemented to bound a high-order zonotope by a lower-order zonotope using the complexity reduction method presented in Chapter 3.

In the literature, there are several authors interested in this estimation problem [37], [38], [39], [2], [3]. In the linear context, the step 1 of the Algorithm 4.2 is similar in these methods. Based on different methods to realize the correction step (the intersection between the predicted state set and the measurement consistent state set), two different approaches presented in the literature will be further detailed: the Singular Value Decomposition-based method [37], the optimization-based method [2].

4.2.1 Singular Value Decomposition-based method

This method was firstly proposed in [37]. The zonotope bounding the disturbance is supposed to be a centered zonotope represented by $W = F\mathbf{B}^{n_x}$. In this presented method, the measurement noise is supposed to belong to a centered parallelotope V, which can be described by $V = \Sigma\mathbf{B}^{n_y}$, with $\Sigma \in \mathbb{R}^{n_y \times n_y}$ an invertible matrix. With these notations, at each sample time k there exists a vector $b_k \in \mathbf{B}^{n_y}$ such that the measurement noise at time instant k is computed by $v_k = \Sigma b_k$.

Let us suppose that at the time instant k the zonotopic guaranteed state estimation at $k-1$ is available: $\hat{X}_{k-1} = \hat{p}_{k-1} \oplus \hat{H}_{k-1}\mathbf{B}^r$, $r \in \mathbb{R}^+$. Using the mathematical model, the predicted state set $\bar{X}_k$ in the first step of Algorithm 4.2, which contains the real state x_k, can be computed by:

$$\begin{aligned}\bar{X}_k &= A\hat{X}_{k-1} \oplus W \\ &= A(\hat{p}_{k-1} \oplus \hat{H}_{k-1}\mathbf{B}^r) \oplus F\mathbf{B}^{n_x} \\ &= A\hat{p}_{k-1} \oplus A\hat{H}_{k-1}\mathbf{B}^r \oplus F\mathbf{B}^{n_x} \\ &= A\hat{p}_{k-1} \oplus \begin{bmatrix} A\hat{H}_{k-1} & F \end{bmatrix} \mathbf{B}^{r+n_x} \\ &= \bar{p}_k \oplus \bar{H}_k\mathbf{B}^{r+n_x}\end{aligned} \tag{4.6}$$

with $\bar{p}_k = A\hat{p}_{k-1}$ and $\bar{H}_k = \begin{bmatrix} A\hat{H}_{k-1} & F \end{bmatrix}$.

***Remark* 4.1.** From further on, in this chapter, the notation $\hat{*}$ will be used to specify the estimation of $*$ and $\bar{*}$ will be used for the prediction of $*$.

The guaranteed state estimation is obtained from the intersection between the measurement consistent state set X_{y_k} and the predicted state set $\bar{X}_k$. The method proposed in [37] considers a slightly different approach in which the measurement consistent state set X_{y_k} is not explicitly computed. This method consists in decomposing the extended space $\mathbb{R}^{r+n_x}$ (called *abstract space* in [37]) of $\bar{X}_k$ into two complementary sub-spaces using the singular value decomposition: one sub-space is influenced by the measurement, while the other sub-space is not influenced. Uniquely the outer approximation in the sub-space containing the information coming from the measurement is considered.

A prediction of the measurement at time instant k can be obtained from the center of $\hat{X}_{k-1}$:

$$\bar{y}_k = C\bar{p}_k \tag{4.7}$$

The real measurement is given from (4.5):

$$y_k = Cx_k + \Sigma b_k \tag{4.8}$$

The difference between y_k and $\bar{y}_k$ reflects the supplementary information coming from the measurement.

$$y_k - \bar{y}_k = C(x_k - \bar{p}_k) + \Sigma b_k \tag{4.9}$$

As Σ is an invertible matrix, by multiplying (4.9) with Σ^{-1} this is equivalent to:

$$\Sigma^{-1}(y_k - \bar{y}_k) = \Sigma^{-1}C(x_k - \bar{p}_k) + b_k \tag{4.10}$$

Denote $\eta = \Sigma^{-1}(y_k - \bar{y}_k)$ and $M = \Sigma^{-1}C$. Because the real state x_k belongs to the predicted state set $\bar{X}_k$ formulated by (4.6), there exists a value $s \in \mathbf{B}^{r+n_x}$

such that $x_k = \bar{p}_k + \bar{H}_k s$. Thus, the following equation is verified:

$$\begin{aligned} \eta - b_k &= M(x_k - \bar{p}_k) \\ &= M(\bar{p}_k + \bar{H}_k s - \bar{p}_k) \\ &= M\bar{H}_k s \end{aligned} \tag{4.11}$$

***Remark* 4.2.** The correction step focuses on the outer approximation of the intersection between $\mathbf{B}^{r+n_x}$ and the domain of possible values of s resulting from the measurement equation (4.8).

The procedure proposed in [37] for computing the zonotopic guaranteed state estimation is based on the Singular Value Decomposition (SVD) of the matrix resulted from the product $M\bar{H}_k \in \mathbb{R}^{n_y \times (r+n_x)}$.

Find the Singular Value Decomposition of $M\bar{H}_k$:

$$M\bar{H}_k = USV^T = \begin{bmatrix} U_1 & U_0 \end{bmatrix} \begin{bmatrix} S_1 & 0 \\ 0 & 0 \end{bmatrix} \begin{bmatrix} V_1^T \\ V_0^T \end{bmatrix} \tag{4.12}$$

with $U^T U = I$ and $V^T V = I$ and S_1 a diagonal matrix with non-zero elements which are the singular values of $M\bar{H}_k$.

The initial measurement space is generated by U_0 and U_1 and the abstract space is generated by V_0 and V_1 [37]. The sub-space generated by V_0 is the kernel of $M\bar{H}_k$ and is not influenced by the output measurement. The sub-space influenced by the output measurement is generated by V_1.

In fact, V_0 and V_1 are the new base and, thus, in the new base, the vector s can be decomposed as:

$$s = V_0\delta_0 + V_1\delta_1 \tag{4.13}$$

and $\delta_0 = V_0^T s$, $\delta_1 = V_1^T s$ with δ_0, δ_1 the coordinate of s in the new base. With these new notations, the equation (4.11) is equivalent to:

$$\eta - b_k = M\bar{H}_k(V_0\delta_0 + V_1\delta_1) \tag{4.14}$$

Replace $M\bar{H}_k$ by its Singular Value Decomposition leads to:

$$\eta - b_k = U_1 S_1 V_1^T (V_0\delta_0 + V_1\delta_1) \tag{4.15}$$

From the expressions $U^T U = I$, $V^T V = I$, it leads to $U_1^T U_1 = I$, $V_0^T V_0 = I$, $V_1^T V_1 = I$, $V_1^T V_0 = 0$, $V_0^T V_1 = 0$. Thus, the equation (4.15) is equivalent to:

$$\delta_1 = S_1^{-1} U_1^T \eta - S_1^{-1} U_1^T b_k \tag{4.16}$$

Because b_k is an interval vector, from the definition of zonotope, a sufficient condition for the equation (4.16) or (4.11) is the following:

$$\delta_1 \in Z_1 = Z(S_1^{-1} U_1^T \eta; S_1^{-1} U_1^T) \tag{4.17}$$

From the equation (4.13), the images of s in the sub-space generated by V_1 and the sub-space generated by V_0 are shown by:

$$\delta_1 \in Z(0; V_1^T), \delta_0 \in Z(0; V_0^T) \tag{4.18}$$

Combining the results of (4.17) and (4.18), it leads to:

$$\delta_1 \in Z_1 \cap Z(0; V_1^T), \delta_0 \in Z(0; V_0^T) \tag{4.19}$$

The next step consists in finding the outer approximation of the intersection between Z_1 and $Z(0; V_1^T)$. This can be computed as the intersection of the interval hulls of the two zonotopes Z_1 and $Z(0; V_1^T)$ (i.e. the intersection of two boxes) which is an easy work:

$$Z(p_{temp}; H_{temp}) = Z(S_1^{-1} U_1^T \eta; rs(S_1^{-1} U_1^T)) \cap Z(0; rs(V_1^T)) \tag{4.20}$$

Coming back in the abstract space (4.13), the approximation of s can be done by combining the information from (4.19) and (4.20):

$$s \in Z(V_1 p_{temp}; \begin{bmatrix} V_1 H_{temp} & V_0 V_0^T \end{bmatrix}) \tag{4.21}$$

Thus the guaranteed state estimation at time instant k is determined by:

$$\hat{X}_k = Z(\bar{p} + \bar{H}_k V_1 p_{temp}; \begin{bmatrix} \bar{H}_k V_1 H_{temp} & \bar{H}_k V_0 V_0^T \end{bmatrix}) \tag{4.22}$$

Detailed explanations about this algorithm can be found in [37], [39]. An improved version of this algorithm which consists in replacing the intersection of two boxes (4.20) by a zonotopic outer approximation of the intersection between two zonotopes is presented in [38]. The singular decomposition method permits to rapidly obtain a guaranteed state estimation but it can not guarantee that the size of this guaranteed state estimation is optimized. For this reason, another method based on the solution of an optimization problem is presented in the next subsection.

4.2.2 Optimization based method

This method presented in [2] is based on the zonotopic approximation of the intersection between a zonotope and a strip. The algorithm presented in [2] is developed for single output systems($n_y = 1$ in (4.5)). The disturbances are bounded by a centered zonotope $W = F\mathbf{B}^{n_x}$. The measurement noise is supposed to belong to a centered interval $V = \sigma\mathbf{B}^1$, $\sigma \in \mathbb{R}^+$. With this assumption, from the mathematical model (4.5) the output measurement can be written in the form $y_k = c^T x_k + v_k$, with $v_k \in V$ and $c^T \in \mathbb{R}^{1 \times n_x}$.

Suppose the guaranteed state estimation at time instant $k-1$ is known at time instant k ($\hat{X}_{k-1} = \hat{p}_{k-1} \oplus \hat{H}_{k-1}\mathbf{B}^r$). Similar to (4.6) the predicted state set is determined as :

$$\bar{X}_k = A\hat{p}_{k-1} \oplus \begin{bmatrix} A\hat{H}_{k-1} & F \end{bmatrix} \mathbf{B}^{r+n_x} = \bar{p}_k \oplus \bar{H}_k \mathbf{B}^{r+n_x} \tag{4.23}$$

In this case the measurement consistent state set is computed as a strip:

$$X_{y_k} = \{|c^T x - y_k| \leq \sigma\} \tag{4.24}$$

The guaranteed state estimation $\hat{X}_k$ can be obtained by intersecting the predicted state set $\bar{X}_k$ with the measurement consistent state set X_{y_k}. As $\bar{X}_k$ is a zonotope and X_{y_k} is a strip, it is convenient to obtain a zonotopic outer bound of the intersection of a zonotope and a strip. The following proposition provides a family of zonotopes (parameterized by a vector λ) that contains the intersection of a zonotope and a strip. Denoting that this method can be extended to the case of Multi-Output systems by considering each measurement gives us a strip in the state-space, then the guaranteed state estimation is obtained by repeating the intersection with each strip of measurement.

***Proposition* 4.1.** ([2]). Given the zonotope $Z = p \oplus H\mathbf{B}^r \subset \mathbb{R}^n$, the strip $S = \{x \in \mathbb{R}^n : |c^T x - d| \leq \sigma\}$ and the vector $\lambda \in \mathbb{R}^n$, define:

- a vector $\hat{p}(\lambda) = p + \lambda(d - c^T p) \in \mathbb{R}^n$;
- a matrix $\hat{H}(\lambda) = [(I - \lambda c^T)H \ \sigma\lambda] \in \mathbb{R}^{n \times (r+1)}$;

then the following expression holds $Z \cap S \subseteq \hat{Z}(\lambda) = \hat{p}(\lambda) \oplus \hat{H}(\lambda)\mathbf{B}^{r+1}$.

Proof Given an element $x \in Z \cap S$, on one hand this means that $x \in Z = p \oplus H\mathbf{B}^r$. Using the definition of a m-zonotope implies that there exists a vector $s \in \mathbf{B}^r$ such that:

$$x = p + Hs \tag{4.25}$$

Adding and subtracting $\lambda c^T Hs$ to the previous equality leads to the following expression:

$$x = p + \lambda c^T Hs + (I - \lambda c^T)Hs \tag{4.26}$$

On the other hand, $x \in Z \cap S$ leads to $x \in S = \{x \in \mathbb{R}^n : |c^T x - d| \leq \sigma\}$. Thus, there exists a value $\alpha \in [-1; 1]$ such that $c^T x - d = \sigma\alpha$. Taking into account the form of the vector x given by (4.25) leads to $c^T(p + Hs) - d = \sigma\alpha$, which is equivalent to $c^T Hs = d - c^T p + \sigma\alpha$. Substituting $c^T Hs$ in equation (4.26), the following expression is obtained:

$$\begin{aligned} x &= p + \lambda(d - c^T p + \sigma\alpha) + (I - \lambda c^T)Hs \\ &= p + \lambda(d - c^T p) + \lambda\sigma\alpha + (I - \lambda c^T)Hs \end{aligned} \tag{4.27}$$

After simple computations and using the notation defined in Proposition 4.1, the following form is obtained:

$$x = \hat{p}(\lambda) + \begin{bmatrix}(I - \lambda c^T)H & \sigma\lambda\end{bmatrix} \begin{bmatrix}s \\ \alpha\end{bmatrix} = \hat{p}(\lambda) \oplus \hat{H}(\lambda) \begin{bmatrix}s \\ \alpha\end{bmatrix} \tag{4.28}$$

and the following inclusion holds:

$$x = \hat{p}(\lambda) \oplus \hat{H}(\lambda) \begin{bmatrix}s \\ \alpha\end{bmatrix} \in \hat{p}(\lambda) \oplus \hat{H}(\lambda)\mathbf{B}^{r+1} = \hat{Z}(\lambda). \tag{4.29}$$

□

Using Proposition 4.1, the guaranteed state estimation at time instant k, is the outer approximation of $\bar{X}_k \cap X_{y_k}$, formulated by:

$$\hat{X}_k(\lambda) = \hat{p}_k(\lambda) \oplus \hat{H}_k(\lambda)\mathbf{B}^{r+n_x+1} \tag{4.30}$$

with $\hat{p}_k(\lambda) = A\hat{p}_{k-1} + \lambda(y_k - c^T A\hat{p}_{k-1})$
and $\hat{H}_k(\lambda) = \begin{bmatrix}(I - \lambda c^T)A\hat{H}_{k-1} & (I - \lambda c^T)F & \sigma\lambda\end{bmatrix}$.

This equation describes a family of zonotopes parameterized by the vector λ, which bounds the intersection between $\bar{X}_k$ and a X_{y_k}. The vector λ is then determined in order to optimize the size of this zonotope $\hat{X}_k(\lambda)$. In the following, two size-based criteria developed in [2] to compute λ will be presented: the minimization of the segments of the zonotope $\hat{X}_k(\lambda)$ and the minimization of the volume of the zonotope $\hat{X}_k(\lambda)$.

4.2.2.1 Minimizing the segments of the zonotope

In this approach proposed in [2], the vector λ is computed such that the Sum Of Squares (SOS) of the generators of the zonotope $\hat{X}(\lambda)$ is minimized (i.e. the SOS of the segments of the zonotope). This is equivalent to minimize the Frobenius norm of the matrix $\hat{H}(\lambda)$. It is convenient to decompose this matrix in the following form [2]:

$$\hat{H}(\lambda) = M + \lambda a^T \tag{4.31}$$

with $M = \begin{bmatrix}H & 0\end{bmatrix}$, $a^T = \begin{bmatrix}-c^T H & \sigma\end{bmatrix}$.

The Frobenius norm of $\hat{H}(\lambda)$ is computed by:

$$\begin{aligned}\|\hat{H}(\lambda)\|_F^2 &= \|M + \lambda a^T\|_F^2 \\ &= tr((M^T + a\lambda^T)(M + \lambda a^T)) \\ &= tr(M^T M) + tr(a\lambda^T M) + tr(M^T \lambda a^T) + tr(a\lambda^T \lambda a^T) \\ &= 2\lambda^T M a + a^T a \lambda^T \lambda + tr(M^T M)\end{aligned} \tag{4.32}$$

The minimum of $\|\hat{H}(\lambda)\|_F^2$ is obtained when $\frac{d\|\hat{H}(\lambda)\|_F^2}{d\lambda} = 0$. This means that:

$$\frac{d(2\lambda^T Ma + a^T a\lambda^T\lambda + tr(M^T M))}{d\lambda} = 0 \tag{4.33}$$

or:

$$2Ma + 2a^T a\lambda^* = 0 \tag{4.34}$$

The optimal value of vector λ is then computed by:

$$\begin{aligned} \lambda^* &= \frac{-Ma}{a^T a} \\ &= \frac{HH^T c}{c^T HH^T c + \sigma^2} \end{aligned} \tag{4.35}$$

This method permits a fast computation of the vector λ which can be used in fast real-time systems; however the result of approximation is sometimes conservative as illustrated in [2].

4.2.2.2 Minimizing the volume of the intersection

In order to improve the performance of the guaranteed state estimation, another criterion is proposed. The vector λ is determined such that the volume of the zonotope $\hat{X}(\lambda)$ is minimized. The volume of a zonotope $Z = p \oplus H\mathbf{B}^m \in \mathbb{R}^n$, with $m \geq n$ is given by the following formula [132], [105]:

$$Vol(Z) = 2^n \sum_{i=1}^{\binom{n}{m}} |det\left[H_{s_1(i)} \quad H_{s_2(i)} \quad \dots \quad H_{s_n(i)}\right]| \tag{4.36}$$

with $\binom{n}{m}$ the number of all the different ways of choosing n elements between m elements, H_i the ith column of H and $s_j(i)$ ($j = 1, \dots, n$ and $i = 1, \dots, \binom{n}{m}$) denotes each one of different ways of choosing n elements from a set of m. These integers satisfy $1 \leq s_1(i) < s_2(i) < \dots < s_n(i) \leq m$.

Using this formula to compute the volume of the zonotope $\hat{X}_k(\lambda) =$

$\hat{p}_k(\lambda) \oplus \hat{H}_k(\lambda)\mathbf{B}^{r+n_x+1}$ leads to:

$$\begin{aligned} Vol(\hat{X}_k(\lambda)) = 2^{n_x} \sum_{i=1}^{\binom{n_x}{r+n_x}} |1 - c^T\lambda||det(D_i)| + \\ +2^{n_x} \sum_{i=1}^{\binom{n_x-1}{r+n_x}} \sigma|det\begin{bmatrix} E_i & q_i \end{bmatrix}||q_i^T\sigma| \end{aligned} \tag{4.37}$$

where D_i is each of different matrices obtained by choosing n_x columns of matrix $\bar{H}_k$, E_i is each of different matrices obtained by choosing $n_x - 1$ columns of matrix $\bar{H}_k$ and q_i is orthonormal to $\mathrm{Im}(E_i)$ with $q_i^T q_i = 1$ and $q_i^T E_i = 0$. The proof of this formula is presented in [2].

The vector λ is chosen to minimize the volume of the zonotope computed by (4.37). As the volume of $\hat{X}_k(\lambda)$ is a convex function of λ, the optimal vector λ^* which minimizes the volume of $\hat{X}_k(\lambda)$ can be found by solving a convex optimization problem. This volume based criterion gives an improved result of the approximation in comparison to the segment based criterion. But the complexity of the equation (4.37) leads to a considerable increase of the computation time. Moreover, minimizing the volume of the zonotope can lead to a very narrow zonotope (i.e. the uncertainty in some directions can remain extremely large, even when the volume of the zonotope tends to zero). For these reasons, in the next section an original approach will be proposed, permitting to obtain a good result with a low complexity.

4.3 Minimizing the P-radius of the guaranteed state estimation

These presented approaches have their advantages and their drawbacks. The Singular Value Decomposition method and the minimization of the volume of the zonotope lead to a good result with a complex online computation. The minimization of the segments of the zonotope offers a fast online computation time with a conservative result. For these reasons, a major challenge is to design an efficient algorithm that has reasonable complexity and precision and can be used not only for Single-Output systems but also Multi-Output systems in the context of systems with interval uncertainties.

This section presents an original approach to obtain the guaranteed state estimation based on the minimization of the P-radius of the zonotopic guar-

anteed state estimation which will be defined in the next paragraph, offering good trade-off between performance and low complexity when computing an outer approximation of the exact uncertain state set using the zonotope-based procedure proposed by Algorithm 4.2. The complex online computation of the Singular Value Decomposition method and the minimization of the volume of the zonotope are replaced by an optimization problem solved off-line. Moreover, this P-radius based method permits to guarantee the non-increasing of the zonotopic guaranteed state estimation. The method is developed in a first time for single-output systems. Two different cases of the Single-Output linear discrete time systems (4.5) are analyzed: a known evolution matrix A and a matrix $[A]$ with coefficients subject to interval uncertainties, respectively. A generalization to uncertain Multi-Output systems is also proposed. Before detailing the proposed method, the definition of the P-radius is presented as follows.

***Definition* 4.3.** The *P-radius* of a zonotope $Z = p \oplus H\mathbf{B}^m$ is defined by the following expression:

$$L = \max_{z \in Z}(\|z - p\|_P^2) \tag{4.38}$$

where P is a symmetric and positive definite matrix ($P = P^T \succeq 0$).

This notation gives us a new criterion to value the quality of the estimation. A small value of P-radius signifies a good quality of the estimation. The P-radius definition is illustrated in Figure 4.2. This figure shows a centered red zonotope Z_1 constructed by a linear image of a centered cube ($p_1 = \begin{bmatrix}0\\0\end{bmatrix}$) in $\mathbb{R}^2$, with $H_1 = \begin{bmatrix}1 & 2 & 3\\3 & 2 & 1\end{bmatrix}$, and a centered blue zonotope constructed by $p_2 = \begin{bmatrix}0\\0\end{bmatrix}$, $H_2 = \begin{bmatrix}1 & 0.4 & 3\\3 & 0.2 & 1\end{bmatrix}$. The associated P-radius of these two zonotopes are $L_1 = \max(\|z\|_P^2) = 72$, with $z \in Z_1 = p_1 \oplus H_1\mathbf{B}^3$, $L_2 = \max(\|z\|_P^2) = 37$, with $z \in Z_2 = p_2 \oplus H_2\mathbf{B}^3$ and $P = \begin{bmatrix}1 & 0\\0 & 1\end{bmatrix}$. The associated P-radius of Z_1 is related to the red ellipsoid $x^T P x \leq L_1$, and the associated P-radius of Z_2 is related to the blue ellipsoid $x^T P x \leq L_2$. From this figure, it can be seen that if the zonotope is large, then the value of its P-radius and its related ellipsoid are large and vice versa. The latter is introduced to characterize the zonotope size by the associated P-radius that is more convenient than the criteria used in different approaches (e.g. in the segment minimization method or in the volume minimization method).

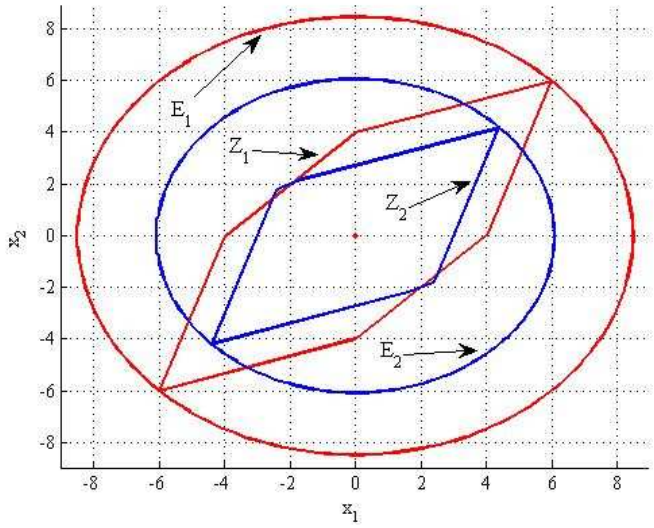

Figure 4.2: Zonotopes and ellipsoids related to the associated P-radius

4.3.1 Linear Time Invariant Single-Output systems

In this subsection, the P-radius based method is developed for linear discrete-time invariant Single-Output systems with a fixed known A matrix: [3]

$$\begin{cases} x_{k+1} = Ax_k + \omega_k \\ y_k = c^T x_k + v_k \end{cases} \tag{4.39}$$

The disturbance is bounded by a centered zonotope $\omega_k \in W = F\mathbf{B}^{n_x}$ and the measurement noise is bounded by a centered interval $v_k \in V = \sigma\mathbf{B}^1 \subset \mathbb{R}$ with $\sigma \in \mathbb{R}^+$. The aim is to find a zonotopic guaranteed state estimation at each sample time. Similar to the previous presented method, this set is the outer approximation of the intersection of the two sets X_{y_k} and $\bar{X}_k$. With the definition of V, the measurement consistent state set at time k is defined as a strip: $X_{y_k} = \{x \in \mathbb{R}^n : |c^T x - y_k| \leq \sigma\}$. As $\bar{X}_k$ is a zonotope and X_{y_k} is a strip, a family of zonotopes (parameterized by a vector λ) which contains the intersection between $\bar{X}_k$ and X_{y_k} is computed using Proposition 4.1. The idea is to find the value of this vector λ that minimizes the size of the zonotopic approximation based on the P-radius minimization criterion in order to overcome the drawbacks of the previous methods proposed in [2], [37].

[3] This is a particular case of (4.5).

Supposing an outer approximation of the state set $\hat{X}_{k-1} = \hat{p}_{k-1} \oplus \hat{H}_{k-1}\mathbf{B}^r$ at the time instant $k-1$ and the measured output y_k at the time instant k, the predicted state set $\bar{X}_k$ and the guaranteed state estimation are obtained similar to the previous two optimization based methods:

$$\bar{X}_k = A\hat{p}_{k-1} \oplus \begin{bmatrix} A\hat{H}_{k-1} & F \end{bmatrix} \mathbf{B}^{r+n_x} = \bar{p}_k \oplus \bar{H}_k \mathbf{B}^{r+n_x} \tag{4.40}$$

$$\hat{X}_k(\lambda) = \hat{p}_k(\lambda) \oplus \hat{H}_k(\lambda)\mathbf{B}^{r+n_x+1} \tag{4.41}$$

with $\hat{p}_k(\lambda) = A\hat{p}_{k-1} + \lambda(y_k - c^T A\hat{p}_{k-1})$
and $\hat{H}_k(\lambda) = \begin{bmatrix} (I-\lambda c^T)A\hat{H}_{k-1} & (I-\lambda c^T)F & \sigma\lambda \end{bmatrix}$.

Denote the P-radius of the state estimation set at the time instant k by $L_k = \max_{x \in \hat{X}_k}(\|x - \hat{p}_k\|_P^2)$. From the definition of the guaranteed state estimation $\hat{X}_k$ in (4.41), it can be rewritten like $L_k = \max_{\hat{z}} \|\hat{H}_k(\lambda)\hat{z}\|_P^2$, with $\hat{z} \in \mathbf{B}^{r+n_x+1}$.

***Proposition* 4.2.** A symmetric positive definite matrix $P = P^T \succ 0$ and a vector λ can be computed such that at each sample time the P-radius of the zonotopic state estimation set $\hat{X}_k$ is not increased, more precisely the value of L_k. This means that the zonotopic state estimation set is non-increasing in time.

This proposition on the non-increasing condition of the P-radius can be visualized in Figure 4.3 where the blue zonotope is the guaranteed state estimation at each iteration and the red ellipsoid $\|x - \hat{p}_k\|_P^2 \leq L_k$ is related to the P-radius of the zonotopic state estimation set $\hat{X}_k$. Namely, the reader should not fear the fact that the zonotope is partially out of the ellipsoid because this ellipsoid is only a criterion to characterize the size of the zonotope.

A constructive proof of Proposition 4.2 is presented in the following. The non-increase of the P-radius can be expressed by a mathematical formulation as follows. The contractiveness of the P-radius, L_k is ensured by the expression $L_k \leq \beta L_{k-1}$, with $\beta \in (0,1)$. Due to the presence of disturbances and measurement noise, this condition is difficult to verify. A relaxation of this condition can be $L_k \leq \beta L_{k-1} + \epsilon$, where ϵ is a positive constant which permits to bound the influence of disturbances and measurement noises. For $\epsilon = \max_s \|Fs\|_2^2 + \sigma^2$, this leads to the following inequality:

$$L_k \leq \beta L_{k-1} + \max_s \|Fs\|_2^2 + \sigma^2 \tag{4.42}$$

with $\beta \in (0,1)$ and $\max_s \|Fs\|_2^2 + \sigma^2 > 0$.

This inequality can be rewritten in an equivalent form:

$$\max_{\hat{z}} \|\hat{H}_k(\lambda)\hat{z}\|_P^2 \leq \max_z \beta \|\hat{H}_{k-1}z\|_P^2 + \max_s \|Fs\|_2^2 + \sigma^2 \tag{4.43}$$

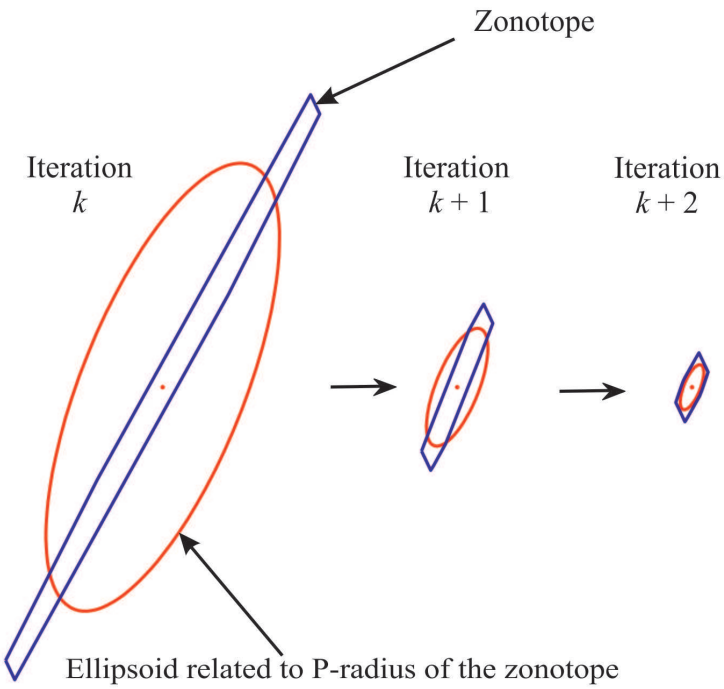

Figure 4.3: Evolution of the guaranteed state estimation

with $\hat{z} = \begin{bmatrix} z^T & s^T & \eta^T \end{bmatrix}^T \in \mathbf{B}^{r+n_x+1}$, $z \in \mathbf{B}^r$, $s \in \mathbf{B}^{n_x}$, $\eta \in \mathbf{B}^1$, and $\beta \in (0,1)$.

Using the reverse triangle inequality [44] leads to a sufficient condition for (4.43):

$$\max_{\hat{z}} (\|\hat{H}_k(\lambda)\hat{z}\|_P^2 - \beta\|\hat{H}_{k-1}z\|_P^2 - \|Fs\|_2^2 - \sigma^2) \leq 0 \tag{4.44}$$

This is equivalent to the following inequality:

$$\hat{z}^T\hat{H}_k^T(\lambda)P\hat{H}_k(\lambda)\hat{z} - \beta z^T\hat{H}_{k-1}^T P\hat{H}_{k-1}z - s^TF^TFs - \sigma^2 \leq 0, \quad \forall z, s, \eta \tag{4.45}$$

Because $\eta \in \mathbf{B}^1$, which is equivalent to $|\eta| \leq 1$, the following expression is obtained:

$$\sigma^2(1 - \eta^2) \geq 0 \tag{4.46}$$

Adding this positive term to the left-side of (4.45) leads to the following sufficient condition for (4.45):

$$\begin{aligned} \hat{z}^T\hat{H}_k^T(\lambda)P\hat{H}_k(\lambda)\hat{z} - \beta z^T\hat{H}_{k-1}^T P\hat{H}_{k-1}z - s^TF^TFs - \sigma^2 + \\ + \sigma^2(1 - \eta^2) \leq 0, \quad \forall z, s, \eta \end{aligned} \tag{4.47}$$

Right multiplying the expression of $\hat{H}_k$ in (4.41) with the explicit form of $\hat{z}$ leads to:

$$\hat{H}_k(\lambda)\hat{z} = (I - \lambda c^T)(A\hat{H}_{k-1}z + Fs) + \sigma\lambda\eta \tag{4.48}$$

Denote $\theta = \hat{H}_{k-1}z$, then the inequality (4.47) can be written in the matrix formulation:

$$\begin{bmatrix}\theta\\ s\\ \eta\end{bmatrix}^T \begin{bmatrix}A_{11} & A_{12} & A_{13}\\ * & A_{22} & A_{23}\\ * & * & A_{33}\end{bmatrix} \begin{bmatrix}\theta\\ s\\ \eta\end{bmatrix} \leq 0, \quad \forall\theta, s, \eta \tag{4.49}$$

with '$*$' denoting the terms required for the symmetry of the matrix and the following additional notations:

$$\begin{cases} A_{11} = ((I - \lambda c^T)A)^T P(I - \lambda c^T)A - \beta P \\ A_{12} = ((I - \lambda c^T)A)^T P(I - \lambda c^T)F \\ A_{13} = ((I - \lambda c^T)A)^T P\sigma\lambda \\ A_{22} = ((I - \lambda c^T)F)^T P(I - \lambda c^T)F - F^T F \\ A_{23} = ((I - \lambda c^T)F)^T P\sigma\lambda \\ A_{33} = \sigma^2\lambda^T P\lambda - \sigma^2. \end{cases} \tag{4.50}$$

Using the Definition 3.11 of positive definite matrix allows to rewrite (4.49) as:

$$\begin{bmatrix}A_{11} & A_{12} & A_{13}\\ * & A_{22} & A_{23}\\ * & * & A_{33}\end{bmatrix} \preceq 0, \quad \forall \begin{bmatrix}\theta\\ s\\ \eta\end{bmatrix} \neq 0 \tag{4.51}$$

Multiplying (4.51) by -1, this is equivalent to:

$$\begin{bmatrix}-A_{11} & -A_{12} & -A_{13}\\ * & -A_{22} & -A_{23}\\ * & * & -A_{33}\end{bmatrix} \succeq 0, \quad \forall \begin{bmatrix}\theta\\ s\\ \eta\end{bmatrix} \neq 0 \tag{4.52}$$

Using the explicit notations (4.50) and doing some manipulations in (4.52), a matrix inequality is derived as:

$$\begin{bmatrix}\beta P & 0 & 0\\ * & F^T F & 0\\ * & * & \sigma^2\end{bmatrix} - \\ - \begin{bmatrix}(A^T - A^T c\lambda^T)P\\ (F^T - F^T c\lambda^T)P\\ \lambda^T P\sigma\end{bmatrix} P^{-1} \begin{bmatrix}(A^T - A^T c\lambda^T)P\\ (F^T - F^T c\lambda^T)P\\ \lambda^T P\sigma\end{bmatrix}^T \succeq 0 \tag{4.53}$$

Using the Schur complement definition (3.14), the expression (4.53) is equivalent to the following matrix inequality:

$$\begin{bmatrix} \beta P & 0 & 0 & A^TP - A^TcY^T \\ * & F^TF & 0 & F^TP - F^TcY^T \\ * & * & \sigma^2 & Y^T\sigma \\ * & * & * & P \end{bmatrix} \succeq 0 \tag{4.54}$$

with a change of variables $Y = P\lambda$ with $P \in \mathbb{R}^{n_x \times n_x}$, $\lambda \in \mathbb{R}^{n_x}$ and $Y \in \mathbb{R}^{n_x}$.

As the 2-norm is a convex function and W is a convex set, the term $\max_{s \in \mathbf{B}^{n_x}} \|Fs\|_2^2$, can be easily computed using the maximum principle [122]. Thus the value of $\epsilon = \max_s \|Fs\|_2^2 + \sigma^2$ can be obtained. Then the condition (4.42) can be written as $L_k \leq \beta L_{k-1} + \epsilon$. At infinity, this expression is equivalent to:

$$L_\infty = \beta L_\infty + \epsilon \tag{4.55}$$

leading to:

$$L_\infty = \frac{\epsilon}{1-\beta} \tag{4.56}$$

Let us consider an ellipsoid $E = \{x : x^TPx \leq \frac{\epsilon}{1-\beta}\}$ which can be normalized to $E = \{x : x^T \frac{(1-\beta)P}{\epsilon} x \leq 1\}$. This ellipsoid is related to the P-radius of the zonotopic guaranteed state estimation at infinity. To minimize the P-radius (i.e. L_∞) of the zonotope, one can find the ellipsoid of smallest diameter [24]. This leads to solve the following Eigenvalue Problem (EVP):

$\max_{\tau,\beta,P} \tau$

subject to the BMI

$$\frac{(1-\beta)P}{\epsilon} \succeq \tau I_{n_x} \tag{4.57}$$

where $I_{n_x} \in \mathbb{R}^{n_x \times n_x}$ is the identity matrix, $\tau \in \mathbb{R}^+$ and $\beta \in (0,1)$ are scalar. Then the smallest diameter is computed by $\frac{2}{\sqrt{\tau^*}}$ [24].

Finally, to find the values of $P = P^T \succ 0 \in \mathbb{R}^{n_x \times n_x}$ and $\lambda \in \mathbb{R}^{n_x}$ the following optimization problem must be solved:

***Method* 4.1.** $\max_{\tau,\beta,P,Y} \tau$

subject to

$$\begin{cases} \frac{(1-\beta)P}{\epsilon} \succeq \tau I \\ \begin{bmatrix} \beta P & 0 & 0 & A^TP - A^TcY^T \\ * & F^TF & 0 & F^TP - F^TcY^T \\ * & * & \sigma^2 & Y^T\sigma \\ * & * & * & P \end{bmatrix} \succeq 0 \\ \tau > 0 \end{cases} \tag{4.58}$$

***Remark* 4.3.** As β is a scalar variable, this optimization problem can be efficiently solved by using a BMI solver (e.g. *Penbmi* [74]) or by executing a simple search-loop on β leading to a LMI problem. In this optimization problem (4.58), the decision variables are: $P = P^T \in \mathbb{R}^{n_x \times n_x}$, $Y \in \mathbb{R}^{n_x}$, $\beta \in (0,1)$ and $\tau \in \mathbb{R}^+$. Thus, the total number of the scalar decision variables is $\frac{n_x(n_x+1)}{2} + n_x + 2$. The dimensions of the inequalities in (4.58) are $n_x \times n_x$, $(3n_x+1) \times (3n_x+1)$ and 1, respectively.

***Remark* 4.4.** In [85], a modification of the problem (4.58) to avoid solving a BMI optimization problem is presented. Instead of optimizing the value of the P-radius, a minimum value of β is searched which permits to have a maximum decreasing speed of the P-radius. This criterion leads to a new LMI optimization problem based on the bisection algorithm [28] on β:

***Method* 4.2.** $\min\limits_{\beta \in (0,1)} \beta$
such that
$\max\limits_{\tau,P,Y} \tau$
subject to

$$\begin{cases} \frac{(1-\beta)P}{\epsilon} \succeq \tau I \\ \begin{bmatrix} \beta P & 0 & 0 & A^TP - A^TcY^T \\ * & F^TF & 0 & F^TP - F^TcY^T \\ * & * & \sigma^2 & Y^T\sigma \\ * & * & * & P \end{bmatrix} \succeq 0 \\ \tau > 0 \end{cases} \tag{4.59}$$

As β is computed by a bissection algorithm, then it is not a decision variable in (4.59). This means that, in this case, the matrix inequalities (4.59) are LMIs.

In order to better undertand the proposed methods, an illustrative example will be further presented.

***Example* 4.1.** Consider the following linear discrete-time invariant system:

$$\begin{cases} x_{k+1} = \begin{bmatrix} 1 & 1 \\ 0 & 1 \end{bmatrix} x_k + 0.02 \begin{bmatrix} -6 \\ 1 \end{bmatrix} \omega_k \\ y_k = \begin{bmatrix} -2 & 1 \end{bmatrix} x_k + 0.2 v_k \end{cases} \tag{4.60}$$

with $\|v_k\|_\infty \leq 1$, $\|\omega_k\|_\infty \leq 1$. The values of v_k and ω_k are generated by random functions with $Matlab^{®}$. The initial state belongs to the box $3\mathbf{B}^2$. The guaranteed state estimation must be determined at each time instant.

***Remark* 4.5.** The order of the m-zonotopes in each example in this chapter is limited to $m \leq 20$ in the interest of a fast simulation. The over-approximation of a high-order zonotope by a lower-order zonotope is done using Proposition 3.4 with an Euclidean norm based criterion and the box approximation method 3.6.3.1. A system of order 2 is chosen to reduce the complexity of the computation and to facilitate the graphical visualization.

The BMI optimization problem (4.58) in Method 4.1 is solved by two different solvers: the *Penbmi* solver and the LMI solver (*mincx*) of $Matlab^{®}$ with search loop on β (the step on β is 10^{-4}, i.e. $\beta = 10^{-4} : 10^{-4} : 1$) which in this case give the same results with $\beta = 0.4090$, $\lambda = \begin{bmatrix} -0.6205 \\ -0.2842 \end{bmatrix}$. The solution of the optimization problem (4.59) in Method 4.2 gives $\beta = 0.0001$, $\lambda = \begin{bmatrix} -0.7500 \\ -0.4999 \end{bmatrix}$. The number of scalar decision variables in the problems (4.58) and (4.59) is 7 and 6, respectively. The dimension of these matrix inequalities is 2×2, 7×7 and 1, respectively. The estimation performance of Methods 4.1 and 4.2 are compared with the results obtained from the minimization of the segments of a zonotope method and the minimization of the volume of a zonotope method.

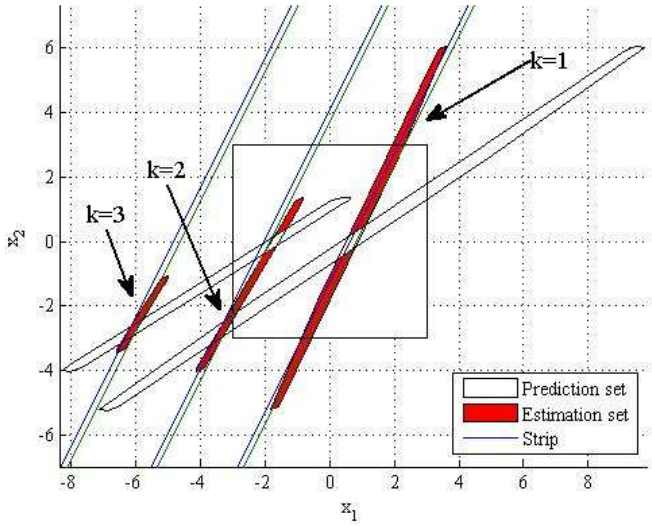

Figure 4.4: Evolution of the guaranteed state estimation by Method 4.1

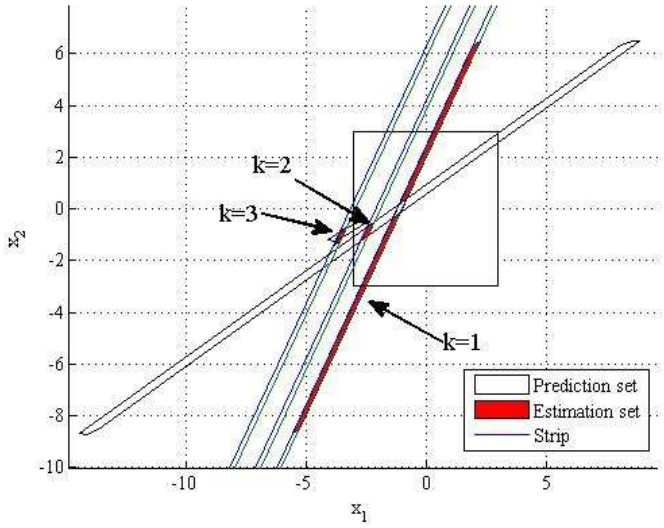

Figure 4.5: Evolution of the guaranteed state estimation by Method 4.2

Figures 4.4 and 4.5 show the evolution of the predicted state set and the outer approximation of state estimation set using Method 4.1 and Method 4.2, respectively. The outer approximations are rapidly reduced at each iteration. The reduction means that the guaranteed state estimation set (an approximation of the real intersection) becomes more and more accurate at each iteration ($k = 1$, $k = 2$, $k = 3$). Comparing these figures shows that the guaranteed state estimation obtained by Method 4.2 is decreased more rapidly than the one obtained by Method 4.1 due to the minimum value of β obtained by Method 4.2.

Figure 4.6 and its zoom (Figure 4.7) show the bounds on x_{2_k} obtained by Method 4.1, Method 4.2 and the two methods developed in [2]. The dash lines show the bounds of x_{2_k} obtained by the segment minimization algorithm. The dash-dot lines represent the bounds of x_{2_k} obtained by the volume minimization algorithm, the solid lines represent the bounds of x_{2_k} obtained by Method 4.1 and the dot lines represent the bounds of x_{2_k} obtained by Method 4.2. The stars represent the real state x_{2_k} of the system. These points are found inside the bounds of x_{2_k} confirming that this bound is well estimated by each method. To compare the performance of these methods, the bound's width of states will be analyzed in the next figures.

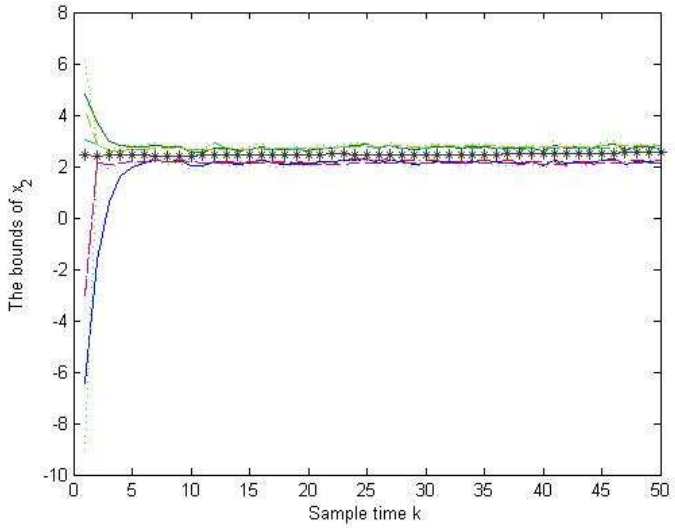

Figure 4.6: Bounds of x_2 obtained by different approaches (Example 4.1)

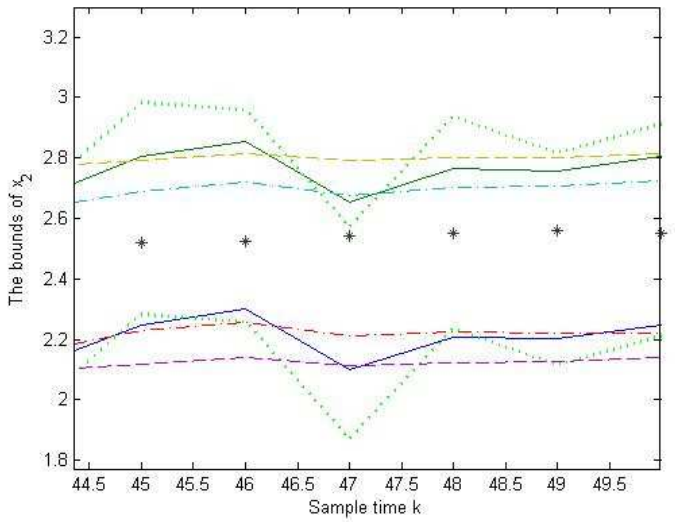

Figure 4.7: Zoom of the bounds of x_2 obtained by different approaches (Example 4.1)

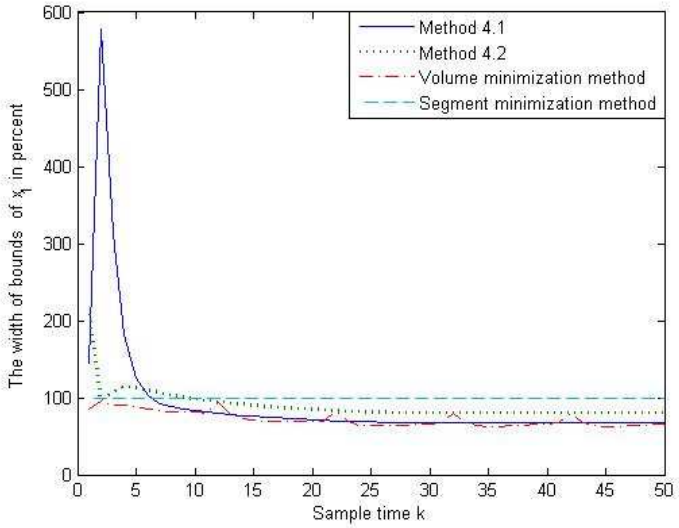

Figure 4.8: Comparison of the bound's width of x_1 obtained by different approaches (Example 4.1)

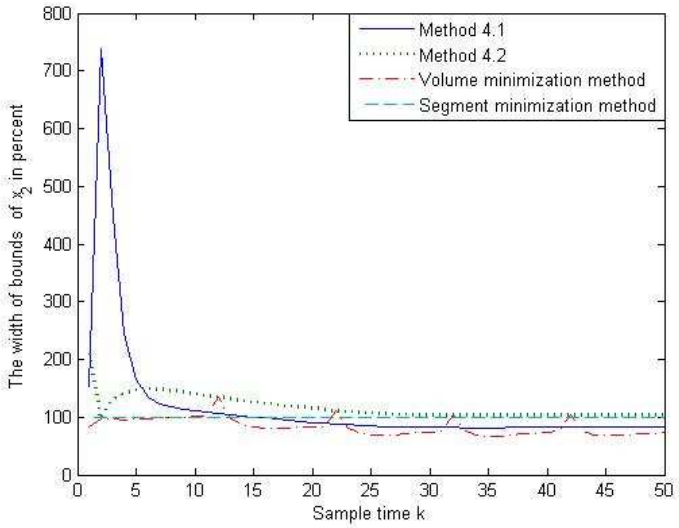

Figure 4.9: Comparison of the bound's width of x_2 obtained by different approaches (Example 4.1)

To confirm the good performance of the P-radius based approach, Figure

4.10 compares the volume of the zonotopic guaranteed state estimation by different approaches (the segment minimization, the volume minimization and the P-radius minimization). The P-radius minimization gives a better performance than the segment minimization and as good as the volume minimization.

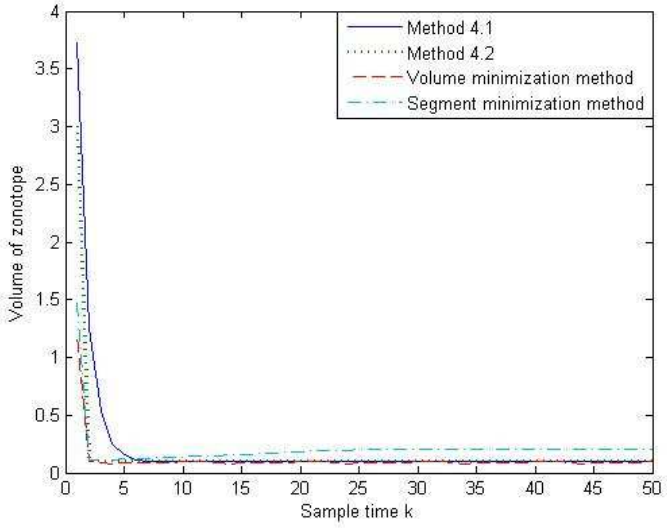

Figure 4.10: Comparison of the volume of guaranteed state estimation obtained by different approaches (Example 4.1)

Table (4.1) shows the computation time of different algorithms. These results are obtained with an Intel Core $i5$ 2.67 GHz. The BMI optimization (4.58) is solved by *Penbmi* solver, the LMI optimization (4.59) is dealt by LMI toolbox ($mincx$) of $Matlab^{®}$, the volume minimization problem is solved by the $fminsearch$ function of Matlab and the segment minimization problem is solved with a simple matrix computation. If the time used to solve LMI optimizations is not taken into account, the computation time of this method is the same as the computation of the segment minimization but the performance of the estimation is better. Even if the LMI optimizations are taken into account, the computation time is 10 times less than the computation time of the volume minimization method. This highlights the advantages on the computation complexity of the proposed method.

Table 4.1: Total computation time of Example 4.1 after 50 time instants

Algorithm	Time(second)
Segment minimization	0.0468
Presented algorithm (without off-line optimization problem included)	0.0312
Method 4.1 (with off-line optimization (4.58) included)	0.9204
Method 2 (with off-line optimization (4.59) included)	0.6240
Volume minimization	10.0153

The segment minimization algorithm has an acceptable performance and a very short computation time (only some computations to obtain λ). The volume minimization algorithm gives a better performance but it needs a longer computation time (215 times more than for the segment minimization method) because an optimization problem must be solved at each sample time. The performance of the presented method can be comparable with the performance obtained by the volume minimization algorithm but λ is computed at the beginning of the program and at each iteration the value of λ does not need to be recomputed leading to a reasonable online complexity. In summary, the proposed P-radius based algorithms combine the advantage of the volume minimization (performance) and of the segment minimization (computation time). In addition, the P-radius based approaches allow to overcome the problem of volume minimization due to a very narrow zonotope. In the next part, the P-radius based technique is further developed to solve the problem in the case of systems with interval parametric uncertainty.

4.3.2 Single-Output systems with interval uncertainties

Consider the following linear uncertain discrete-time varying system:

$$\begin{cases} x_{k+1} = Ax_k + \omega_k \\ y_k = c^T x_k + v_k \end{cases} \tag{4.61}$$

With the same notations as in Subsection 4.3.1, the proposition 4.2 presented in Subsection 4.3.1 can be extended in this case with the same assumptions on W and V. An additional assumption is considered: the unknown matrix A belongs to a Schur stable interval matrix $[\![A]\!]$ (i.e. all the matrices in the interval matrix $[\![A]\!]$ are Schur stable [97], [112]). This assumption is not very restrictive because in many applications the matrix A is given by a closed-loop matrix $A + BK$, where A and B are the open-loop matrices and A belongs to the interval matrix $[\![A]\!]$. A stabilizing feedback gain K can be computed by solving a LMI problem [98], [5].

The computation of the guaranteed state estimation can be easily modified in order to estimate the guaranteed bound of the state of the system

(4.61). The vector λ and the matrix $P = P^T \succ 0$ are computed such that at each iteration the P-radius of the zonotopic guaranteed state estimation set is non-increasing.

The problem can be formulated in a similar way as described in the previous subsection. The predicted state set $\bar{X}_k$ and guaranteed state estimation set $\hat{X}_k$ at time instant k are described as:

$$\bar{X}_k = A\hat{p}_{k-1} \oplus \begin{bmatrix} A\hat{H}_{k-1} & F \end{bmatrix} \mathbf{B}^{r+n_x} \tag{4.62}$$

$$\hat{X}_k(\lambda) = \hat{p}_k(\lambda) \oplus \hat{H}_k(\lambda)\mathbf{B}^{r+n_x+1} \tag{4.63}$$

with the parametrized vector $\hat{p}_k(\lambda) = A\hat{p}_{k-1} + \lambda(y_k - c^T A\hat{p}_{k-1})$ and the parametrized matrix $\hat{H}_k(\lambda) = \begin{bmatrix}(I - \lambda c^T)\begin{bmatrix} A\hat{H}_{k-1} & F \end{bmatrix} & \sigma\lambda \end{bmatrix}$. Denote that the difference between these equations and the equations (4.40), (4.41) in the last subsection is that the matrix A is known in (4.40), (4.41) and unknown in this case.

Similar to the procedure to obtain the BMI (4.54), the non-increasing condition on the P-radius of the zonotopic guaranteed state estimation leads to the following matrix inequality:

$$\begin{bmatrix} \beta P & 0 & 0 & A^T P - A^T c Y^T \\ * & F^T F & 0 & F^T P - F^T c Y^T \\ * & * & \sigma^2 & Y^T \sigma \\ * & * & * & P \end{bmatrix} \succeq 0 \tag{4.64}$$

where A belongs to the interval matrix $[A]$.

As $\mathbf{[}A\mathbf{]}$ is a convex set, by using the maximum principle [122], if (4.64) is true on each vertex of $\mathbf{[}A\mathbf{]}$, then it is true for all $A \in \mathbf{[}A\mathbf{]}$. In summary, the vector λ can be found by solving the following optimization problem:

$$\max_{\tau,\beta,P,Y} \tau$$

subject to

$$\begin{cases} \frac{(1-\beta)P}{\epsilon} \succeq \tau I \\ \begin{bmatrix} \beta P & 0 & 0 & \tilde{A}_i^T P - \tilde{A}_i^T c Y^T \\ * & F^T F & 0 & F^T P - F^T c Y^T \\ * & * & \sigma^2 & Y^T \sigma \\ * & * & * & P \end{bmatrix} \succeq 0 \\ \tau > 0 \end{cases} \tag{4.65}$$

for $i = 1, ..., 2^q$, where $\tilde{A}_i$ are the vertices of the interval matrix $\mathbf{[}A\mathbf{]}$, q is the number of interval elements of $\mathbf{[}A\mathbf{]}$ and $Y = P\lambda$.

***Remark* 4.6.** As A is unknown but belongs to the interval matrix $\mathbf{[}A\mathbf{]}$, the predicted state set $\bar{X}_k$ can not be directly computed by the expression (4.62)

at each iteration. This set is replaced by a zonotopic outer approximation using the following property.

***Property* 4.1.** Given an interval matrix $[\![M]\!] \in \mathbb{I}^{n\times p}$ and a real matrix $N \in \mathbb{R}^{p\times q}$, the center and the radius of the interval matrix defined by the product $[\![M]\!]N$ are given by $mid([\![M]\!]N) = mid([\![M]\!])N$ and $rad([\![M]\!]N) = rad([\![M]\!])|N|$, where $|N|$ designates the matrix formed with the absolute value of each element of N.

Proof It is evident by using matrix multiplication. Also note that the elements of the radius of an interval matrix are always positive. □

Using this property, a zontopic outer approximation of $\bar{X}_k$ is computed as follows. The starting point is given by equation (4.62):

$$\bar{X}_k = A\hat{p}_{k-1} \oplus \begin{bmatrix} A\hat{H}_{k-1} & F \end{bmatrix} \mathbf{B}^{r+n_x} \tag{4.66}$$

As A belongs to the interval matrix $[\![A]\!]$, an outer approximation of $\bar{X}_k$ can be obtained by $[\![A]\!]\hat{p}_{k-1} \oplus \begin{bmatrix} [\![A]\!]\hat{H}_{k-1} & F \end{bmatrix} \mathbf{B}^{r+n_x}$.

Using Property 4.1 the following expression is true:

$$[\![A]\!]\hat{p}_{k-1} \in mid([\![A]\!])\hat{p}_{k-1} \oplus rs(rad([\![A]\!])|\hat{p}_{k-1}|)\mathbf{B}^{n_x} \tag{4.67}$$

In addition, Property 3.5 implies that:

$$[\![A]\!]\hat{H}_{k-1}\mathbf{B}^r \in \begin{bmatrix} mid([\![A]\!])\hat{H}_{k-1} & rs(rad([\![A]\!])|\hat{H}_{k-1}|) \end{bmatrix} \mathbf{B}^{r+n_x} \tag{4.68}$$

The Minkowski sum of the last two expressions (4.67) and (4.68) leads to:

$$\begin{aligned}[\![A]\!]\hat{p}_{k-1} \oplus [\![A]\!]\hat{H}_{k-1}\mathbf{B}^r \subset mid([\![A]\!])\hat{p}_{k-1} \oplus rs(rad([\![A]\!])|\hat{p}_{k-1}|)\mathbf{B}^{n_x} \oplus \\ \oplus \begin{bmatrix} mid([\![A]\!])\hat{H}_{k-1} & rs(rad([\![A]\!])|\hat{H}_{k-1}|)) \end{bmatrix} \mathbf{B}^{r+n_x}\end{aligned} \tag{4.69}$$

Therefore, the zonotopic outer approximation of $\bar{X}_k$ is:

$$Z(mid([\![A]\!])p_{k-1}; \begin{bmatrix} mid([\![A]\!])\hat{H}_{k-1} & rs(rad([\![A]\!])|\hat{H}_{k-1}|) & rs(rad([\![A]\!])|\hat{p}_{k-1}|) & F \end{bmatrix}) \tag{4.70}$$

This zonotope is formed by generators which depend on $\hat{H}_{k-1}$ and $\hat{p}_{k-1}$. As $A \in [A]$ is a Schur stable matrix, the states of the system converge to a set containing the origin and thus, the generator $rad([A])|\hat{p}_{k-1}|$ is bounded. Moreover, the computation of vector λ depends only on the vertices of the interval matrix $[\![A]\!]$ and not $\bar{X}_k$ and this outer approximation is done at each time instant. Thus this implies that the approximation does not change the non-increasing property of the guaranteed bound on the system states.

***Remark* 4.7.** The number of decision variables in (4.65) is the same as in (4.58), the only difference is that the optimization problem (4.65) has $2^q - 1$ additional BMIs compared to (4.58). Even if the complexity of this optimization increases exponentially when q is increased, this optimization is solved off-line and thus it does not limit the application of the proposed method.

***Example* 4.2.** Consider the following linear discrete time-variant system [2]:

$$\begin{cases} x_{k+1} = \begin{bmatrix} 0 & -0.5 \\ 1 & 1+0.3\delta \end{bmatrix} x_k + 0.02 \begin{bmatrix} -6 \\ 1 \end{bmatrix} \omega_k \\ \\ y_k = \begin{bmatrix} -2 & 1 \end{bmatrix} x_k + 0.2 v_k \end{cases} \tag{4.71}$$

with $|\delta| \leq 1$ the interval parametric uncertainty, $\|v_k\|_\infty \leq 1$ and $\|\omega_k\|_\infty \leq 1$. The values of δ, v_k and ω_k are generated by the random functions of $Matlab^{\textcircled{R}}$. In this example the number of parametric interval elements is equal to $q = 1$. The initial state belongs to the box $3B^2$.

Solving the optimization problem (4.65) by *Penbmi* solver gives $\beta = 0.1981$, $\lambda = \begin{bmatrix} -0.2137 \\ 0.5726 \end{bmatrix}$. The number of scalar decision variables is 7, the optimization problem (4.65) contains 2 BMIs constraints of size 2×2, 7×7 and one scalar LMI. Even if the number of BMIs in (4.54) has an exponential dependency on the number of interval uncertainties, due to the capacity of existing solvers, a system of order n_x up to 50 can be considered. To facilitate the comparison of the result, we do not simulate the solution of the optimization problem (4.59). The importance is to show that the P-radius based approach can work in the context of interval parametric uncertainty systems, thus the solution obtained from (4.65) is compared with the performance of the segment minimization approach and the volume minimization approach.

Figure 4.11 shows the evolution of the predicted state set and the outer approximation of state estimation set at time instants $k = 1$, $k = 2$ and $k = 3$. Note that this estimation set is decreased at each sample time.

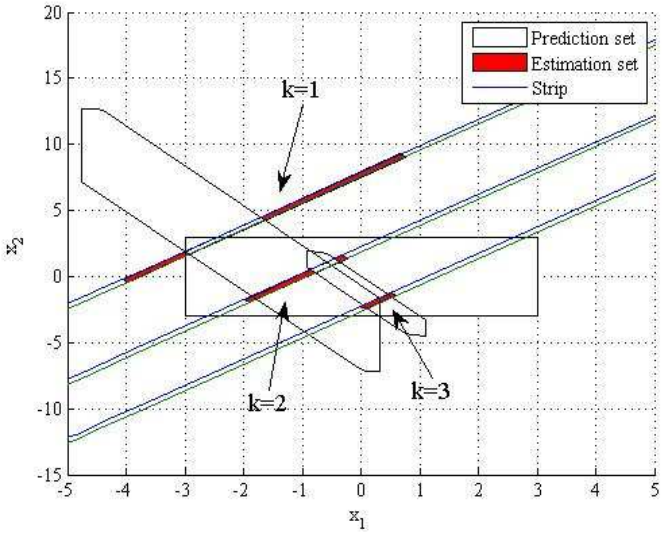

Figure 4.11: Evolution of the guaranteed state estimation $\hat{X}_k$ (Example 4.2)

The comparison of the bounds of x_{1_k} and x_{2_k} in percent obtained via the segment minimization of the zonotope, the volume minimization of the zonotope and minimization of the P-radius of the zonotope is proposed in Figures 4.14 and 4.15. These figures show a smaller bound obtained by the P-radius based approach than the bound obtained by the segment minimization approach and similar compared to the bound obtained by the volume minimization approach. To better understand, the volume of the zonotopic guaranteed state estimation is compared in Figure 4.16. This confirms the good performance (a small bound on each state, a small volume of the guaranteed state estimation) of the proposed P-radius-based approach. On one hand, the proposed approach is better than the segment minimization approach and comparable to the volume minimization approach. On the other hand the computation time of proposed approach is significantly less than the one of the volume minimization approach (see Table 4.2). Due to the effect of the uncertainty in the system parameters, the computation time in this example is increased in comparison to the Example 4.1 but it is denoted that the increasing time is added to the off-line computation in the proposed approach and to the online computation in the volume minimization approach. This remark gives us an important advantage related to the computation complexity of the proposed approach recommanding the application of the approach developed in this PhD thesis for fast time applications.

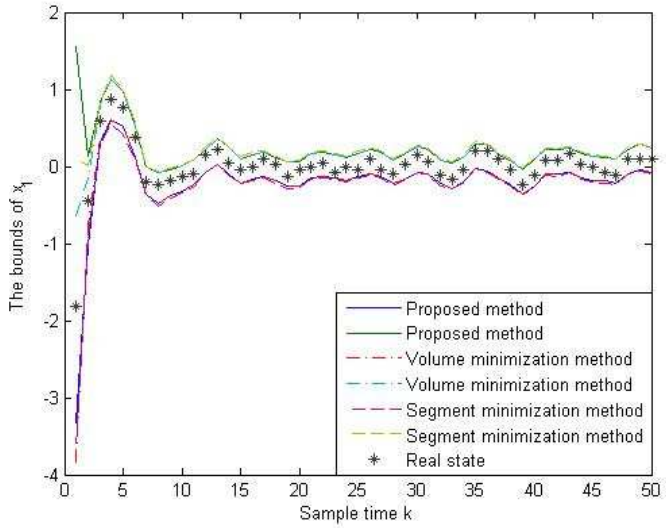

Figure 4.12: Guaranteed bound of x_1 obtained by different methods (Example 4.2)

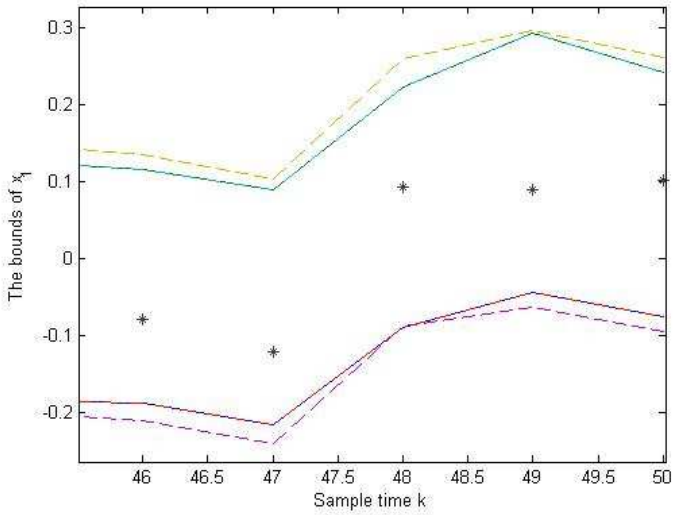

Figure 4.13: Zoom of the guaranteed bound of x_1 obtained by different methods (Example 4.2)

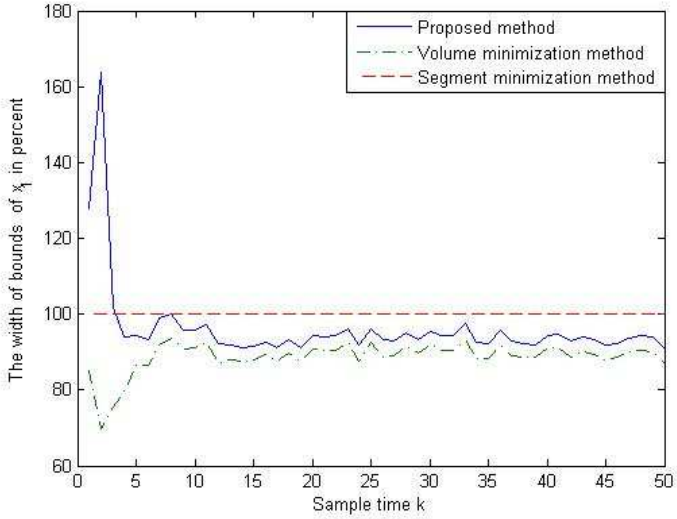

Figure 4.14: Comparison of the bound's width of x_1 obtained by different methods in percent (Example 4.2)

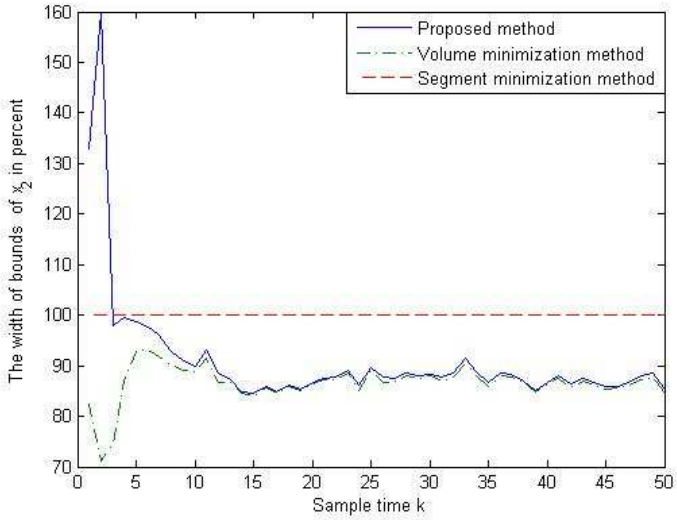

Figure 4.15: Comparison of the bound's width of x_2 obtained by different methods in percent (Example 4.2)

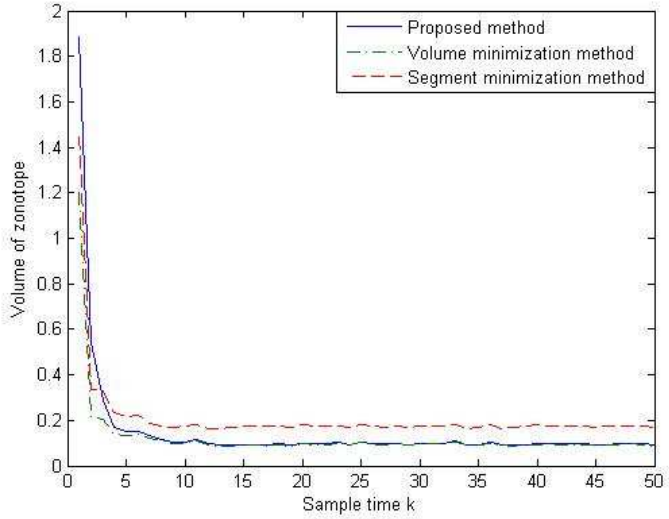

Figure 4.16: Comparison of the volume of zonotopic state estimation set obtained by different methods (Example 4.2)

Table 4.2: Total computation time of Example 4.2 after 50 time instants

Algorithm	Time(second)
Segment minimization	0.0312
P-radius minimization (without off-line optimization (4.65) included)	0.0312
P-radius minimization (with off-line optimization (4.65) included)	0.9828
Volume minimization	10.3273

To recapitulate the advantages of each of estimation method, the table 4.3 classifies the complexity of the computation and the accuracy of the estimation for each method from 1 to 4. The number 1 means the best accuracy and the less complexity of computation. The number 4 means the worst accuracy and the most complex from the computation point of view.

Table 4.3: Table of recapitulation of different estimation approaches (Single-Output case)

Algorithm	Complexity	Accuracy
Segment minimization method	1	4
Volume minimization method	4	1
Method 4.1	2	2
Method 4.2	2	3

***Example* 4.3.** To better understand the influence of the parameter uncertainty on the performance of estimation, the same system with more parametrric uncertainties in the matrix A_k is considered:

$$\begin{cases} x_{k+1} = \begin{bmatrix} 0 + 0.2\delta_1 & -0.5 + 0.1\delta_2 \\ 1 + 0.2\delta_3 & 1 + 0.3\delta_4 \end{bmatrix} x_k + 0.02 \begin{bmatrix} -6 \\ 1 \end{bmatrix} \omega_k \\ y_k = \begin{bmatrix} -2 & 1 \end{bmatrix} x_k + 0.2 v_k \end{cases} \tag{4.72}$$

The parametric uncertainties are bounded by $-1 \leq \delta_1, \delta_2, \delta_3, \delta_4 \leq 1$. The bound on the disturbance ω_k, on the measurement noise v_k and on the initial state are the same as the Example 4.2. Figure 4.17 shows that in this case, the non-increase of the zonotopic guaranteed state estimation based on the P-radius minimization is always ensured. Moreover, by comparing Figure 4.17 and Figure 4.16, the influence of parameter uncertainties on the performance of estimation is illustrated: the volume of the zonotopic guaranteed estimation in this example (4 parametric uncertainties) is larger than the one in the Example 4.2 (1 parametric uncertainty); the complexity of computation is higher which is reflected by a longer computation time (Compare Table 4.4 and Table 4.2).

Until now the performance of the P-radius minimization approach is illustrated in the case of Single-Output systems (Examples 4.1, 4.2, 4.3). To complete the solution, the case of Multi-Output systems will be solved in the next subsection.

Table 4.4: Total computation time of Example 4.3 after 50 time instants

Algorithm	Time(second)
Segment minimization	0.0312
P-radius minimization (without off-line optimization (4.65) included)	0.0312
P-radius minimization (with off-line optimization (4.65) included)	1.0761
Volume minimization	11.0917

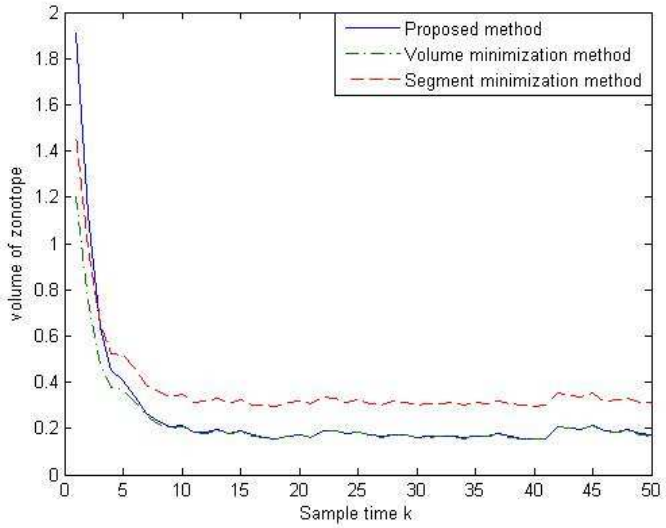

Figure 4.17: Comparison of the volume of zonotopic state estimation set obtained by different methods (Example 4.3)

4.3.3 Extension to Multi-Output uncertain systems

The presented estimation methodology is further extended to the case of Multi-Outputs systems. The diagram proposed in Figure 4.18 recapitulates the solution of the estimation problem for Multi-Output system where the natural Single-Output extension is presented in this subsection and the direct Multi-Output solution is described in the next subsection. Firstly, a general procedure for Multi-Output system is described, allowing to introduce new useful notations. Secondly, a simple but conservative solution consists in decoupling the multi-output system in n_y independent single-output sub-systems. Thirdly, a sub-optimal solution (with reduced conservatism) considers the coupling effect between the measurements offering a trade-off between the computation complexity of the Multi-Outputs problem and the accuracy of the estimation. Finally, a solution permitting to consider the information of all measurements at the same time is proposed which leads to a Polynomial Matrix Inequality problem. This PMI problem is solved using the relaxation technique proposed in [62]. Note that all these three presented solutions are original results.

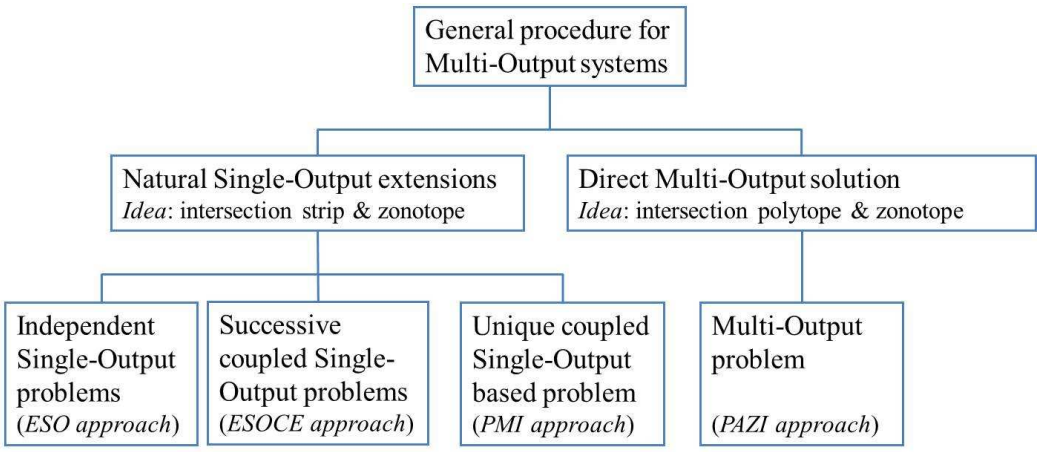

Figure 4.18: Classification of proposed solution for Multi-Output systems

4.3.3.1 General formulation

Considering the Multi-Output system (4.5), the guaranteed state estimation set $\hat{X}_k$ can be found by successively repeating the guaranteed state intersection described in Subsection 4.3.1 for each component of the output measurement vector y_k, denoted $y_{k/i}$:

$$y_{k/i} = c_i^T x_k + v_{k/i}, i = 1, \ldots, n_y \tag{4.73}$$

Here c_i^T is the i-th row of matrix C and the noise $v_{k/i}$ is bounded by the interval $V_i = \sigma_i \mathbf{B}^1$, with $\sigma_i = \Sigma_{ii}$. Thus, the measurement noise v_k belongs to a box $V = diag(\sigma_1, \ldots, \sigma_{n_y})\mathbf{B}^{n_y}$. If this assumption is not satisfied, an outer approximation of V by a box can be used. To simplify the manuscript, a known matrix A is considered. The extension to the case of an interval matrix $[A]$ is similar to the Subsection 4.3.2 and hence immediate.

Supposing an outer approximation of the state set $\hat{X}_{k-1} = \hat{p}_{k-1} \oplus \hat{H}_{k-1}\mathbf{B}^r$ at the time instant $k-1$, then the predicted state set at the next time instant $\bar{X}_k$ can be computed as in (4.40). The exact estimation set will be obtained after intersecting the predicted state set with the measurement consistent state set of the measured output vector y_k (as described in Algorithm 4.2). In a general way, the outer approximation of this set can be found by using the guaranteed state intersection as follows.

Similar to (4.41), an outer approximation of the intersection between the strip created by the first component of the output vector ($y_{k/1}$) and the predicted state set ($\bar{X}_k$) is represented by:

$$\hat{X}_{k/1}(\lambda_1) = \hat{p}_{k/1}(\lambda_1) \oplus \hat{H}_{k/1}(\lambda_1)\mathbf{B}^{r+n_x+1} \tag{4.74}$$

where $\hat{p}_{k/1}(\lambda_1) = A\hat{p}_{k-1} + \lambda_1(y_{k/1} - c_1^T A\hat{p}_{k-1})$
and $\hat{H}_{k/1}(\lambda_1) = \begin{bmatrix}(I - \lambda_1 c_1^T)A\hat{H}_{k-1} & (I - \lambda_1 c_1^T)F & \sigma_1\lambda_1\end{bmatrix}$.
Then this set $\hat{X}_{k/1}(\lambda_1)$ is intersected with the strip obtained from the second component of the measured output vector $(y_{k/2})$ leading to:

$$\hat{X}_{k/2}(\lambda_1, \lambda_2) = \hat{p}_{k/2}(\lambda_1, \lambda_2) \oplus \hat{H}_{k/2}(\lambda_1, \lambda_2)\mathbf{B}^{r+n_x+2} \tag{4.75}$$

with $\hat{p}_{k/2}(\lambda_1, \lambda_2) = \hat{p}_{k/1}(\lambda_1) + \lambda_2(y_{k/2} - c_2^T\hat{p}_{k/1}(\lambda_1))$
and $\hat{H}_{k/2}(\lambda_1, \lambda_2) = \begin{bmatrix}(I - \lambda_2 c_2^T)\hat{H}_{k/1}(\lambda_1) & \sigma_2\lambda_2\end{bmatrix}$.

This procedure is repeated until the last component of the measured output vector (y_{k/n_y}) leading to the zonotopic guaranteed state estimation set at time instant k:

$$\begin{aligned}\hat{X}_{k/n_y}(\lambda_1, ..., \lambda_{n_y}) = \hat{p}_{k/n_y}(\lambda_1, ..., \lambda_{n_y})\oplus \\ \oplus\hat{H}_{k/n_y}(\lambda_1, ..., \lambda_{n_y})\mathbf{B}^{r+n_x+n_y}\end{aligned} \tag{4.76}$$

with the recursive notations:

$$\begin{aligned}\hat{p}_{k/n_y}(\lambda_1, ..., \lambda_{n_y}) = \hat{p}_{k/n_y-1}(\lambda_1, ..., \lambda_{n_y-1})+ \\ + \lambda_{n_y}(y_{k/n_y} - c_{n_y}^T\hat{p}_{k/n_y-1}(\lambda_1, ..., \lambda_{n_y-1}))\end{aligned} \tag{4.77}$$

and

$$\hat{H}_{k/n_y}(\lambda_1, ..., \lambda_{n_y}) = \begin{bmatrix}(I - \lambda_{n_y} c_{n_y}^T)\hat{H}_{k/n_y-1}(\lambda_1, ..., \lambda_{n_y-1}) & \sigma_{n_y}\lambda_{n_y}\end{bmatrix} \tag{4.78}$$

Finally, the zonotopic guaranteed state estimation set at instant k is provided by:

$$\hat{X}_k(\lambda_1, ..., \lambda_{n_y}) = \hat{p}_k(\lambda_1, ..., \lambda_{n_y}) \oplus \hat{H}_k(\lambda_1, ..., \lambda_{n_y})\mathbf{B}^{r+n_x+n_y} \tag{4.79}$$

with $\hat{p}_k(\lambda_1, ..., \lambda_{n_y}) = \hat{p}_{k/n_y}(\lambda_1, ..., \lambda_{n_y})$
and $\hat{H}_k(\lambda_1, ..., \lambda_{n_y}) = \hat{H}_{k/n_y}(\lambda_1, ..., \lambda_{n_y})$.

This procedure can be visualized in Figure 4.19 for the case of two outputs. Suppose at the time instant k from the guaranteed state estimation set $\hat{X}_{k-1}$ the predicted state set is determined (represented by the green zonotope $\bar{X}_k$). Firstly, this set is intersected with the first element of the measured output denoted by the red strip $|c_1^T x - y_{k/1}| \leq \sigma_1$. Then this intersection is approximated by the black zonotope $\hat{X}_{k/1}$ by using Proposition 4.2. The procedure is repeated with the second element of the measured output (the strip $|c_2^T x - y_{k/2}| \leq \sigma_2$). Proposition 4.2 is used again to obtain the outer approximation of the intersection between $\hat{X}_{k/1}$ and the second strip. The guaranteed state estimation set is then the magenta zonotope $\hat{X}_{k/2}$.

Further on, in the general case of n_y outputs, three original procedures are proposed to compute the vectors λ_1,...,λ_{n_y}.

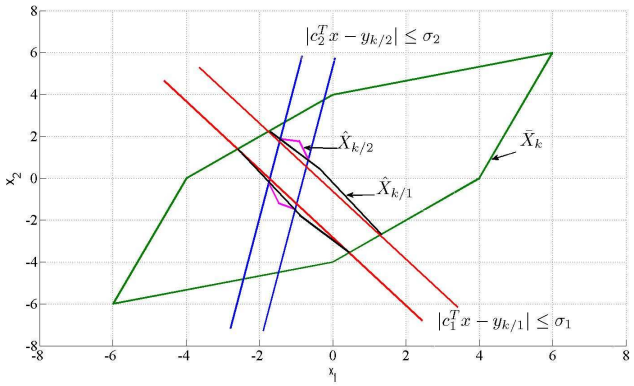

Figure 4.19: State estimation for a two-output system

4.3.3.2 Equivalent Single-Output approach

In this approach, the system is considered as n_y independent Single-Output systems. This leads to independently compute the vectors λ_1, ..., λ_{n_y} by off-line solving independently n_y separate optimization problems (4.58) or (4.59). This approach is named as Equivalent Single-Output approach (ESO). The guaranteed state estimation is determined using the following algorithm:

***Algorithm* 4.3.**

1. For $j = 1, ..., n_y$
   Step j: Using the strip of the measurement $y_{k/j}$ compute λ_j;
   End.

2. The guaranteed state estimation is computed by the equation (4.79) with the known vectors $\lambda_1, \ldots, \lambda_{n_y}$.

***Remark* 4.8.** This approach proposes a simple solution for the state estimation of Multi-Output systems but this solution can lead to a conservative result due to the possible multi-outputs coupling effect. In the next subsection, another solution is proposed to improve the performance of the guaranteed state estimation.

4.3.3.3 Equivalent Single-Output with Coupling Effect approach

Secondly, to reduce the conservatism of the previous method, the following procedure is proposed. Using $y_{k/1}$, the predicted state set $\bar{X}_k$ and method

4.1, method 4.2 or (4.65) in the case of interval parametric uncertainty leads to λ_1 and a smaller zonotope $\hat{X}_{k/1}$. Intersecting this new zonotope with the strip corresponding to $y_{k/2}$ (supposing λ_1 known from the previous step) leads to λ_2 and another zonotope $\hat{X}_{k/2}$. This procedure is repeated until the last component of the output vector y_{k/n_y} (supposing all the previous vectors λ_1,..., λ_{n_y-1} to be known). This approach is called as Equivalent Single-Output with Coupling Effect approach (ESOCE). The following algorithm describes this off-line procedure.

***Algorithm* 4.4.**

1. Step 1: Using the measurement $y_{k/1}$ and (4.65), compute λ_1;
2. For $j = 2, ..., n_y$
   Step j: Using the measurement $y_{k/j}$ and the previous obtained vectors $\lambda_1, ..., \lambda_{j-1}$, compute λ_j.

   End.

The computation of λ_j is detailed as follows. The guaranteed state estimation set at Step j is computed as:

$$\hat{X}_{k/j}(\lambda_1, ..., \lambda_j) = \hat{p}_{k/j}(\lambda_1, ..., \lambda_j) \oplus \hat{H}_{k/j}(\lambda_1, ..., \lambda_j)\mathbf{B}^{r+n_x+j} \tag{4.80}$$

The non-increasing condition on the P-radius of the zonotopic estimation set is applied leading to:

$$\max_{\hat{z}} \|\hat{H}_{k/j}\hat{z}\|_P^2 \leq \max_{z} \beta\|\hat{H}_{k-1}z\|_P^2 + \max_{s} \|Fs\|_2^2 + \sigma_1^2 + ... + \sigma_j^2 \tag{4.81}$$

with $\hat{z} = \begin{bmatrix} z^T & s^T & \eta_1 & ... & \eta_j \end{bmatrix}^T \in \mathbf{B}^{r+n_x+j}$, $z \in \mathbf{B}^r$, $s \in \mathbf{B}^{n_x}$, $\eta_j \in \mathbf{B}^1$, and $\beta \in (0, 1)$.

Using the reverse triangle inequality leads to a sufficient condition for (4.81):

$$\max_{\hat{z}}(\|\hat{H}_{k/j}\hat{z}\|_P^2 - \beta\|\hat{H}_{k-1}z\|_P^2 - \|Fs\|_2^2 - \sigma_1^2 - ... - \sigma_j^2) \leq 0 \tag{4.82}$$

Because $\eta_i \in \mathbf{B}^{n_y}$, with $i = 1, \ldots, j$ the following expression is obtained:

$$\begin{bmatrix} \sigma_1^2 & ... & \sigma_j^2 \end{bmatrix} \left(\begin{bmatrix} 1 \\ \vdots \\ 1 \end{bmatrix} - \begin{bmatrix} \eta_1^2 \\ \vdots \\ \eta_j^2 \end{bmatrix} \right) \geq 0 \tag{4.83}$$

Adding this term to the left-side of (4.82) leads to the following sufficient condition for (4.82):

$$\begin{aligned}\hat{z}^T\hat{H}_{k/j}^T P\hat{H}_{k/j}\hat{z} - \beta z^T\hat{H}_{k-1}^T P\hat{H}_{k-1}z - s^T F^T Fs - \\ -\sigma_1^2\eta_1^2 - ... - \sigma_j^2\eta_j^2 \leq 0\end{aligned} \tag{4.84}$$

Similar to the Subsections 4.3.1 and 4.3.2, the expression (4.84) is equivalent to:

$$\begin{bmatrix}\theta\\ s\\ \eta_1\\ \vdots\\ \eta_j\end{bmatrix}^T \begin{bmatrix}\beta P & 0 & 0 & ... & 0 & B_1\\ * & F^TF & 0 & ... & 0 & B_2\\ * & * & \sigma_1^2 & ... & 0 & B_3\\ ... & ... & ... & ... & ... & ...\\ * & * & * & ... & \sigma_j^2 & B_{j+2}\\ * & * & * & ... & * & P\end{bmatrix} \begin{bmatrix}\theta\\ s\\ \eta_1\\ \vdots\\ \eta_j\end{bmatrix} > 0, \forall\theta, s, \eta_1, \ldots, \eta_j \tag{4.85}$$

with $\theta = H_{k/j}z$ and the notations:

$$\begin{aligned}B_1 &= ((\prod_{i=1}^{j}(I - \lambda_{j+1-i}c_{j+1-i}^T))A)^T P\\ B_2 &= ((\prod_{i=1}^{j}(I - \lambda_{j+1-i}c_{j+1-i}^T))F)^T P\\ B_3 &= (\prod_{i=1}^{j-1}(I - \lambda_{j+1-i}c_{j+1-i}^T)\sigma_1\lambda_1)^T P\\ &\vdots\\ B_j &= ((I - \lambda_j c_j^T)(I - \lambda_{j-1}c_{j-1}^T)\sigma_{j-2}\lambda_{j-2})^T P\\ B_{j+1} &= ((I - \lambda_j c_j^T)\sigma_{j-1}\lambda_{j-1})^T P\\ B_{j+2} &= (\sigma_j\lambda_j)^T P\end{aligned} \tag{4.86}$$

Using the definition of positive definite matrix, and the minimization of the P-radius, the following optimization problem is obtained:

$$\max_{\tau,\beta,P,Y_j} \tau$$

subject to

$$\begin{cases}\frac{(1-\beta)P}{\sigma_1^2+...+\sigma_j^2+\max\limits_{s\in\mathbf{B}^{n_x}}\|Fs\|_2^2} \succeq \tau I\\ \begin{bmatrix}\beta P & 0 & 0 & ... & 0 & B_1\\ * & F^TF & 0 & ... & 0 & B_2\\ * & * & \sigma_1^2 & ... & 0 & B_3\\ ... & ... & ... & ... & ... & ...\\ * & * & * & ... & \sigma_j^2 & B_{j+2}\\ * & * & * & ... & * & P\end{bmatrix} \succeq 0\\ \tau > 0\end{cases} \tag{4.87}$$

As the vectors $\lambda_1, \ldots, \lambda_{j-1}$ are computed in the previous steps, (4.86) is a BMI optimization problem whose decision variables are $Y_j = P\lambda_j$, $P = P^T$, β and τ.

***Example* 4.4.** The same dynamic system with the same assumptions as in Example 4.2 is considered with a second output in order to compare the performance in these two examples.

$$\begin{cases} x_{k+1} = \begin{bmatrix} 0 & -0.5 \\ 1 & 1+0.3\delta \end{bmatrix} x_k + 0.02 \begin{bmatrix} -6 \\ 1 \end{bmatrix} \omega_k \\ \\ y_k = \begin{bmatrix} -2 & 1 \\ 1 & 1 \end{bmatrix} x_k + \begin{bmatrix} 0.2 & 0 \\ 0 & 0.2 \end{bmatrix} v_k \end{cases} \tag{4.88}$$

In this example, the results obtained by the ESO approach in Subsection 4.3.3.2 and ESOCE approach in Subsection 4.3.3.3 are compared with the results obtained by the segment minimization approach and the volume minimization approach [2] applied for the multivariable case. The ESO approach gives the correction factors $\lambda_1 = \begin{bmatrix} -0.2137 \\ 0.5726 \end{bmatrix}$ and $\lambda_2 = \begin{bmatrix} 0.3684 \\ 0.3570 \end{bmatrix}$. The correction factors computed by Algorithm 4.4 (ESOCE) are $\lambda_1 = \begin{bmatrix} -0.2137 \\ 0.5726 \end{bmatrix}$ and $\lambda_2 = \begin{bmatrix} 0.2839 \\ 0.5085 \end{bmatrix}$.

The simulation result shows a good performance of these proposed approaches as in the previous examples. The volume minimization approach gives the best result of the estimation with an important online computation time. The segment minimization approach offers a fast computation with a degradation of the guaranteed state estimation set. The proposed approaches give good compromise solutions between the complexity of the computation on one hand and the precision of the state estimation in the other hand (Figures 4.22, 4.23, 4.24, Table 4.5).

Figure 4.20 shows the decrease of the zonotopic guaranteed state estimation at each time instant ($k = 1$, $k = 2$, $k = 3$). Figures 4.22, 4.23, 4.24 show that the performance of the ESOCE algorithm is better than the one of the ESO algorithm which confirms a less conservative result of the ESOCE method.

Moreover, the simulation results show that in Example 4.4 one more output is added which induces a better state estimation in comparison with the results of Example 4.2 (compare with Figures 4.11, 4.20 and 4.16, 4.24, respectively).

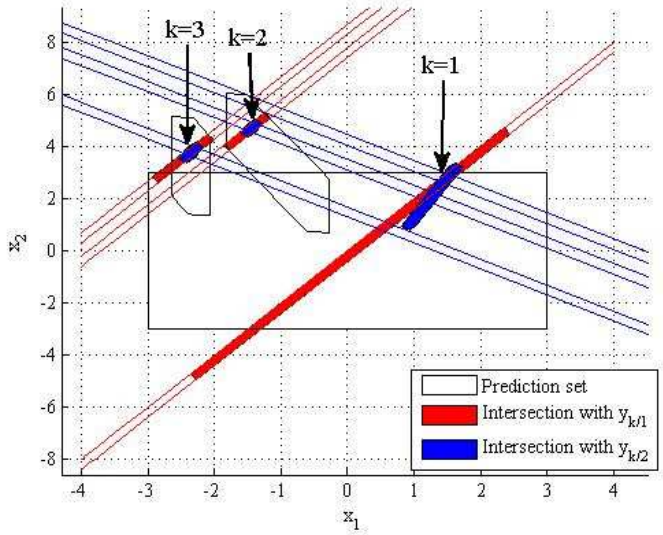

Figure 4.20: Intersection $\hat{X}_k$ between the predicted state set $\bar{X}_k$ and the measurement X_{y_k} using ESOCE approach

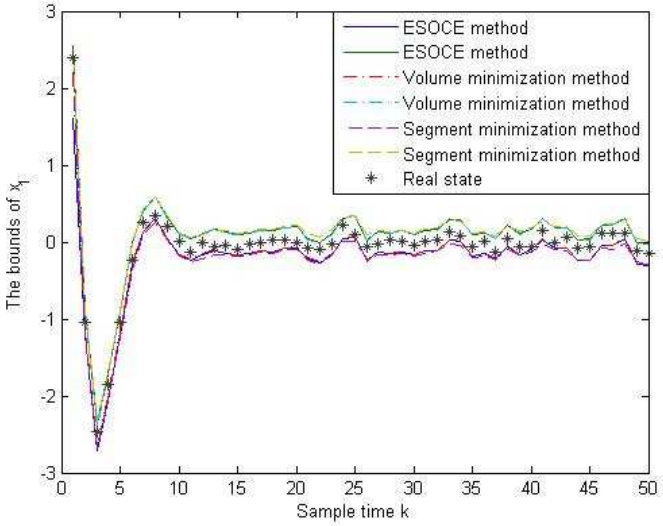

Figure 4.21: Guaranteed bound of x_1 obtained by different methods

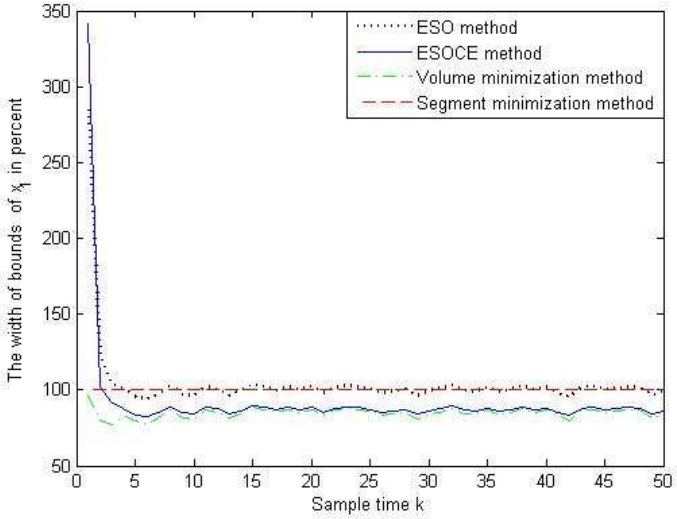

Figure 4.22: Comparison of the bound's width of x_1 obtained by different methods in percent

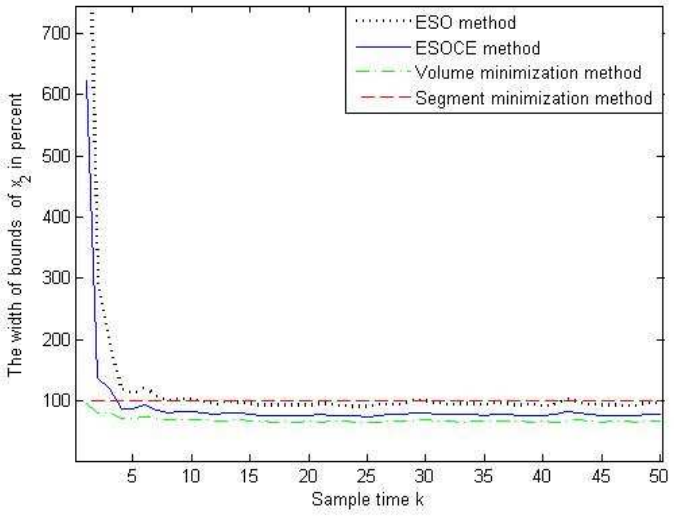

Figure 4.23: Comparison of the bound's width of x_2 obtained by different methods in percent

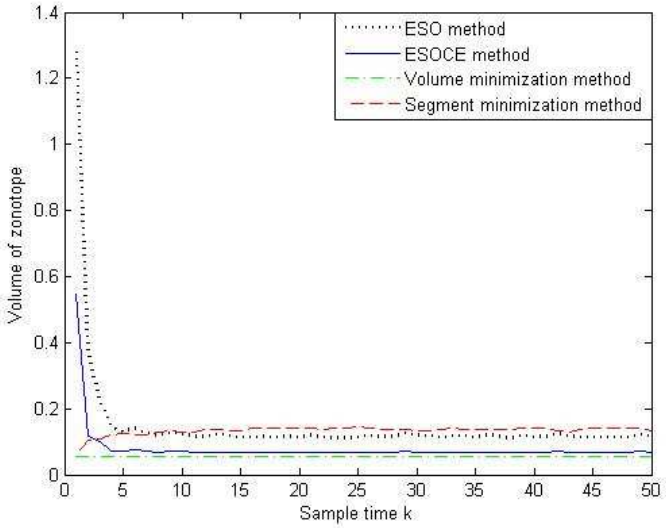

Figure 4.24: Comparison of the volume of zonotopic state estimation set obtained by different methods

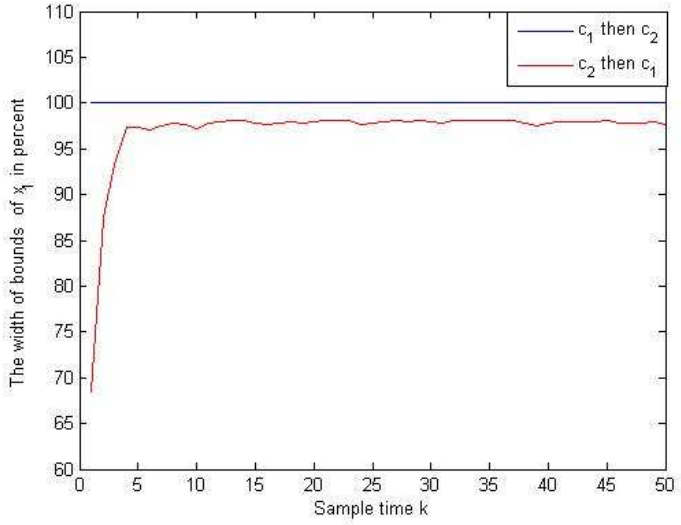

Figure 4.25: Comparison of the bound's width of x_1 with interchanged output measurements

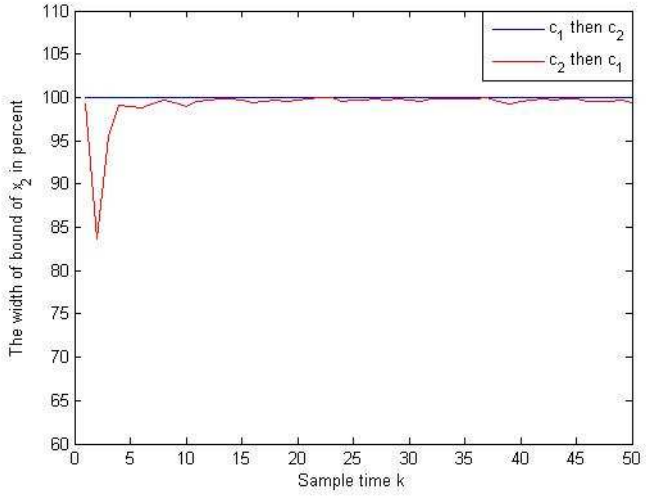

Figure 4.26: Comparison of the bound's width of x_2 with interchanged output measurements

Table 4.5: Total computation time of Example 4.4 after 50 time instants

Algorithm	Time(second)
Segment minimization	0.0624
Presented algorithms (ESO and ESOCE) (without off-line optimization included)	0.0624
ESO algorithm (with off-line optimization included)	1.3884
ESOCE algorithm (with off-line optimization included)	1.4664
Volume minimization	27.2534

Figures 4.25 and 4.26 compare the performance of the estimation when the order of taking into account the measurements is changed (the vector c_1 is replaced by c_2 and vice versa). The comparison leads to the following conclusion: the order of taking into account the measurement can influence to the performance of the estimation. Thus to obtain the best result of the approximation in the case of Multi-Output systems, $n_y!$ different combinations of output measurements must be tried and compared, and then, the best solution must be chosen for the implementation. The Singular Value Decomposition method which is a method dedicated to Multi-Output system has the same problem (4.12 is different when the rows of the C matrix are changed. Thus the performance of estimation is influenced). Note that for systems with a large number of outputs this operation can be time consuming. To overcome the conservativeness of these approaches, a new method is proposed in the next subsection.

4.3.3.4 Polynomial Matrix Inequality approach

In the previous approaches, the vectors $\lambda_1, \ldots, \lambda_{n_y}$ are separately computed which can lead to a conservative result. To overcome this problem, the solution proposed now is to compute $\lambda_1, \ldots, \lambda_{n_y}$ in the same time. All the vectors λ_i, with $i = 1, \ldots, n_y$, are computed such that the condition on the non-increasing property of the P-radius is ensured. This condition leads to a similar inequality as (4.82), with the modification that j is replaced by n_y.

Similar to the ESOCE approach, the following optimization problem is obtained: $\max_{\tau,\beta,P,\lambda_1,\ldots,\lambda_{n_y}} \tau$
subject to

$$\begin{cases} \frac{(1-\beta)P}{\sigma_1^2+\ldots+\sigma_{n_y}^2+\max\limits_{s\in\mathbf{B}^{n_x}}\|Fs\|_2^2} \succeq \tau I \\ \begin{bmatrix} \beta P & 0 & 0 & \ldots & 0 & B_1 \\ * & F^TF & 0 & \ldots & 0 & B_2 \\ * & * & \sigma_1^2 & \ldots & 0 & B_3 \\ \ldots & \ldots & \ldots & \ldots & \ldots & \ldots \\ * & * & * & \ldots & \sigma_{n_y}^2 & B_{n_y+2} \\ * & * & * & \ldots & * & P \end{bmatrix} \succeq 0 \\ \tau > 0 \end{cases} \tag{4.89}$$

with the notations:

$$\begin{aligned} B_1 &= ((\prod_{i=1}^{n_y}(I-\lambda_{n_y+1-i}c_{n_y+1-i}^T))A)^TP \\ B_2 &= ((\prod_{i=1}^{n_y}(I-\lambda_{n_y+1-i}c_{n_y+1-i}^T))F)^TP \\ B_3 &= (\prod_{i=1}^{n_y-1}(I-\lambda_{n_y+1-i}c_{n_y+1-i}^T)\sigma_1\lambda_1)^TP \\ &\vdots \\ B_{n_y} &= ((I-\lambda_{n_y}c_{n_y}^T)(I-\lambda_{n_y-1}c_{n_y-1}^T)\sigma_{n_y-2}\lambda_{n_y-2})^TP \\ B_{n_y+1} &= ((I-\lambda_{n_y}c_{n_y}^T)\sigma_{n_y-1}\lambda_{n_y-1})^TP \\ B_{n_y+2} &= (\sigma_{n_y}\lambda_{n_y})^TP \end{aligned} \tag{4.90}$$

As the vectors $\lambda_1, \ldots, \lambda_{n_y}$ are the unknown variables, the optimization problem (4.89) is not any more a BMI optimization problem as the previous subsection.

From the definition 3.15 of Polynomial Matrix Inequality, the problem (4.89) is a PMI optimization problem. PMI problems can be solved using several relaxation techniques [31], [61], [72], [64], [62]. In this thesis the method presented in [62] which is the most recent technique, is chosen to

solve the PMI optimization problem (4.90). This method is based on an insertion of lifting variables to reduce the polynomial terms to linear terms. By using these new variables, the PMI problem becomes a LMI problem, which can be easily solved (see [62] for more details).

In the Polynomial Matrix inequality problem (4.89), with the notations (4.90), the decision variables are: $P = P^T \in \mathbb{R}^{n_x \times n_x}$, $\lambda_1, ..., \lambda_{n_y} \in \mathbb{R}^{n_x}$ and the scalar β and τ. Thus the total number of scalar decision variables is: $\frac{n_x(n_x+1)}{2} + n_y n_x + 2$. The degree of the PMI (4.89) is $n_y + 1$. This PMI can be solved by using the first order LMI relaxation methodology [62].

***Example* 4.5.** To better understand, the first order LMI relaxation method [62] is illustrated in the following example:

$\min_x (x_1^2 - x_2^2)$

subject to PMI: $\begin{bmatrix} 1 + x_1 x_2 & x_1 \\ x_1 & 1 - x_1^2 - x_2^2 \end{bmatrix} \succeq 0$

First, the following change of variables is done: $y_{10} = x_1$, $y_{01} = x_2$, $y_{20} = x_1^2$, $y_{02} = x_2^2$, $y_{11} = x_1 x_2$.
Using these new variables, the PMI optimization problem is relaxed by the following LMIs:

$\min_x (y_{20} - y_{02})$

subject to LMIs:

$$\begin{cases} \begin{bmatrix} 1 & y_{10} & y_{01} \\ * & y_{20} & y_{11} \\ * & * & y_{02} \end{bmatrix} \succeq 0 \\ \begin{bmatrix} 1 + y_{11} & y_{10} \\ * & 1 - y_{20} - y_{02} \end{bmatrix} \succeq 0 \end{cases} \tag{4.91}$$

Using this technique, the PMI optimization (4.89) can be solved as in the following algorithm:

***Algorithm* 4.5.**

1. All the $\frac{n_x(n_x+1)}{2} + n_y n_x + 2$ *scalar decision variables* are denoted as follows: τ, $y_{10...0}$, $y_{01...0}$, ..., $y_{00...10}$, $y_{00...01}$. For expression (4.89), this leads to $\beta = y_{100...0}$, $P = \begin{bmatrix} y_{01...0} & \cdots & y_{00...1...0} \\ \cdots & \cdots & \cdots \end{bmatrix}$, $\lambda_1^T = \begin{bmatrix} y_{00...1...0} & \cdots \end{bmatrix}$,..., $\lambda_{n_y}^T = \begin{bmatrix} y_{00...1...0} & \cdots & y_{00...01} \end{bmatrix}$.

2. The *polynomial decision elements* in (4.89) are rewritten as the result of a change of variables based on the previous scalar decision variables such as: $y_{20...0} = y_{10...0} \cdot y_{10...0}$, $y_{11...0} = y_{10...0} \cdot y_{01...0}$ etc. In this way,

expression (4.89) becomes a LMI. If the LMI relaxation of the PMI optimization problem (4.90) is used, then the following LMI problem must be solved (see [62] for more details):

$\max \tau$
subject to the LMIs

$$\begin{cases} M_1 = \begin{bmatrix} 1 & * & * & * \\ y_{10\ldots0} & y_{20\ldots0} & \cdots & * \\ y_{01\ldots0} & y_{11\ldots0} & \cdots & * \\ \vdots & \vdots & \ddots & \vdots \\ y_{00..111} & \cdots & \cdots & y_{00\ldots222} \end{bmatrix} \succeq 0 \\ M_2 \succeq 0 \end{cases} \tag{4.92}$$

where M_1 is called moment matrix and M_2 denotes the equivalent LMI expressions obtained from the PMI in (4.89) using the new scalar decision variables ($y_{10\ldots0}$, $y_{20\ldots0}$, etc.).

***Remark* 4.9.** Denote $l = \frac{n_x(n_x+1)}{2} + n_y n_x + 1$. As the degree of the PMI in (4.89) is $n_y + 1$, then the dimensions of LMIs (4.92) are:

- M_1: $q \times q$, with $q = 1 + l + \binom{2}{l} + \ldots + \binom{round(\frac{n_y+1}{2})}{l}$;
- M_2: $n_x \times n_x$, $(3n_x + n_y) \times (3n_x + n_y)$ and 1 respectively.

The number of scalar decision variables in this optimization problem is $\frac{q(q+1)}{2}$.

***Remark* 4.10.** Using the relaxation method proposed in [62] permits to relax the PMI optimization problem to a LMI optimization problem which is easier to solve. Even if the obtained LMIs problem is solved off-line this method leads to a large size LMI problem (see the size of matrix M_1 and the number of scalar decision variables) which limits its application.

***Example* 4.6.** Consider the following linear discrete time system:

$$\begin{cases} x_{k+1} = \begin{bmatrix} 0 & -0.5 \\ 1 & 1 \end{bmatrix} x_k + 0.02 \begin{bmatrix} -6 \\ 1 \end{bmatrix} \omega_k \\ y_k = \begin{bmatrix} -2 & 1 \\ 1 & 1 \end{bmatrix} x_k + 0.2 v_k \end{cases} \tag{4.93}$$

with $\|v_k\|_\infty \leq 1$, $\|\omega_k\|_\infty \leq 1$. The values of v_k and ω_k are generated by the random functions of $Matlab^{\textcircled{R}}$. The initial state is unknown and belongs to the box $3B^2$.

Denote $\beta = y_{10000000}$, $P = \begin{bmatrix} y_{01000000} & y_{00100000} \\ * & y_{00010000} \end{bmatrix}$, $\lambda_1^T = \begin{bmatrix} y_{00001000} & y_{00000100} \end{bmatrix}$, $\lambda_2^T = \begin{bmatrix} y_{00000010} & y_{00000001} \end{bmatrix}$. Thus the dimensions of the LMIs of the considered optimization problem (4.92) are:

- M_1: 37×37;

- M_2: 2×2, 7×7 and 1.

As $l = 8$ and $q = 37$, the total number of scalar decision variables of the LMI problem (4.92) is $\frac{37 \cdot 38}{2} + 1 = 704$, which is still reasonable for any LMI solver.

Figures 4.27 and 4.28 show the evolution of the predicted state set and the outer approximation of the state estimation set at the time instant $k = 1$, $k = 8$, respectively. Comparing these figures confirms the contractiveness of the guaranteed state estimation. Figures 4.29, 4.30 show the obtained guaranteed bounds on x_1 and x_2, respectively. The real states (black star) are found inside these bounds, which confirms good performance of the estimation. Figure 4.31 shows the evolution of the zonotopic guaranteed state estimation. Note that these guaranteed bounds and the volume of zonotope are decreased in time leading to a more and more accurate estimation.

Table 4.6 shows the computation time of the PMI approach after 50 time instants. Even if the solution of the PMI problem is computed off-line, the computation time of this approach is significantly increased due to the big number of decision variables in the LMIs problem (4.92) (the reader can compare Table 4.5 and Table 4.6). Even if the contractiveness property of the guaranteed state estimation is always preserved, the proposed method gives an unsatisfying result of estimation. The poor result of estimation obtained in this example may be due to the relaxation method used to solve the PMI optimization problem. To reduce the conservatism of this solution, a higher order of the LMI relaxation (a higher order ofthe moment matrix M_1) can be used leading to a more complex LMI optimization problem than the first order LMI relaxation (see [62]). In the recent paper [63], the author proposed an inner approximation of the PMI set instead of the outer approximation [62] used in this example which can lead to a less conservative result of the guaranteed state estimation.

To conclude, Table 4.6 recapitulates the complexity and the performance of the proposed approaches to solve the estimation problem for the Multi-Output system, numbers from 1 to 5 being associated to each approach. The number 1 means the best accuracy and the less complexity of the computation. The number 5 means the worst accuracy and the most complex from the computation point of view.

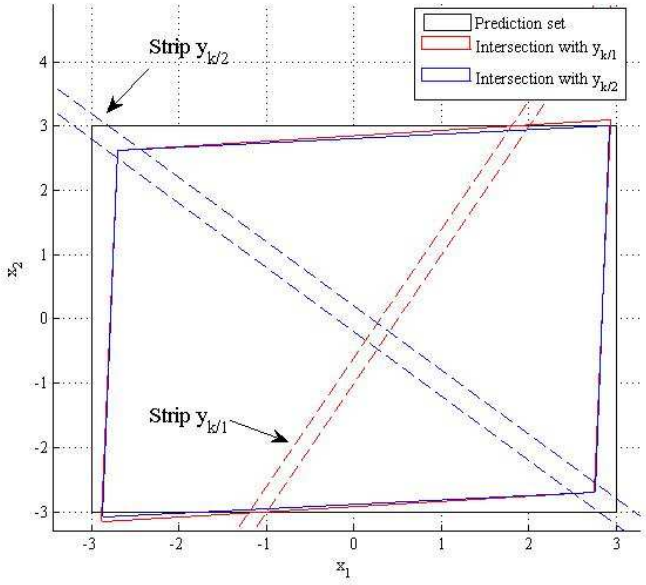

Figure 4.27: Guaranteed state estimation at the time instant $k = 1$

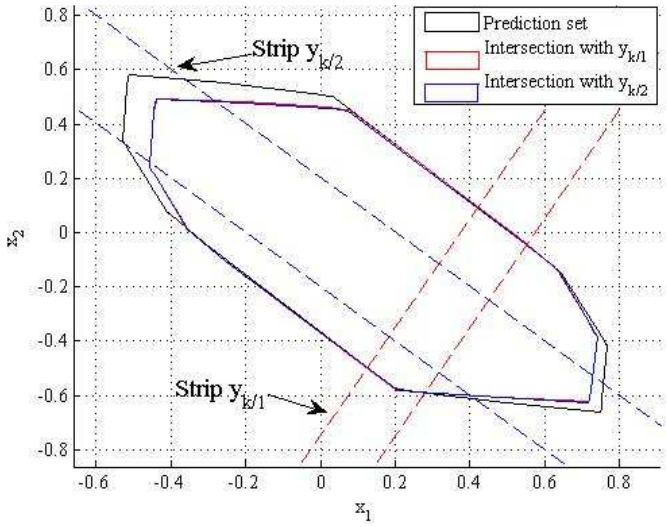

Figure 4.28: Guaranteed state estimation at the time instant $k = 8$

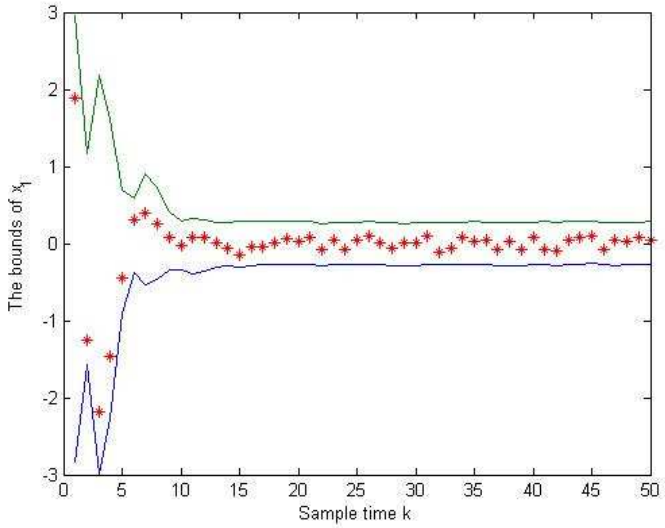

Figure 4.29: Guaranteed bounds of x_1 by PMI-based approach

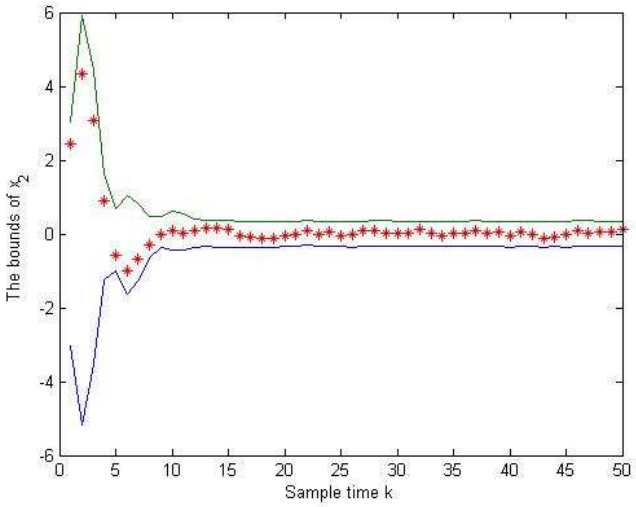

Figure 4.30: Guaranteed bounds of x_2 by PMI-based approach

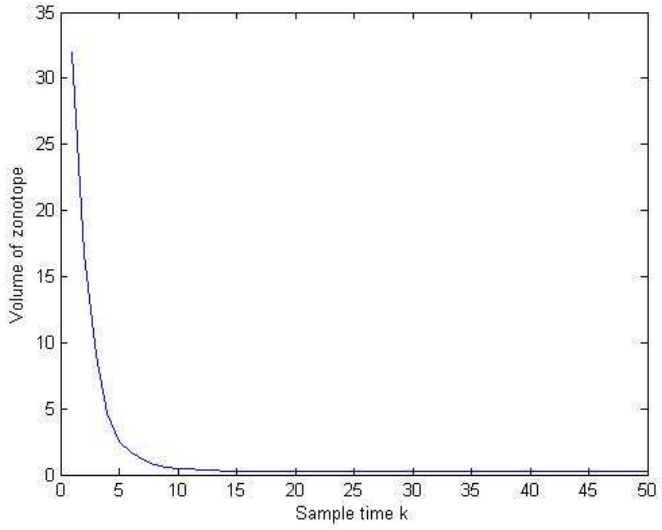

Figure 4.31: Evolution of the volume of the guaranteed state estimation obtained by PMI-based approach

Table 4.6: Total computation time of Example 4.5 after 50 time instants

Algorithm	Time(second)
PMI algorithm (without off-line LMI relaxed optimization included)	0.0780
PMI algorithm (with off-line LMI relaxed optimization included)	3436.1

Table 4.7: Table of recapitulation of different estimation approaches (Multi-Output case)

Algorithm	Complexity	Accuracy
Segment minimization method	1	4
Volume minimization method	4	1
ESO method	2	3
ESOCE method	2	2
PMI method	5	5

To avoid solving a PMI problem and its inconvenient related to its poor performance due to the choice of the relaxation procedure, in the next part a new solution will be proposed to avoid solving the PMI optimization problem.

4.3.4 Polytope and Zonotope intersection approach for Multi-Output systems

In the previous subsections, the guaranteed state estimation set is obtained using step by step algorithms (ESO method, ESOCE method and PMI based method). This means that the predicted state set intersects with the first measurement leading to a zonotopic outer approximation of this intersection. Then this approximation is intersected with the second measurement leading to a zonotopic outer approximation of this intersection and so on. This step by step algorithm does not quite respect Algorithm 4.2, where the measurement consistent state set induced by the measurement is intersected with the predicted state set. Moreover, the order used to take into account the different measurements is important. The different order used gives a different result of the state estimation, thus all the possible re-arrangements of the output vector components must be tested to find the optimum order. All these tests lead to increased the computation complexity.

The new solution, called Polytope and Zonotope Intersection (PAZI), proposed in this subsection consists in intersecting directly the measurement consistent state set with the predicted state set. As each measurement is represented by a strip $|c_i^T x - y_{k/i}| \leq \sigma_i$, the measurement consistent state set is the intersection of n_y strips or more precisely a H-polytope. As the predicted state set is a zonotope, it is convenient to determine the intersection between a zonotope and a polytope. The problem of finding the intersection between a zonotope Z and a polytope P can be solved in an easy way: the zonotope Z is transformed from the generator representation to the H-representation. Then the intersection between Z and Po can be easily computed using the Multi-Parametric Toolbox (MPT) [79]. This way gives an exact computation of the intersection between the zonotope Z and the polytope Po. Unfortunately, this intersection is not always a zonotope and is represented by a polytope in the H-representation. In order to continue the next step, an outer approximation of this polytope by a zonotope must be found. In the literature, the approximation of a polytope by a zonotope is studied by many authors; however this problem still remains complex (see [141], [11], [59]). Therefore, to overcome this difficult problem, a an original simpler way to have a zonotope represented by its generators characterizing the intersection between a polytope and a zonotope will be presented below.

***Proposition* 4.3.** Given the zonotope $Z = p \oplus H\mathbf{B}^r \subset \mathbb{R}^n$, the polytope $Po = \{x \in \mathbb{R}^n : |Cx - d| \leq \begin{bmatrix} \sigma_1 \\ \vdots \\ \sigma_m \end{bmatrix}\}$ $(d \in \mathbb{R}^m,\ \sigma_i \in \mathbb{R}^+,\ i = 1, \ldots, m)$ and

the matrix $\Lambda \in \mathbb{R}^{n\times m}$, define a vector $\hat{p}(\Lambda) = p + \Lambda(d - Cp) \in \mathbb{R}^{n_x}$ and a matrix $\hat{H}(\Lambda) = \begin{bmatrix}(I - \Lambda C)H & \Lambda\Sigma\end{bmatrix}$ with $\Sigma = \begin{bmatrix}\sigma_1 & 0 & \dots & 0 \\ 0 & \sigma_2 & \dots & 0 \\ \vdots & \vdots & \ddots & \vdots \\ 0 & 0 & \dots & \sigma_m\end{bmatrix} \in \mathbb{R}^{m\times m}$ a diagonal matrix . Then a family of zonotopes (parameterized by the matrix Λ) that contains the intersection of the zonotope Z and the polytope Po is obtained such as $Z \cap Po \subseteq \hat{Z}(\Lambda) = \hat{p}(\Lambda) \oplus \hat{H}(\Lambda)B^{r+m}$.

Proof Consider an element $x \in Z \cap Po$, on one hand this means that $x \in Z = p \oplus H\mathbf{B}^r$. Using the definition of a zonotope implies that there exists a vector $s_1 \in \mathbf{B}^r$ such that:

$$x = p + Hs_1 \tag{4.94}$$

Adding and subtracting ΛCHs_1 to the previous equality leads to the following expression:

$$x = p + \Lambda CHs_1 + (I - \Lambda C)Hs_1 \tag{4.95}$$

On the other hand, from $x \in Z \cap Po$, it is inferred that:

$$x \in Pp = \{x \in \mathbb{R}^n : |Cx - d| \leq \begin{bmatrix}\sigma_1 \\ \vdots \\ \sigma_m\end{bmatrix}\} \tag{4.96}$$

Thus, there exists a vector $s_2 \in \mathbf{B}^m$ such that $Cx - d = \Sigma s_2$. Taking into account the form of the vector x given by (4.94) leads to $C(p+Hs_1)-d = \Sigma s_2$, which is equivalent to $CHs_1 = d-Cp+\Sigma s_2$. Substituting CHs_1 in equation (4.95), the following expression is obtained:

$$\begin{aligned} x &= p + \Lambda(d - Cp + \Sigma s_2) + (I - \Lambda C)Hs_1 \\ &= p + \Lambda(d - Cp) + \Lambda\Sigma s_2 + (I - \Lambda C)Hs_1 \end{aligned} \tag{4.97}$$

After simple computations and using the notation defined in Proposition 4.3, the following form is obtained:

$$x = \hat{p}(\Lambda) + \begin{bmatrix}(I - \Lambda C)H & \Lambda\Sigma\end{bmatrix}\begin{bmatrix}s_1 \\ s_2\end{bmatrix} = \hat{p}(\Lambda) \oplus \hat{H}(\Lambda)\begin{bmatrix}s_1 \\ s_2\end{bmatrix} \tag{4.98}$$

and the following inclusion holds:

$$x = \hat{p}(\Lambda) \oplus \hat{H}(\Lambda)\begin{bmatrix}s_1 \\ s_2\end{bmatrix} \in \hat{p}(\Lambda) \oplus \hat{H}(\Lambda)\mathbf{B}^{r+m} = \hat{X}(\Lambda). \tag{4.99}$$

□

This proposition is illustrated in the following example.

***Example* 4.7.** Consider a centered zonotope $Z(p;H)$ with $p = \begin{bmatrix}0 & 0\end{bmatrix}$ and $H = \begin{bmatrix}0.1 & 0.2 & 0.3\\ 0.3 & 0.2 & 0.1\end{bmatrix}$ and a polytope Po described by the intersection of 3 strips: $|Cx - d| < \begin{bmatrix}\sigma_1\\ \sigma_2\\ \sigma_3\end{bmatrix}$, with $C = \begin{bmatrix}5 & 1\\ -4 & 1\\ 1 & 2\end{bmatrix}$, $d = \begin{bmatrix}-0.1163\\ -0.2935\\ -0.6928\end{bmatrix}$, $\sigma_1 = 0.2$, $\sigma_2 = 0.2$ and $\sigma_3 = 0.3$.

Figure 4.32 shows a zonotopic outer approximation of the zonotope Z and the polytope Po using Proposition 4.3. The matrix Λ is determined using the minimization of segments of the zonotope which is simple to compute $\Lambda = \begin{bmatrix}0.1123 & -0.1044 & 0.0035\\ 0.1914 & 0.2646 & 0.2026\end{bmatrix}$. As Λ is a free matrix, the method of computation of Λ can influence on the quality of the approximation.

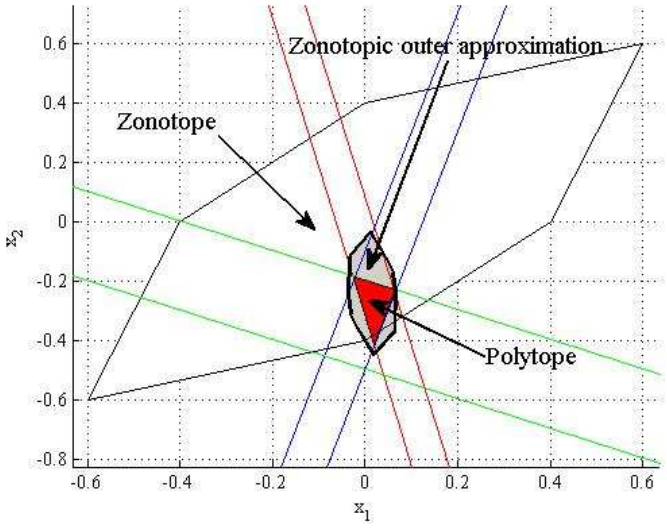

Figure 4.32: Outer approximation of the the intersection between a zonotope and a polytope

Similar to the previous subsections, the predicted state set is computed by (4.6). The measurement consistent state set X_{y_k} is a polytope described by:

$$X_{y_k} = \{x \in \mathbb{R}^n : |Cx - y_k| \leq \begin{bmatrix}\sigma_1\\ \vdots\\ \sigma_{n_y}\end{bmatrix}\} \tag{4.100}$$

Thus, the exact uncertain state set is the intersection between $\bar{X}_k$ (a zonotope) and X_{y_k} (a polytope). Using Proposition 4.3 the guaranteed state estimation of the Multi-Output system (4.5) obtained by intersecting the zonotope $\bar{X}_k$ and the polytope X_{y_k} is a family of zonotopes parameterized by the matrix Λ:

$$\hat{X}_k(\Lambda) = \hat{p}_k(\Lambda) \oplus \hat{H}_k(\Lambda)\mathbf{B}^{r+n_x+n_y} \tag{4.101}$$

with $\hat{p}_k(\Lambda) = A\hat{p}_{k-1} + \Lambda(y_k - CA\hat{p}_{k-1})$
and $\hat{H}_k(\Lambda) = \begin{bmatrix}(I-\Lambda C)A\hat{H}_{k-1} & (I-\Lambda C)F & \Lambda\Sigma\end{bmatrix}$.

This matrix Λ is computed such that the P-radius of the guaranteed state estimation is non-increasing. Similar to the procedure in the previous subsection this condition leads to the following optimization problem:

$$\max_{\tau,\beta,P,Y} \tau$$

subject to

$$\begin{cases} \frac{(1-\beta)P}{\sigma_1^2+\ldots+\sigma_{n_y}^2+\max\limits_{s\in\mathbf{B}^{n_x}}\|Fs\|_2^2} \succeq \tau I \\ \begin{bmatrix} \beta P & 0 & 0 & A^TP - A^TC^TY^T \\ * & F^TF & 0 & F^TP - F^TC^TY^T \\ * & * & \Sigma^T\Sigma & Y^T\Sigma \\ * & * & * & P \end{bmatrix} \succeq 0 \\ \tau > 0 \end{cases} \tag{4.102}$$

with a change of variables $Y = P\Lambda$.

***Remark* 4.11.** In this optimization problem (4.102), the decision variables are: $P = P^T \in \mathbb{R}^{n_x\times n_x}$, $Y \in \mathbb{R}^{n_x\times n_y}$, $\beta \in (0,1)$ and $\tau \in \mathbb{R}$. The total number of the scalar decision variables is $\frac{n_x(n_x+1)}{2}+n_xn_y+2$. The dimensions of matrix inequalities in (4.102) are $n_x \times n_x$, $(3n_x+n_y)\times(3n_x+n_y)$, 1, respectively. The dimensions of matrix inequalities and the number of scalar decision variables of this method is similar to the other methods (ESO, ESOCE) but the number of matrix inequalities is less than the one of ESO and ESOCE methods.

***Remark* 4.12.** The goal of computing all of the correction factors λ_i as mentioned in the PMI approach is obtained by the proposed solution in this subsection. Moreover, the number of scalar decision variables of this optimization problem is significantly decreased in comparison with the one of the relaxed LMIs obtained from the PMI approach.

The following schema recaps the proposed methods to solve the estimation problem for Multi-Output systems.

***Example* 4.8.** Consider the following linear variant Multi-Output system:

$$\begin{cases} x_{k+1} = \begin{bmatrix} 0 & -0.5 \\ 1 & 1+0.3\delta \end{bmatrix} x_k + \begin{bmatrix} 0.1 & 0 \\ 0 & 0.1 \end{bmatrix} \omega_k \\ \\ y_k = \begin{bmatrix} -2 & 1 \\ 1 & 1 \end{bmatrix} x_k + \begin{bmatrix} 0.2 & 0 \\ 0 & 0.2 \end{bmatrix} v_k \end{cases} \tag{4.103}$$

The disturbances and the noises are always considered bounded by w_k, $v_k \in \mathbf{B}^2$. The initial state is unknown but belongs to the box $3\mathbf{B}^2$. The proposed method PAZI will be compared with the Singular Value Decomposition method [37], and the ESOCE method. Note that, the comparison is done only with the Singular Value Decomposition method because in the literature only this method can solve the case of Multi-Output systems.

The solution of the PAZI approach (4.102) obtained by *Penbmi* solver gives $\beta = 0.0452$, $\Lambda = \begin{bmatrix} -0.3136 & 0.2678 \\ 0.3591 & 0.5811 \end{bmatrix}$ and the solution of Algorithm 4.4 is $\lambda_1 = \begin{bmatrix} -0.2108 \\ 0.5784 \end{bmatrix}$, $\lambda_2 = \begin{bmatrix} 0.2946 \\ 0.5420 \end{bmatrix}$.

The simulation results are shown in Figures 4.33, 4.34, 4.35. The guaranteed state estimation obtained by the PAZI method is quickly decreased at each sample time (Figure 4.33). Figures 4.34 and 4.35 compare the performance of the proposed method with the one of the Singular Value Decomposition method (Subsection 4.2.1 and [37]) and the one of the ESOCE method. The bound obtained by the proposed method are smaller (compared in percent) than the one obtained by the singular value decomposition method with a reduced complexity of the computation (see Table 4.8). Moreover, this polytope intersection solution obtains a similar performance of the estimation as the performance of the ESOCE method but the computation time is significantly decreased (0.2808s and 1.4464s comparing the result of Table 4.8).

Table 4.8: Total computation time of Example 4.6 after 50 time instants

Algorithm	Time(second)
Polytope and Zonotope Intersection algorithm (without off-line optimization included)	0.0468
Polytope and Zonotope Intersection algorithm (with off-line optimization included)	0.2808
Singular Value Decomposition algorithm [37]	1.5444

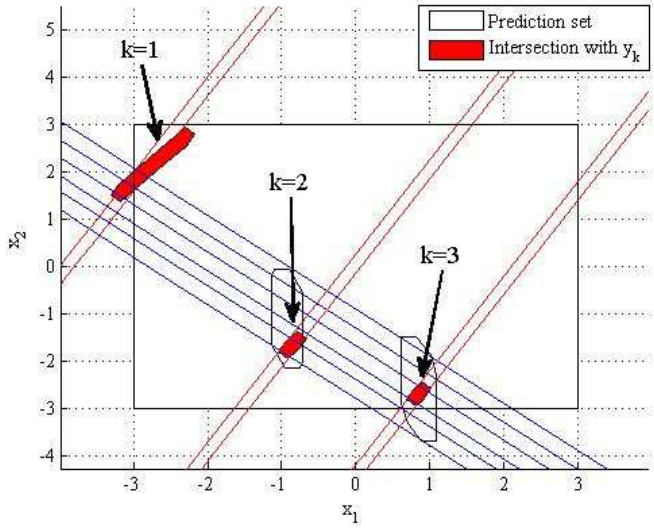

Figure 4.33: Evolution of the guaranteed state estimation obtained by PAZI approach

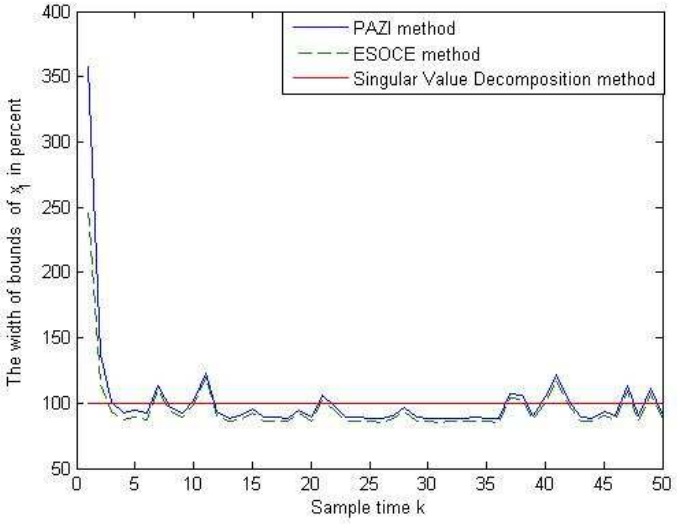

Figure 4.34: Comparison of the bound's width of x_1 in Example 4.6 obtained by different methods in percent

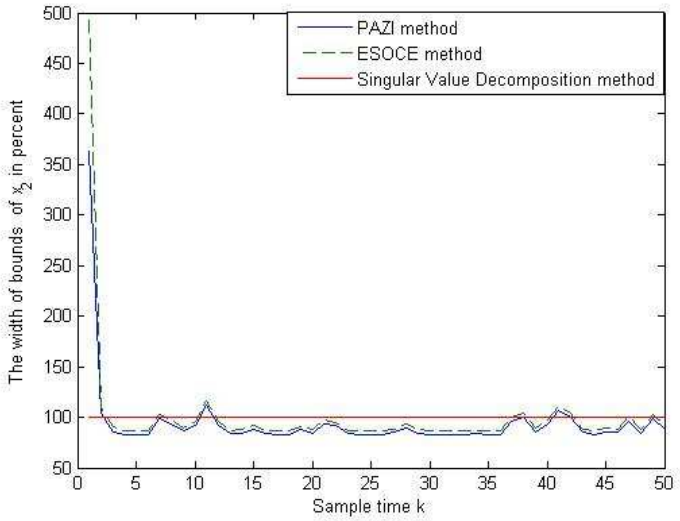

Figure 4.35: Comparison of the bound's width of x_2 in Example 4.6 obtained by different methods in percent

4.4 Conclusion

This chapter proposes an exhaustive methodology to compute a zonotopic set containing all the possible states of the system that are consistent with the uncertain model and the measurement noise at each sample time. The chapter begins with the state of the art on the state estimation technique. When the system is modeled by the deterministic approach, the set-membership estimation using zonotopes is proposed as a suitable solution. A recall on the zonotopic set-membership techniques presented in the literature is done. The zonotopic set-membership procedures presented in this chapter are illustrated in Figure 4.36, where the contributions of this PhD thesis have been highlighted in red blocks. This permits to give a general view on the advantages and the problems of each methodology.

The main part of this chapter consists in introducing a new methodology to compute a zonotopic outer approximation of the exact uncertain state set based on the minimization of the P-radius of this zonotopic guaranteed state estimation. The proposed method permits to overcome the weak points of the existent methods: minimization of the segments and of the volume of the zonotope [2] and Singular Value Decomposition method [37]. The size of this zonotopic guaranteed state estimation is non-increasing at each sample time leading to a more and more accurate estimation after each time instant.

The complexity of the computation is reduced by performing an off-line optimization problem which is a major advantage for real-time applications. The problem is firstly solved for the linear discrete time invariant system with Single-Output. By using the maximum principle [122], the proposed method is extended to the case of Single-Output linear stable discrete-time systems with interval uncertainties. Based on the result for Single-Output system, the solution for Multi-Output systems is next developed. The simplest solution should be to consider a multi-output system as a several separated Single-Output systems. But this solution leads to a conservative result due to neglecting the coupling effect of Multi-Output system.

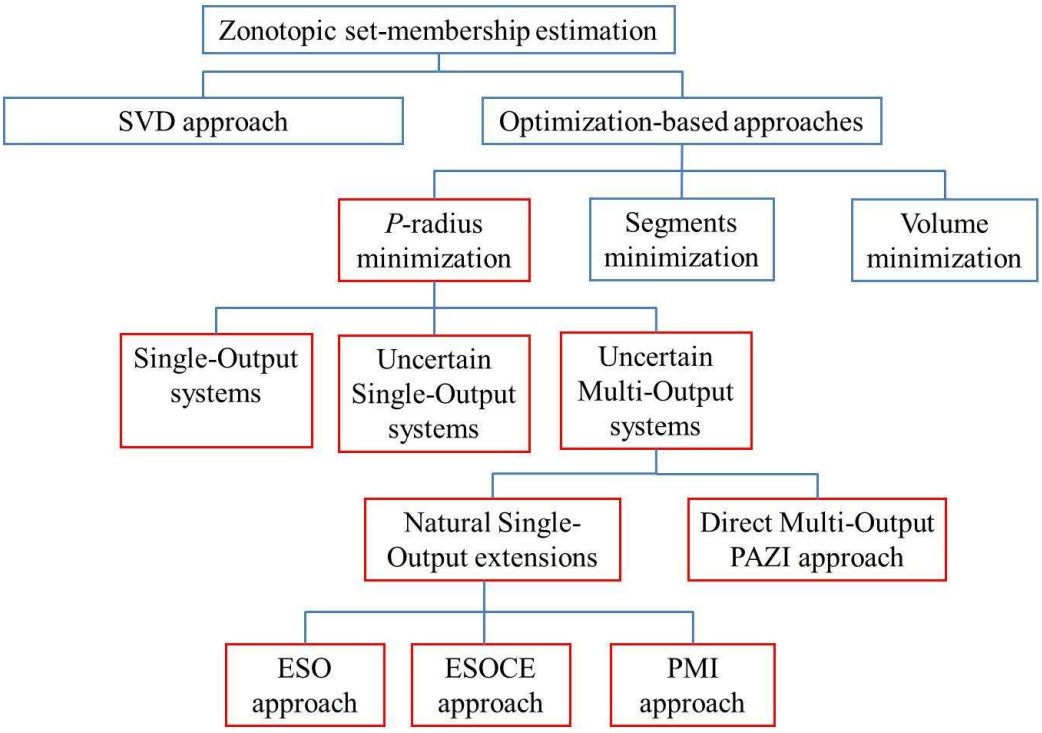

Figure 4.36: Classification of the zonotopic guaranteed state estimation methods

To improve the estimation performance, another solution is proposed. Compute the correction factor λ_i (corresponding to the i-th measurement) successively in the same way as in the first solution, while considering known the previous correction factors $\lambda_1, \ldots, \lambda_{i-1}$. If all the correction factors λ_i are computed at the same time, this leads to a PMI optimization problem which is difficult to solve. The LMI relaxation approach proposed by [62]

is further used to find a sub-optimal solution of this PMI problem, but the size and the number of decision variables of the obtained LMIs can become very large. In addition, the performances of the proposed methods depend on the order of the measurement, and thus on the order of computing the correction factors. The best results must be chosen from all the $n_y!$ possible orders, increasing the time computing. The proposed solutions can solve the Multi-Output problem but these methods do not directly compute the measurement consistent state set X_{y_k} as mentioned in Algorithm 4.2, which is a polytope (intersection of finite number of half-spaces). In order to overcome the mentioned problems introduced by the Multi-Output system, another new solution is proposed. This solution is based on the approximation of the intersection of a polytope and a zonotope. Thus, in Subsection 4.3.4 an improved result is presented which consists in a zonotopic approximation of the intersection between a zonotope and a polytope. The simulation result shows an improvement of the estimation performance and the computation time compared to existing approaches.

Finally, the proposed set-membership estimation by zonotopes in this chapter will be used in the context of output feedback control for uncertain systems in the next chapter.

Chapter 5

Model Predictive Control based on zonotopic set-membership estimation

5.1 Introduction

Model Predictive Control (MPC) can be considered today as a mature domain, both from the research and the industrial applications points of view. The application of MPC can be found in many industrial processes (e.g. petroleum industry [49], aerospace [21]), specially when the trajectory to be tracked by the system is given in advance, such as the trajectory of a robot arm [34]. The large application of MPC [117] is mainly due to an easy implementation, a generic solution that can deal both with SISO and MIMO systems and, the most important, to its ability to handle hard constraints, which often appear when dealing with real plants [29], [54]. The strategy of MPC can be decomposed into three steps:

1. Based on the appropriate system model the system output is predicted at a future time horizon;

2. A control sequence is computed by optimizing an objective function on the future behavior of the system, and then only the first element of the control sequence is applied;

3. The horizon is receded into the future, and the computation is repeated at the next time instant.

Due to the receding strategy, the MPC is also called receding horizon predictive control or moving horizon control. From this algorithm, it must be

noticed that the role of the system model is important and thus the choice of the model influences the performance of the MPC strategy. However, if the performance of the controlled system is not "good enough", the system modeling can be reworked in order to choose a better model [123].

The receding horizon control strategy is illustrated in Figure 5.1. The future output is predicted over a horizon N_y called the prediction horizon. The control sequence of length N_u ($N_u \leq N_y$) is computed by minimizing an objective function to track the reference trajectory. Then the first element of the control sequence $u(k)$ is applied to the system. The difference between the MPC and the classical control is that in the MPC case, the control law is determined from the future error between the system output and the reference and in the classical control, the action is computed from the error in the past. Thus, when the desired trajectory is known, the MPC technique is more natural than the classical control.

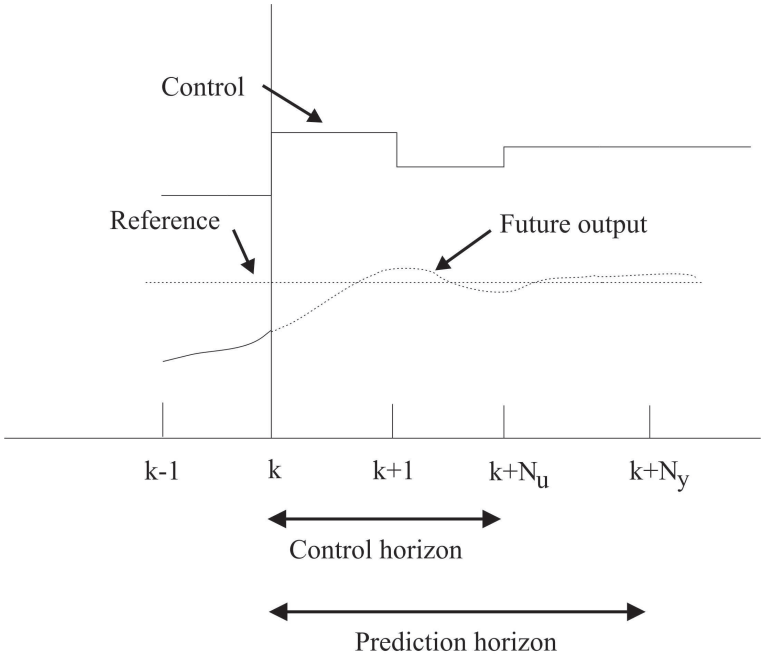

Figure 5.1: Strategy of Model Predictive Control

To better understand the principle of MPC, let us have a look on the history of predictive control. That started at the end of 70's. In the following, a list of some popular algorithms of MPC is presented.

- Model predictive heuristic control (MHRC) or later known as Model algorithmic control (MAC) is proposed in [121]. This technique is used

to control a multivariable industrial process. The control which is based on an impulse response model is computed by minimizing the tracking error.

- Dynamic Matrix Control (DMC) proposed in [41] uses the step response to predict the trajectory of the future output and then minimizes the prediction error.

- Extended Horizon Adaptive Control (EHAC) is developed in [149] based on a parametric process model. This strategy elaborates a control sequence in order to minimize the error between the reference and the future output which is computed by solving a Diophantine equation at a period of time after the process delay.

- Extended Prediction Self-Adaptive Control (EPSAC) proposed by De Keyser and Van Cauwenberghe in [43] uses a discrete transfer function and a constant control signal while using a sub-optimal predictor instead of solving a Diophantine equation used in EHAC method.

- Generalized Predictive Control (GPC) is one of the most popular approaches proposed in [35]. This technique is based on a Controlled Auto-Regressive Integrated Moving Average (CARIMA) model which can track both varying and constant future set-points. There are some other predictive controllers based on the same idea such as: Predictive Functional Control (PFC) [121], Multipredictor Receding Horizon Adaptive Control (MURHAC) [90], Multistep Multivariable Adaptive Control (MUSMAR) [55], Unified Predictive Control (UPC) [133].

- Constrained Receding Horizon Predictive Control (CRHPC) developed by Clarke and Scatollini in [36] imposes an additional terminal equality constraints on the output over a finite horizon beyond the prediction horizon.

- State-space Model Predictive Control is a mature predictive control technique [108] based on the use of a state-space model. This model facilitates the stability study [70], [128], [101] and the generalization of MPC to multivariable systems, non-linear systems and systems with disturbances and measurement noises. Moreover, when the system state is not available as mentioned in the previous chapter, it is more convenient to implement a state estimation (Luenberger observer, Kalman filter, set-membership estimation).

Due to the existence of uncertainties in the mathematical model, the robustness of the MPC became a key problem. The robust MPC in the presence of uncertainties and disturbances is studied by many authors [30], [73], [146], [96], [17] [101], [80], [102], [100], [33], [111], [135]. A simple way to deal with the model uncertainty is to take into account these uncertainties in the optimization problem, it means that the online optimization problem on the objective function is transformed into a min-max problem with constraints (the worst case of the objective function is computed on the uncertainty set and then this value of the worst case is minimized) [30]. In [73] and [146], an upper-bound of the worst case is determined and then the min-max problem is transformed to a LMI optimization problem. To simplify the computation, [4] proposed a sub-optimal solution based on a quadratic programming (QP) problem. Other ways to enhance robustness are based on the deterministic model predictive control by ignoring the disturbances over the prediction horizon [129], [33], [92], [102], [100]. These methods require full knowledge of the state which usually cannot be reached due to measurement noises acting on real systems. In [146], [100], the Luenberger observer is implemented to estimate the system state. In the previous chapter, the set-membership estimation has proven its efficiency in estimating the system state in the presence of uncertainties. In addition, in [17], the author used the set-membership estimation based on parallelotopes to estimate the state. Due to the efficiency of the zonotopes, in this chapter the application of the set-membership estimation using zonotopes in the context of robust MPC is considered.

5.2 General set-up

Consider the general description of a Multi-Output linear discrete-time invariant system:

$$\begin{cases} x_{k+1} = Ax_k + Bu_k + F\omega_k \\ y_k = Cx_k + v_k \end{cases} \tag{5.1}$$

where $x_k \in \mathbb{R}^{n_x}$ is the state of the system, $y_k \in \mathbb{R}^{n_y}$ is the measured output at time instant k. The vector $\omega_k \in \mathbb{R}^{n_x}$ represents the state perturbation vector and $v_k \in \mathbb{R}^{n_y}$ is the measurement noise. It is assumed that the uncertainties and the initial state are bounded by the following sets: $\omega_k \in W$, $v_k \in V$ and $x_0 \in X_0$, with W a zonotope containing the origin, V a box and X_0 a zonotope.

The system (5.1) is subject to state and input constraints: $x_k \in X$, $u_k \in U$, where X and U are two compact and convex sets containing the origin as an interior point. It is assumed that system (5.1) is stabilizable and

detectable. In the sequel, two control techniques will be considered. First, an open-loop model predictive control which is simple to apply is presented. Despite its simplicity, this technique does not guarantee the stability and the feasibility of the control law. For this reason, a feedback control based on invariant tube of uncertain trajectories [100] is presented. This control permits to improve the performance of the control system and it can also guarantee the stability of the system and the feasibility of the control law.

5.3 Open-loop MPC design

In this section, a simple MPC control law is proposed to control the system (5.1). Because the system (5.1) is subject to disturbances and measurement noises, the system state is unavailable and is estimated using the zonotopic set-membership estimation based on the P-radius minimization. Due to the non-increasing property of the guaranteed state estimation based on the P-radius optimization, the bound of the estimation error is non-increasing in time. Thus, the simplest solution to control this system is to neglect the estimation errors and to use the state estimation as if it were the true system state. If the state estimation is controlled to steer to the desired point, then the true state which belongs to the guaranteed state estimation converges to a set containing this point.

As mentioned in the previous subsection, Model Predictive Control solves online an optimization problem at each time instant and the performance measure largely used in the MPC history is the quadratic norm [100], [33], [92], [80]. By using this norm, the large deviation is penalized more than the small deviation. In addition, due to the use of the quadratic norm, a connection between predictive control and linear quadratic control (LQ) is immediate. In MPC context, another norm can be used to formulate the optimization problem: the 1-norm or the ∞-norm [30], [6]. The advantage of using the 1-norm and ∞-norm is that the optimization problem can be solved using linear programming. However, using these norms leads sometimes to a deterioration of the closed-loop performance [120]. Moreover, with the development of powerful solvers the quadratic programming optimization in the quadratic norm cost function can be easily solved.

The control objective is to have the system output following a desired reference trajectory. To solve this tracking problem, define the following cost function:

$$J_k = \sum_{i=1}^{N} \|\hat{y}_{k+i} - y_{k+i}^{ref}\|_Q^2 + \sum_{i=0}^{N-1} \|u_{k+i} - u_{k+i}^{ref}\|_R^2 \tag{5.2}$$

with $\hat{y}_{k+i} = C\hat{x}_{k+i}$ and $\hat{x}_{k+i}$ the center of the zonotopic guaranteed state estimation set at time instant $k+i$, N the prediction horizon, y_{k+i}^{ref} the desired future output, u_{k+i}^{ref} the desired future input. The weighting matrix Q is a symmetric positive definite matrix and the weighting matrix R a positive definite matrix. This optimization problem is subject to the following constraints:

$$\begin{cases} u_{k+i} \in U, i = 0, \ldots, N-1 \\ x_{k+i} \in X, i = 1, \ldots, N \end{cases} \tag{5.3}$$

With the notations used in Chapter 4, suppose the guaranteed state estimation at time instant k:

$$\hat{X}_k = p_k \oplus H\mathbf{B}^r \in X \tag{5.4}$$

The state constraint can be reformulated as follows.

As the estimated state $\hat{x}_k$ is the center of the zonotope $\hat{X}_k$ (i.e. $\hat{x}_k = p_k$), there exists a value of $s \in \mathbf{B}^r$ such that:

$$x_k = \hat{x}_k + Hs \tag{5.5}$$

Assume that the state constraint X is described in the H-representation form: $H_1 x \leq K_1$. Thus the condition $x_{k+1} \in X$ can be rewritten as follows:

$$x_{k+1} = Ax_k + Bu_k + \omega_k \in X \tag{5.6}$$

Replacing x_k by the expression (5.5) leads to:

$$x_{k+1} = A\hat{x}_k + AHs + Bu_k + \omega_k \in X \tag{5.7}$$

Using the H-representation of X, the condition $x_{k+1} \in X$ is equivalent to $H_1 x_{k+1} \leq K_1$, thus a sufficient condition for (5.7) is the following:

$$H_1 Bu_k \leq K_1 - H_1 A\hat{x}_k - \max_s H_1 AHs - \max_{\omega_k} H_1 \omega_k \tag{5.8}$$

Due to the convex property of $\mathbf{B}^2$ and W, the terms $\max_s H_1 AHs$ and $\max_{\omega_k} H_1\omega_k$ are easily computed using the maximum principle. Similar to this procedure, the constraint $x_{k+i} \in X$ can be described in the form of linear inequality on u_{k+i-1}, with $i = 1, \ldots, N-1$. The control applied to the system is the solution of the optimization problem $\min_{u_{k+i}} J_k$ subject to the constraint (5.3). This control law is illustrated in the next example.

***Example* 5.1.** Consider the following system [17]:

$$\begin{cases} x_{k+1} = \begin{bmatrix} 1.6463 & -0.7866 \\ 1 & 0 \end{bmatrix} x_k + \begin{bmatrix} 1 \\ 0 \end{bmatrix} u_k + \omega_k \\ y_k = \begin{bmatrix} 0.1404 & 0 \end{bmatrix} x_k + v_k \end{cases} \tag{5.9}$$

The disturbance ω_k and the measurement noise v_k are assumed to be bounded: $\|\omega_k\|_\infty \leq 0.01$, $|v_k| \leq 0.05$. The initial state belongs to the box $0.25\mathbf{B}^2$. The control objective is to make the output y_k track the reference $y^{ref} = 1$. The weighting matrices in the cost function are $Q = I_2$ and $R = 0.1$. The prediction horizon is $N = 4$. This system is subject to the hard constraint:

$$-1 \leq \begin{bmatrix} -1.9313 & 2.2121 \end{bmatrix} x_k \leq 3 \tag{5.10}$$

Figure 5.2 illustrates the evolution of the zonotopic guaranteed state estimation based on the P-radius minimization which is stabilized around the equilibrium point. Figure 5.3 shows that the output system tracks well the reference $y^{ref} = 1$. Figure 5.4 shows that the system fulfills the state constraint (5.10) (the constraint value is between -1 and 3). Even if the result simulation shows a good tracking performance the open loop MPC does not have any stability guarantees for the controlled system or any feasibility proof of the optimization problem (5.2). For this reason in the next subsection, a different scheme of MPC with stability and feasibility guarantees will be presented.

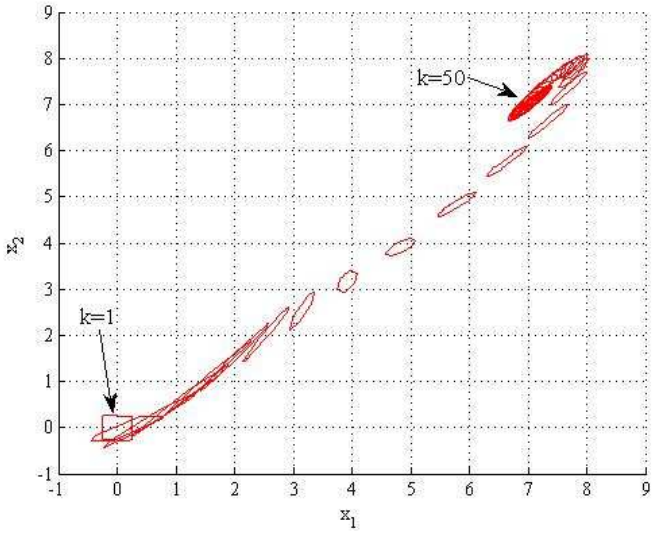

Figure 5.2: Evolution of the state estimation set

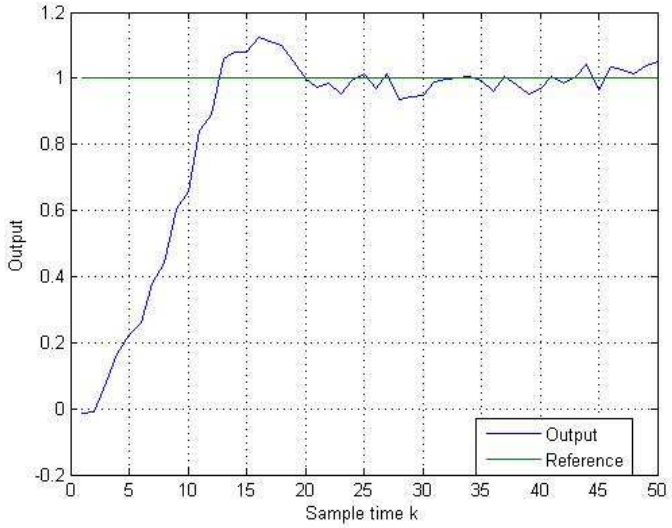

Figure 5.3: Evolution of the system output and reference output

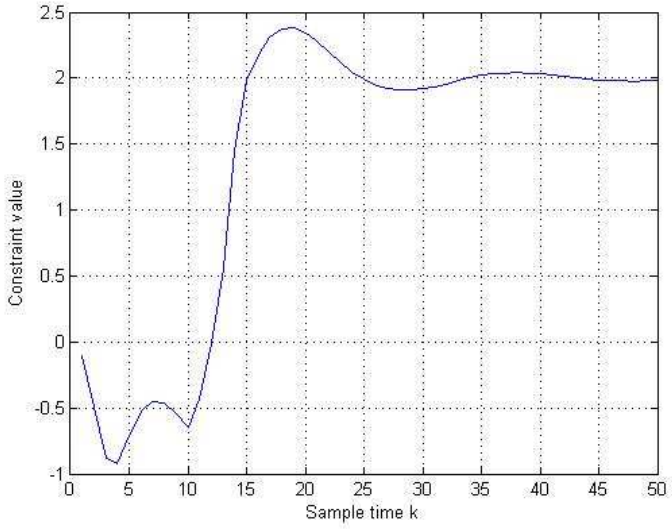

Figure 5.4: Evolution of the constraint value in (5.10)

5.4 Tube-based output feedback MPC design

Different to the proposed control law in the previous section, which is an open-loop MPC control, in this section another MPC technique is proposed based on feedback control, which can be less conservative specially when uncertainties are present [89], [16], [18], [101]. In feedback MPC, the decision variable is a control policy, which is a sequence of control laws. In this section, a feedback MPC, called Tube-based Model Predictive Control (TMPC), is presented. The idea of the TMPC is to construct a tube of all the possible trajectories around the nominal trajectory ensuring robust constraints satisfaction and stability guarantees of the controlled system, using invariant set techniques. During the last years, the TMPC has been investigated by many authors: [80], [33], [102], [92], [91], [100]. In the following part, the TMPC developed in [102], [100] will be summarized. In this approach, the optimization problem of the true system state is replaced by the nominal state one (the state of the nominal system which is not influenced by disturbances and measurement noises). In addition, the nominal state is considered as a decision variable in the optimal control problem solved online. This consideration permits to facilitate the proof of stability and attractivity of the terminal set. Moreover, the complexity of the controller is similar to that required for nominal MPC. This technique is developed for LTI systems with the hypothesis that the system states are known [102]. When the system state is unknown, the state is estimated using an observer. Then the estimation error is considered as unknown but bounded uncertainty which can be taken into account in the control law. In [100] the Luenberger observer is used to estimate the system state. The gain matrix of the Luenberger observer plays an important role for the performances of the observer, and thus the global performance of the controlled system. The main difficulty comes from the fact that the choice of this gain matrix is not unique. For this reason, in this section the set-membership estimation presented in the previous chapter is chosen to replace the Luenberger observer to combine with the TMPC. By using this zonotopic set membership estimation, the bound of the error estimation is minimized and, thus, the performance of the controlled system is improved.

Note that for pedagogical reason the same notations as in [100] have been used. Consider now the system (5.1), due to the presence of the disturbances and the measurement noise, the system state is estimated using the zonotopic guaranteed state estimation presented in the previous chapter. The center of the zonotopic guaranteed state estimation at time instant k is considered as the estimation state at time instant k: $\hat{x}_k = \hat{p}_k$. Similar to the equation (4.93) with the added control law u_k, the dynamics of the estimation state

is determined by the following equation:

$$\begin{aligned}\hat{x}_{k+1} &= A\hat{x}_k + Bu_k + \Lambda(y_{k+1} - \hat{y}_{k+1}) \\ &= A\hat{x}_k + Bu_k + \Lambda(y_{k+1} - C(A\hat{x}_k + Bu_k))\end{aligned} \tag{5.11}$$

Replacing $y_{k+1} = Cx_{k+1}+v_{k+1}$, with $x_{k+1} = Ax_k+Bu_k+\omega_k$, this is equivalent to:

$$\begin{aligned}\hat{x}_{k+1} &= A\hat{x}_k + Bu_k + \Lambda(CAx_k + CBu_k + C\omega_k + v_{k+1} - CA\hat{x}_k - CBu_k) \\ &= A\hat{x}_k + Bu_k + \Lambda CA(x_k - \hat{x}_k) + \Lambda C\omega_k + \Lambda v_{k+1}\end{aligned} \tag{5.12}$$

Denote the estimation error as $\tilde{x}_k = x_k - \hat{x}_k$, from the equations (5.1) and (5.12) the dynamics of the estimation error is described by:

$$\tilde{x}_{k+1} = (I - \Lambda C)A\tilde{x}_k + \omega_k^e \tag{5.13}$$

with $\omega_k^e = (I - \Lambda C)\omega_k - \Lambda v_{k+1}$. From the hypotheses $\omega_k \in W$, $v_k \in V$, the following expression holds:

$$\omega_k^e \in W^e = (I - \Lambda C)W \oplus (-\Lambda V) \tag{5.14}$$

Consider that the estimation error at time instant k is bounded by a set S_k^e, the equation (5.13) leads to the following recursive expression:

$$\tilde{x}_{k+1} \in S_{k+1}^e = (I - \Lambda C)AS_k^e \oplus W^e \tag{5.15}$$

In order to ensure the stability of the controlled system, the estimation error must be taken into account in the control law. The main idea behind the design of the TMPC control law comes from the non-increasing property of the set S_{k+1}^e which bounds the future estimation error. In the following, this property is provided by the robust positive invariance of the set S_{k+1}^e, which is defined in the following.

***Definition* 5.1.** [22] A set Ω is called *robust positive invariant set* for the system $x_{k+1} = Ax_k + \omega_k$ subject to the constraints $(x_k, \omega_k) \in (X, W)$, if $Ax_k + \omega_k \in \Omega$ and $\Omega \in X$, $\forall \omega_k \subseteq W$ and $\forall x_k \in \Omega$.

Thus, the *maximal robust positive invariant set* Ω_{max} for the same system is the smallest robust positive invariant set that contains all the robust positive invariant sets of this system. The *minimal robust positive invariant set* Ω_{min} of the same system is the robust positive invariant set which is contained in any robust positive invariant set of this system.

***Proposition* 5.1.** [100] If the set S_0^e is robust positively invariant for the system (5.13), then the sets S_k^e are robust positively invariant for the system (5.13), too. The set sequence $\{S_k^e\}$ is monotonic non-increasing and converges in the Hausdorff metric to a robust positively invariant set $S_\infty^e = (I - \Lambda C)AS_\infty^e \oplus W^e$.

Denote that the original idea behind the use of the zonotopic set membership estimation in this PhD work in comparison with the use of Luenberger observer in [100] is that the matrix Λ is computed to optimize the size of the set S_∞^e.

The observer equation can be rewritten as:

$$\hat{x}_{k+1} = A\hat{x}_k + Bu_k + \omega_k^{co} \tag{5.16}$$

with $\omega_k^{co} = \Lambda(CA\tilde{x}_k + C\omega_k + v_{k+1})$. As $\tilde{x}_k \in S_k^e$, the following expression is true:

$$\omega_k^{co} \in W_k^{co} = \Lambda CAS_k^e \oplus \Lambda CW \oplus \Lambda V \tag{5.17}$$

Because the set sequence $\{S_k^e\}$ is monotonic non-increasing as presented in Proposition 5.1 and W_k^{co} is linearly dependent on S_k^e, thus the set sequence $\{W_k^{co}\}$ is monotonic non-increasing, too.

Consider now the nominal system which is not affected by disturbances:

$$\underline{x}_{k+1} = A\underline{x}_k + B\underline{u}_k \tag{5.18}$$

To counteract the disturbances, the trajectory of the real system is desired to lie close to the nominal system trajectory. If the nominal system is steered to the origin, then the center of the zonotopic state estimation as well as the real state of the system are bounded by a compact set. In order to have all the possible trajectories inside a tube around the nominal trajectory, a control law u_k can be defined as:

$$u_k = \underline{u}_k + K(\hat{x}_k - \underline{x}_k) \tag{5.19}$$

where $\underline{u}_k$ is the control law applied to the nominal system (5.18) at time instant k.

Combining (5.16) and (5.18), the error between the estimation state and the nominal state denoted by $e_k = \hat{x}_k - \underline{x}_k$ satisfies the difference equation:

$$\begin{aligned} e_{k+1} &= \hat{x}_{k+1} - \underline{x}_{k+1} \\ &= (A\hat{x}_k + Bu_k + w_k^{co}) - (A\underline{x}_k + B\underline{u}_k) \end{aligned} \tag{5.20}$$

Replacing u_k by (5.19), e_{k+1} can be further written as:

$$e_{k+1} = (A + BK)e_k + w_k^{co} \tag{5.21}$$

The gain matrix K is chosen such that the matrix $A + BK$ is Schur stable. Consequently, if at time k, e_k lies in the set S_k^{co}, then e_{k+1} lies in the set $S_{k+1}^{co} = (A + BK)S_k^{co} \oplus W_k^{co}$.

***Proposition* 5.2.** [100] If e_0 belongs to an initial set S_0^{co}, then the set sequence $\{S_k^{co}\}$ converges to a robust positive invariant set S_∞^{co} which satisfies $S_\infty^{co} = (A + BK)S_\infty^{co} \oplus W_\infty^{co}$. If S_0^e is robust positive invariant for the system (5.13) and S_0^{co} is robust positive invariant for the system (5.21) with $\omega_0^{co} \in W_0^{co}$, then the set sequence $\{S_k^{co}\}$ is robust positive invariant for the system (5.21) with $\omega_k^{co} \in W_k^{co}$ and monotonic non-increasing ($S_{k+1}^{co} \subseteq S_k^{co}$).

Based on the procedure proposed in [100], let us define $S_k = S_k^e \oplus S_k^{co}$. Because S_k^e and S_k^{co} converge to S_∞^e and S_∞^{co}, respectively, then S_k tends to $S_\infty = S_\infty^e \oplus S_\infty^{co}$.

In this context, the robust TMPC can be summarized as follows. At time k a state estimation set is computed and a nominal optimal control problem is solved online. Define the cost function for the nominal system as:

$$V_N(\underline{x}_k, \underline{u}) = \frac{1}{2} V_f(\underline{x}_{k+N}) + \sum_{i=0}^{N-1} \frac{1}{2} l(\underline{x}_{k+i}, \underline{u}_{k+i}) \tag{5.22}$$

where N is the prediction horizon and $\bar{u}$ is the control sequence:

$$\underline{u} = \{\underline{u}_k, \underline{u}_{k+1}, \ldots, \underline{u}_{k+N-1}\} \tag{5.23}$$

The stage cost function $l(\underline{x}_k, \underline{u}_k)$ and the terminal cost function $V_f(\underline{x}_{k+N})$ are defined by:

$$\begin{cases} l(\underline{x}_k, \underline{u}_k) = \frac{1}{2}(\underline{x}_k^T Q \underline{x}_k + \underline{u}_k^T R \underline{u}_k) \\ V_f(\underline{x}_{k+N}) = \frac{1}{2} x_{k+N}^T P_f \underline{x}_{k+N} \end{cases} \tag{5.24}$$

where P_f, Q, R are positive definite matrices. With these notations, the time varying constraints at current time k are:

$$\begin{cases} \underline{u}_{k+i} \in \underline{U}_{k+i},\ i = 0, \ldots, N-1 \\ \underline{x}_{k+i} \in \underline{X}_{k+i},\ i = 0, \ldots, N-1 \\ \underline{x}_{k+N} \in \underline{X}_f \end{cases} \tag{5.25}$$

with $\underline{U}_{k+i} = U \ominus K S_{k+i}^{co}$ (this tight constraint comes from the equation (5.19)), $\underline{X}_{k+i} = X \ominus S_{k+i}$ (this constraint comes from the fact that $x_k = \underline{x}_k + \tilde{x}_k + e_k$).

To ensure the feasibility and the stability of this control law, the following conditions are assumed [100].

***Assumption* 5.1.** Consider $S_0 = S_0^{co} \oplus S_0^e \subset X$ and $K S_0^{co} \subset U$.

This condition is assumed in order to ensure that the initial condition satisfies the constraint.

The terminal cost V_f and the terminal constraint set $\underline{X}_f$ are assumed to satisfy the stabilizing condition [101] (Assumptions 5.2 and 5.3).

***Assumption* 5.2.** $\underline{X}_f$ is a proper C-set, is positive invariant for $\underline{x}_{k+1} = (A+BK)\underline{x}_k$ and satisfies $\underline{X}_f \subseteq \underline{X}_N$ and $K\underline{X}_f \subseteq \underline{U}_N$.

***Assumption* 5.3.** $V_f(.)$ is a local control Lyapunov function for $\underline{x}_{k+1} = (A+BK)\underline{x}_k$ for all $\underline{x} \in \underline{X}_f$. There exist constants c_1, $c_2 > 0$ such that $c_1|\underline{x}_k|^2 \leq V_f(\underline{x}_k) \leq c_2|\underline{x}_k|^2$ and $V_f((A+BK)\underline{x}_k) + l(\underline{x}_k, K\underline{x}_k) \leq V_f(\underline{x}_k)$. This means that the Lyapunov function is decreased at the next sampling time.

Denote the set of admissible control sequences at instant k, with the nominal state $\underline{x}_k$:

$$\mathcal{U}_N(\underline{x}_k) = \{\underline{u} : \underline{u}_{k+i} \in \underline{U}_{k+i}, \underline{x}_{k+i} \in \underline{X}_{k+i}, \underline{x}_{k+N} \in \underline{X}_f, \\ i = 0, \ldots, N-1\} \quad (5.26)$$

Then the nominal optimal control problem is:

$$V_N^0(\underline{x}_k) = \min_{\underline{u}} \{V_N(\underline{x}_k, \underline{u}) : \underline{u} \in \mathcal{U}_N(\underline{x}_k)\} \quad (5.27)$$

At each time instant k, the feasible domain of $\underline{x}_k$:

$$\underline{X}_N(k) = \{\underline{x}_k : \mathcal{U}_N(\underline{x}_k) \neq 0\} \quad (5.28)$$

then $\underline{X}_N(k) \subseteq \underline{X}_N(k+1)$.

***Proposition* 5.3.** [100] There exists two constants c_1 and c_2 such that $\forall \underline{x}_k \in \underline{X}_N(k)$, $k \in \mathbb{N}^+$ the following expressions hold:

1. $c_1|\underline{x}_k| \leq V_N^0(\underline{x}_k) \leq c_2|\underline{x}_k|$
2. $V_N^0(\underline{x}_{k+1}) \leq V_N^0(\underline{x}_k) - c_1|\underline{x}|^2$

This proposition establishes the exponential stability at the origin for the nominal system.

Consider now the optimization control problem solved online:

$$V_N^*(\hat{x}_k) = \min_{\underline{x}_k, \underline{u}} \{V_N(\underline{x}_k, \underline{u}) : \underline{u} \in \mathcal{U}_N(\underline{x}_k), \hat{x}_k \in \underline{x}_k \oplus S_k^{co}\} \quad (5.29)$$

Let us consider the solution of this optimization problem:

$$\underline{x}_k^*(\hat{x}_k), \underline{u}^*(\hat{x}_k) = arg \min_{\underline{x}_k, \underline{u}} \{V_N(\underline{x}_k, \underline{u}) : \underline{u} \in \mathcal{U}_N(\underline{x}_k), \hat{x}_k \in \underline{x}_k \oplus S_k^{co}\} \quad (5.30)$$

then using (5.19) the control law applied to the system is obtained:

$$\kappa_N(\hat{x}_k) = \hat{u}_k^*(\hat{x}_k) + K(\hat{x}_k - \underline{x}^*(\hat{x}_k)) \tag{5.31}$$

with $\hat{u}_k^*(\hat{x}_k)$ the first element of the sequence $\underline{u}^*(\hat{x}_k)$.

Using this control law it can be proved that $(x_k, \hat{x}_k)$ is robustly steered to $S_\infty \times S_\infty^{co}$ exponentially fast satisfying all constraints [100]. This robust TMPC control law is illustrated in the following example.

***Example* 5.2.** Consider a second-order system:

$$\begin{cases} x_{k+1} = \begin{bmatrix} 1 & 1.1 \\ 0 & 1 \end{bmatrix} x_k + \begin{bmatrix} 1 \\ 1 \end{bmatrix} u_k + \omega_k \\ y_k = \begin{bmatrix} -2 & 1 \end{bmatrix} x_k + v_k \end{cases} \tag{5.32}$$

The disturbances and measurement noise are assumed to be bounded $(\omega, v) \in W \times V$, where $W = \{\omega \in \mathbb{R}^2 : \|\omega\|_\infty \leq 0.1\}$ and $V = \{v \in \mathbb{R} : |v| \leq 0.05\}$. The state and control constraints are $(x_k, u_k) \in X \times U$, where $X = \{x \in \mathbb{R}\}^2 : x_1 \in [-50, 3], x_2 \in [-50, 3]\}$ and $U = \{u \in \mathbb{R} : |u| \leq 9\}$. This system must be stabilized around the origin while respecting the aforementioned state and control constraints.

The weighting matrices in the cost function are $Q = I_2$ and $R = 0.01$. The terminal cost $V_f(\underline{x})$ is the value function $\underline{x}^T P_f \underline{x}$ for the unconstrained optimal control problem for the nominal system $\underline{x}_{k+1} = A\underline{x}_k + B\underline{u}_k$ and $\underline{u}_k = K\underline{x}_k$ is the associated Linear Quadratic Regulator (LQR) control $K = \begin{bmatrix} -0.6029 & -1.0567 \end{bmatrix}$. The initial sets S_0^e, S_0^{co} are computed using a recursive algorithm to compute an outer approximation of the minimal invariant set [119]. The initial state belongs to the zonotope $Z(\begin{bmatrix} 0 \\ -15 \end{bmatrix}, S_0^e)$. The prediction horizon is chosen $N = 13$ such that the optimization is feasible at the initial time instant.

The terminal constraint set $\underline{X}_f$ (the black set depicted in Figure 5.7) is the maximal positive invariant set for the system $\underline{x}_{k+1} = (A + BK)\underline{x}_k$ under the tighter constraints $\underline{X}_N = X \ominus S_N$ and $\underline{U}_N = U \ominus K S_N^{co}$ obtained using the recursive algorithm proposed by [52]. This algorithm is based on a search of the maximal value of t such that $(A + BK)^{t+1}\underline{x} \in \underline{X}_N$ subject to the constraint $(A + BK)^k \underline{x} \in \underline{X}_N$, with $k = 0, \ldots, t$.

Figure 5.5 compares the state estimation sets of three approaches: the segment minimization, the volume minimization and the P-radius minimization. The zonotopic guaranteed state estimation obtained by P-radius minimization is non-increasing in time. This figure confirms the compromise of the

P-radius minimization between the segment minimization and the volume minimization.

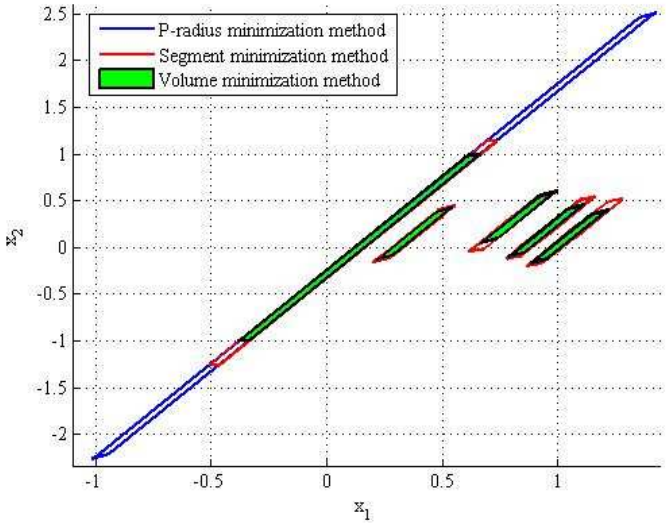

Figure 5.5: Evolution of the zonotopic state estimation set

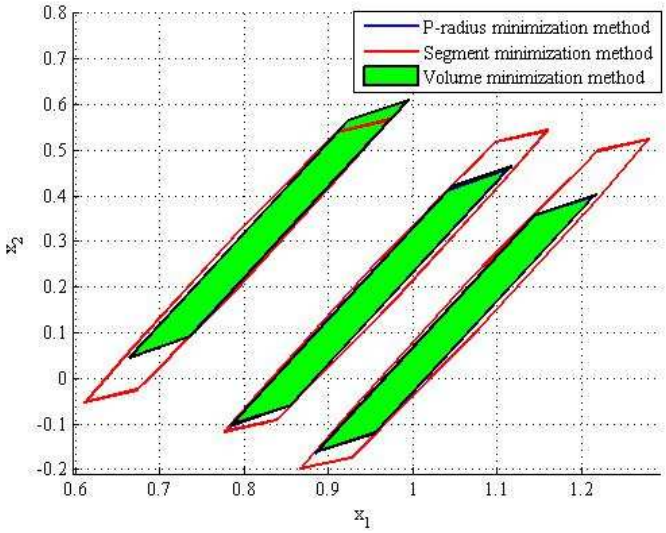

Figure 5.6: Zoom of the evolution of the zonotopic state estimation set

Figure 5.7 shows the tube trajectory of the system. The largest zonotope (red) is the set $\bar{x}^*(\hat{x}_k, k) \oplus S_k$. The real state is guaranteed to belong to this tube section centered at the nominal state. The smaller zonotope (green) is the set $\bar{x}^*(\hat{x}_k, k) \oplus S_k^{co}$, the state estimation is guaranteed to belong to this set. The smallest (blue) is the guaranteed state estimation set $\hat{x}_k \oplus S_k^e$. Denote that the red zonotope which is the section of the tube trajectory at each time instant is the Minkowski sum of the blue zonotope and the green zonotope $S_k = S_k^{co} \oplus S_k^e$. Due to the non-increase in time of the guaranteed state estimation, the section of tube is non-increasing in time. This trajectory is put in the box of the state contraint (Figure 5.8) in order to illustrate that the system respects the constraint. Figure 5.9 shows the stability of this output feedback system respecting the constraints. Due to the presence of the uncertainty, the system state does not converge to the origin but it converges, thus, to a set containing the origin.

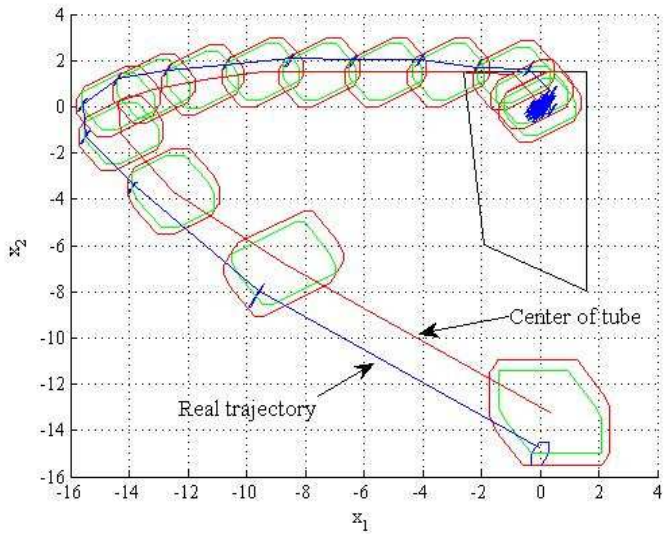

Figure 5.7: Tube trajectory of the closed-loop system

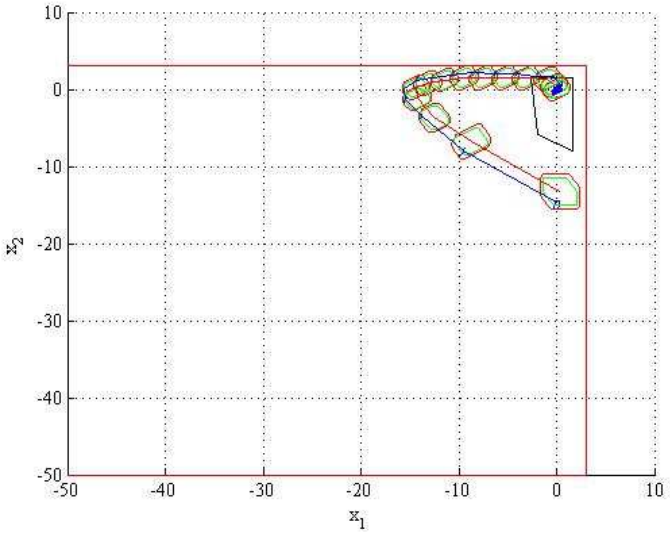

Figure 5.8: Tube trajectory of the closed-loop system fulfilling the state constraints

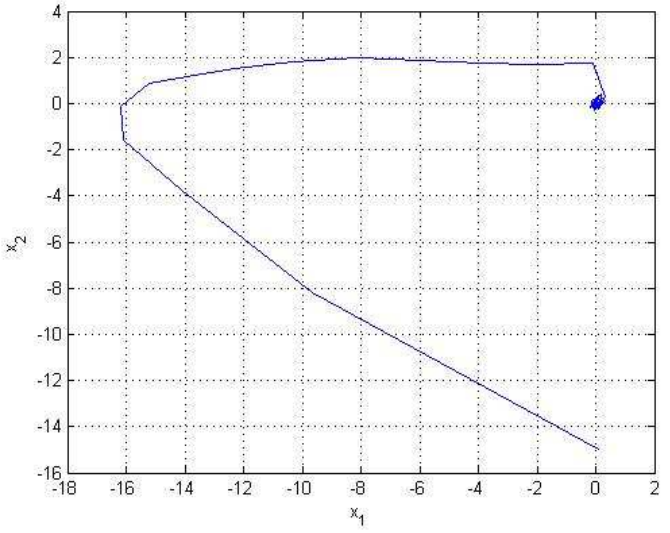

Figure 5.9: Closed-loop response of the system

5.5 Open problem for the control of systems with interval parametric uncertainties

Even if promising simulation results are obtained through these examples, the output feedback control of systems with interval parametric uncertainties still remains an open problem due to the following difficulties.

In the case of open-loop control, if the A matrix has some interval elements, the condition $x_{k+i} \in X$ can not be formulated anymore as linear inequalities on u_{k+i-1} as presented in the previous subsection and thus the optimization problem (5.2) can not be solved. For example, when $i = 1$, we have : $x_{k+i} = x_{k+1}$ and the condition $x_{k+1} = Ax_k + Bu_k + \omega_k \in X$ is equivalent to:

$$H_1 B u_k \leq K_1 - \max_{A} H_1 A x_k - \max_{A,s} H_1 A H s - \max_{\omega_k} H_1 \omega_k \tag{5.33}$$

Different to (5.8), the term $\max_{A,s} H_1 A H s$ is not easily computed due to the non convex problem. In addition, when $i > 1$ the non convexity becomes higher, thus it is more difficult to manipulate the state constraint condition.

In this case, a simple solution can be to use another cost function such as:

$$J_k = (\hat{y}_{k+1} - y_{k+1}^{ref})^2, \forall k \geq 0 \tag{5.34}$$

with $\hat{y}_{k+1} = C(mid([A])\hat{x}_k + Bu_k)$ subject to the constraint $x_{k+1} \in X$.

Suppose at time instant k the guaranteed state estimation is $\hat{X}_k = \hat{x}_k \oplus H\mathbf{B}^r$, thus similar to (4.70) the real state at time instant $k+1$ will belong to the set:

$$\bar{X}_k = Z(mid([A])\hat{x}_k + Bu_k; \begin{bmatrix} mid([A])H & rs(rad([A])|H|) & rs(rad([A])|\hat{x}_k|) & F \end{bmatrix}) \tag{5.35}$$

The condition $x_{k+1} \in X$ becomes $\bar{X}_{k+1} \in X$, which is easy to formulate similar to (5.8):

$$H_1 B u_k \leq K_1 - \max_{s} H_1 \begin{bmatrix} mid([A])H & rs(rad([A])|H|) & rs(rad([A])|\hat{x}_k|) & F \end{bmatrix} s - \\ - H_1 mid([A])\hat{x}_k \tag{5.36}$$

The control law is computed by minimizing the cost function (5.34) subject to the constraint (5.36).

***Remark* 5.1.** In the case of TMPC, due to the interval uncertainties in the A matrix, the problem of finding the initial robust invariant set S_0^e as in Proposition

5.1 is not evident. Thus the recursive feasibility of the optimization problem (5.29) is not ensured due to the fact that S^e_{k+1} may not be contained in S^e_k even if this possibility of this problem is low.

***Example* 5.3.** The open-loop control technique for systems with interval parametric uncertainties is illustrated in the following example. Consider the following linear-discrete time varying system:

$$\begin{cases} x_{k+1} = \begin{bmatrix} 0+0.1\delta_1 & -0.5+0.1\delta_2 \\ 1+0.1\delta_3 & 1+0.1\delta_4 \end{bmatrix} x_k + \begin{bmatrix} 1 \\ 1 \end{bmatrix} u_k + 0.02 \begin{bmatrix} -6 \\ 1 \end{bmatrix} \omega_k \\ y_k = \begin{bmatrix} 1 & 1 \end{bmatrix} x_k + 0.1 v_k \end{cases} \tag{5.37}$$

The disturbances and measurement noise are assumed to be bounded $(\omega, v) \in W \times V$, where $W = \{\omega \in \mathbb{R}^2 : \|\omega\|_\infty \leq 0.1\}$ and $V = \{v \in \mathbb{R} : |v| \leq 0.05\}$. The parameter uncertainties are bounded $|\delta_i| \leq 1$, $i = 1, \ldots, 4$. The system is subject to the state and control constraint $x_k \in X = 10\mathbf{B}^2$, $|u_k| \leq 10$. The initial state is unknown but belongs to the box $3\mathbf{B}^2$. The control objective is to make the output y_k track the reference $y^{ref} = 5$.

Figures 5.10, 5.11 and 5.12 show that the system output tracks well the reference respecting the control constraint ($|u_k| \leq 10$) and the state constraint $x_k \in 10\mathbf{B}^2$. This example shows that despite the presence of interval parametric uncertainties, the controlled system can satisfy the tracking problem. The problem of finding a control law which has stability and feasibility guarantees for the parameter uncertainties systems is still an open problem.

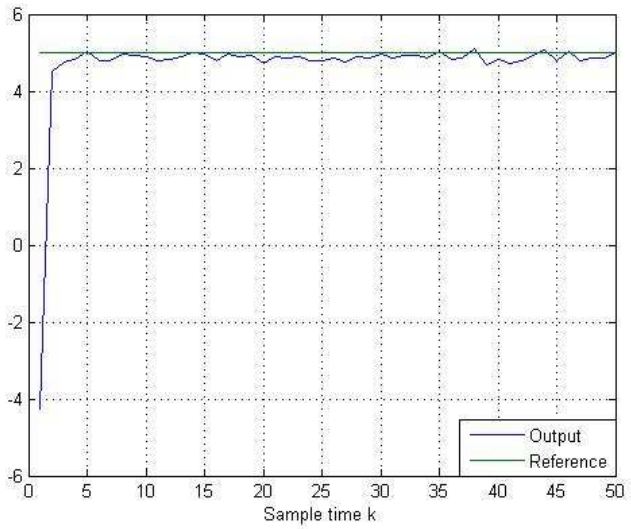

Figure 5.10: Evolution of the system output

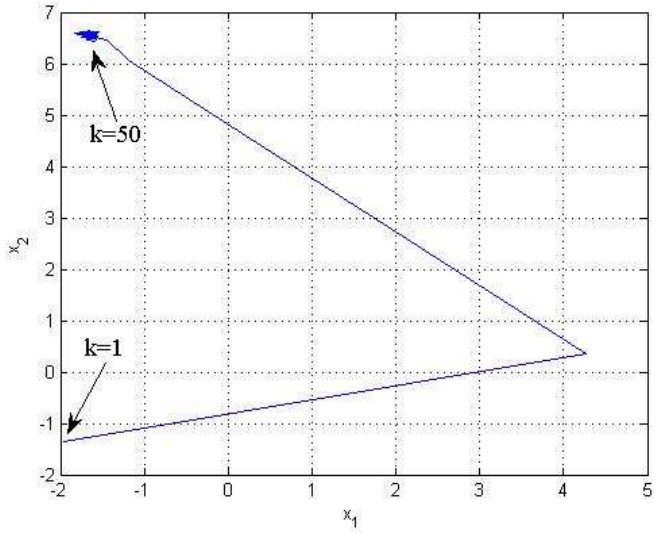

Figure 5.11: Evolution of the system state

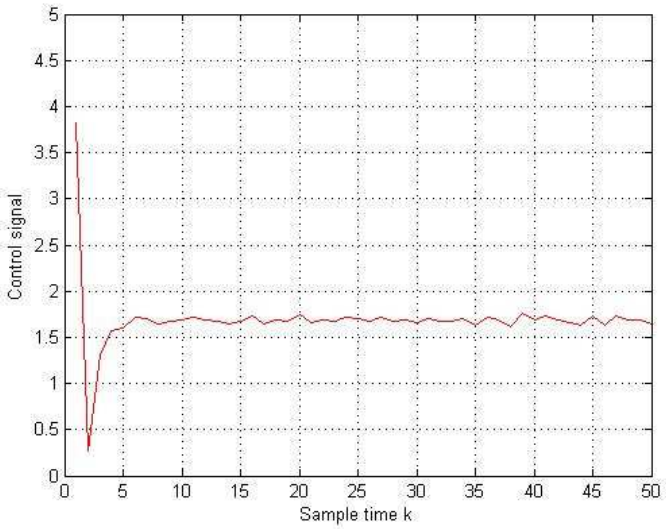

Figure 5.12: Control signal

5.6 Conclusion

This chapter proposes a Model Predictive Control law based on the zonotopic set-membership estimation, when the state is not available. It starts with a general presentation of predictive control history. Due to its robustness and its ability to deal with constraints, predictive control is more and more used to control uncertain constraint system. When the state estimation is implemented, the simplest scheme control is to consider the state estimation as the real state and to minimize a cost function. This solution is simple but it does not take into account the estimation error when designing the controller. Even if the control law and the state estimation are stable, due to the presence of uncertainties the stability of uncertain closed-loop system can not be guaranteed using the separation principle. For this reason, a feedback control law based on a tube of uncertain trajectories (around the nominal trajectory) of the uncertain system is presented. This control law considers the estimation error in the control problem using the invariant set approach in order to guarantee the stability of the system. Based on these control techniques, the control problem of systems with interval parametric uncertainties is considered. The interval uncertainties lead to solve a non convex optimization problem and thus the open-loop control can not be identical to the case of linear time invariant system. A solution consists in modifying the cost function proposed to solve this problem. For systems with interval uncertainties, the Tube-based Model Predictive Control method can not guarantee the recursive feasibility of the control law and thus the stability of the closed-loop system. For these reasons, the problem of finding an appropriate control law for system with interval parametric uncertainties subject to disturbances and measurement noise still remains an open problem. In the next chapter, an application of the proposed set-membership estimation and control techniques are presented to illustrate the performances of these approaches, even if restricted configurations are considered (monovariable system with disturbances and measurement noise).

Chapter 6

Application

6.1 Introduction

In this chapter, the control and estimation approaches proposed in this thesis will be applied to the model of a real system: the magnetic levitation system. The goal is to test the zonotopic set-membership estimation and the association between this estimation and the open-loop Model Predictive Control or the Tube-based Model Predictive Control (TMPC). The chapter proposes first a general description and the mathematical model of the magnetic levitation system. Based on this model, in the next part the model predictive control law is built using the zonotopic set-membership estimation. First, the simulation is done with the open-loop Model Predictive Control method and then, the system is controlled by the TMPC. The simulation results show that these predictive control methods based on the zonotopic set membership estimation can stabilize this system fulfilling the considered constraints, despite the disturbances and measurement noises acting on the system.

6.2 System description

In this section, the general description of the magnetic levitation device will be done. This system is composed of a mobile iron pendulum in a vertical magnetic field created by a fixed electromagnet (Figure 6.1). This electromagnet is supplied by a variable current which permits to vary the magnetic force and thus to vary the vertical position of the pendulum. This system is assumed to have a perfect radial symmetry.

The control goal is to stabilize the vertical position of the pendulum around the equilibrium point. Figure 6.2 illustrates a general schematic block diagram of the closed-loop system with z the position of the pendulum relative to the sensor position center in an absolute reference frame, i the current given by the actuator. In the next part, the model of the magnetic levitation without the

actuator is considered in order to simplify the computation and to mentain a simple visualisation (i.e. 2D).

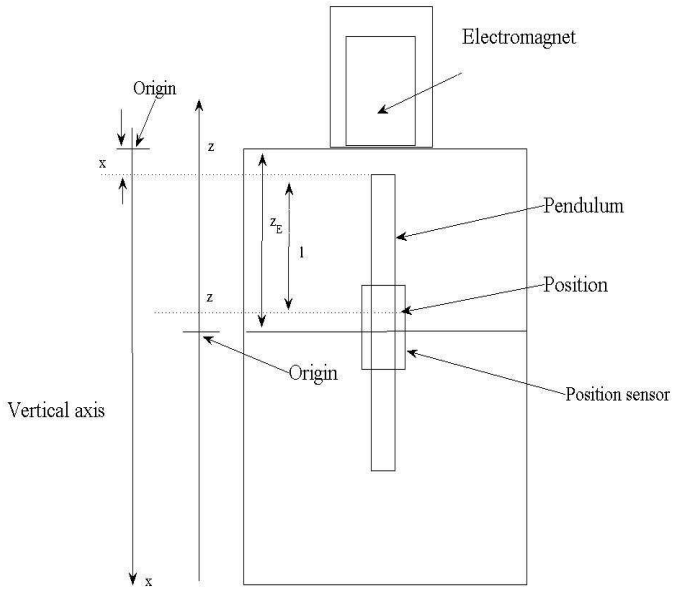

Figure 6.1: Magnetic levitation system

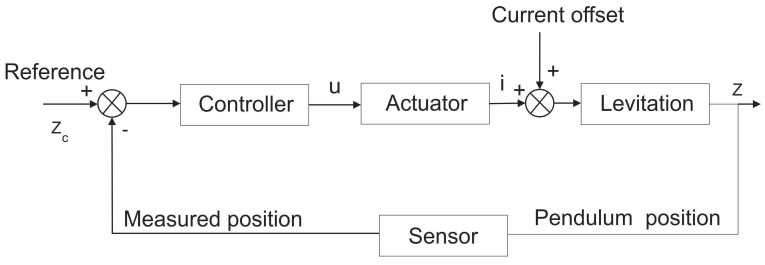

Figure 6.2: Block diagram of the closed-loop system

The force applied on the pendulum created by the electromagnet has the fol-

lowing form:

$$F_m(t) = c\frac{i(t)}{x^2(t)} \tag{6.1}$$

with i the current in the electromagnet, x the distance between the pendulum and the electromagnet and c a constant. Using the fundamental relation of the pendulum dynamics, the movement of the pendulum can be described by the following differential equation:

$$-m\ddot{x}(t) = -mg + \frac{ci(t)}{x^2(t)} \tag{6.2}$$

where m is the pendulum mass and g is the gravitational constant. Replacing $x(t) = x_0 - z(t)$ in equation (6.2), with $x_0 = z_E - l$ (Figure 6.1), leads to:

$$m\ddot{z}(t) = -mg + \frac{ci(t)}{x_0^2(1 - \frac{z(t)}{x_0})^2} \tag{6.3}$$

Consider a small variation of $z(t)$ around the origin (with $|z(t)| << x_0$) and $i(t)$ around i_0 (with i_0 the current at the equilibrium point, $i(t) = i_0 + i_1(t)$ and $|i_1(t)| << i_0$ a small variation around i_0). Keeping only the first order terms, the equation (6.3) is then approximated by:

$$\begin{aligned} m\ddot{z}(t) &\approx -mg + \frac{ci(t)}{x_0^2}(1 + \frac{2z(t)}{x_0}) \\ &\approx -mg + \frac{ci(t)}{x_0^2} + \frac{2ci(t)z(t)}{x_0^3} \end{aligned} \tag{6.4}$$

Writing the equation (6.3) at the equilibrium point ($z(t) = 0$), leads to:

$$\frac{ci_0}{x_0^2} - mg = 0 \tag{6.5}$$

Replacing (6.5) and $i(t) = i_0 + i_1(t)$ in equation (6.4), the following expression is obtained:

$$\frac{ci_0}{gx_0^2}\ddot{z}(t) = \frac{ci_1(t)}{x_0^2} + \frac{2ci(t)z(t)}{x_0^3} \tag{6.6}$$

Because $i_1(t) << i_0$, the following approximation can be done $i(t) \approx i_0$. Replacing this approximation in the equation (6.6) leads to:

$$\frac{ci_0}{gx_0^2}\ddot{z}(t) \approx \frac{ci_1(t)}{x_0^2} + \frac{2ci_0z(t)}{x_0^3} \tag{6.7}$$

or multiplying (6.7) by $\frac{x_0^2}{c}$ leads to:

$$\frac{i_0}{g}\ddot{z}(t) = i_1(t) + \frac{2i_0}{x_0}z(t) \tag{6.8}$$

Based on this differential equation (6.8), the dynamics of the magnetic levitation in continuous-time can be described as the following state-space representation:

$$\begin{cases} \dot{x} = \begin{bmatrix} 0 & 1 \\ \frac{2g}{x_0} & 0 \end{bmatrix} x + \begin{bmatrix} 0 \\ \frac{g}{i_0} \end{bmatrix} u \\ y = \begin{bmatrix} 1 & 0 \end{bmatrix} x \end{cases} \tag{6.9}$$

where $x = \begin{bmatrix} x_1 & x_2 \end{bmatrix}$ correspond to the position z and the speed of the pendulum $\dot{z}$ respectively, u corresponds to the electromagnet current $i_1(t)$, y the position measurement, $g = 9,81(m/s^2)$, $x_0 = 0,019(m)$, $i_0 = 0,436(A)$. As the magnetic levitation system is a nonlinear system, this model is only a local model linearized around the origin. The eigenvalues of the open-loop evolution matrix are 32.1346 and -32.1346. This means that the open-loop system is unstable, which confirms the unstable physical behavior of the magnetic levitation system. Note that even if the position is measured by a position sensor, due to the disturbances and measurement noises the zonotopic set-membership estimation is implemented to estimate not only the position but also the speed of the pendulum.

6.3 Control problem

As The system (6.9) is an unstable system in open-loop and, thus, the control problem is to stabilize this unstable system around the origin under the following constraints $(x, u) \in X \times U$, with $X = \{x \in \mathbb{R}^2 : x_1 \in [-0.5; 0.5](m), x_2 \in [-10; 10](m/s)\}$ and $U = \{u \in \mathbb{R} : |u| \leq 5(A)\}$. The equation (6.9) is discretized using the zero-order hold on the inputs with the sample time $T_s = 0.1(s)$. The obtained linearized discrete-time invariant system is the following:

$$\begin{cases} x_{k+1} = \begin{bmatrix} 12.4526 & 0.3863 \\ 398.8660 & 12.4526 \end{bmatrix} x_k + \begin{bmatrix} 0.2495 \\ 8.6909 \end{bmatrix} u_k + \begin{bmatrix} 0.001 \\ 0.01 \end{bmatrix} \omega_k \\ y_k = \begin{bmatrix} 1 & 0 \end{bmatrix} x_k + v_k \end{cases} \tag{6.10}$$

ω_k and v_k are added to the model disturbances and measurement noise: $\omega \in W = \{w \in \mathbb{R} : |w| \leq 1\}$, $v \in V = \{v \in \mathbb{R} : |v| \leq 0.05(m)\}$. This control problem will be solved using the two proposed control laws in Chapter 5: the open-loop Model Predictive Control and the Tube-based Model Predictive Control.

The first simulation result consists in comparing the guaranteed state estimation obtained by Method 4.2 in subsection 4.3.1, based on the minimization of the P-radius of the zonotopic guaranteed state estimation with the volume minimization method and the segment minimization method [2] at time instants $k = 1$ and $k = 2$ (Figure 6.4). In this example these methods give similar estimation results. The minimization of the P-radius method has the same computation time as the segment minimization method and smaller than the volume minimization method (Table 6.1).

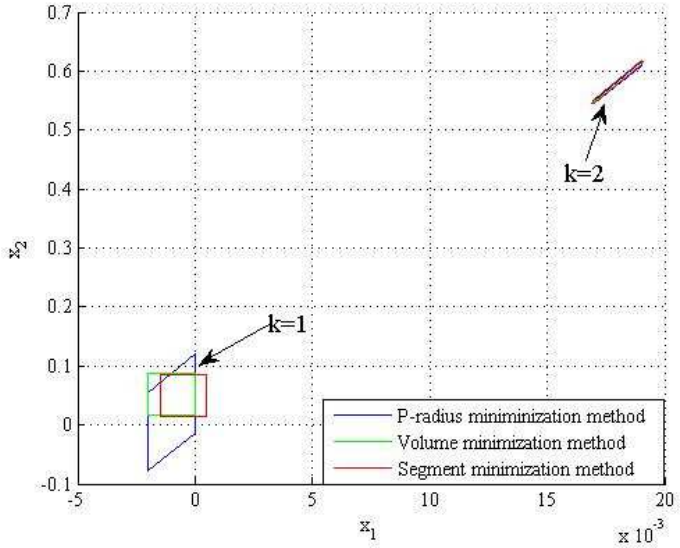

Figure 6.3: Comparison of the zonotopic guaranteed state estimation obtained by different approaches

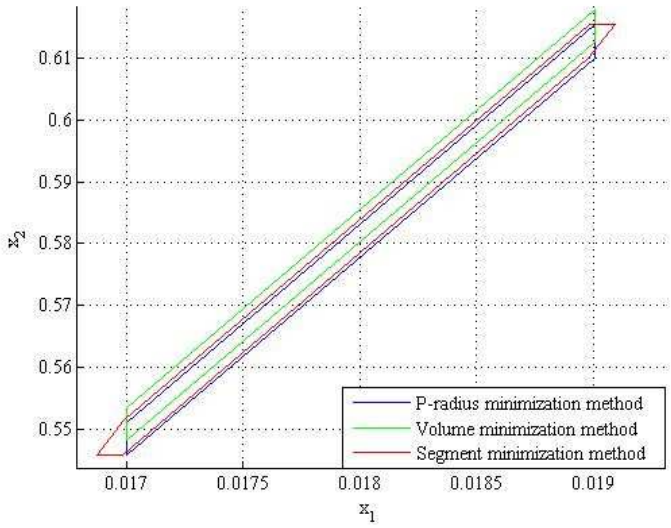

Figure 6.4: Comparison of the zonotopic guaranteed state estimation obtained by different approaches with zoom

Table 6.1: Total computation time of the estimation problem of the magnetic levitation system after 50 time instants

Algorithm	Time(second)
Segment minimization	0.0468
Method 4.2 (without off-line optimization included)	0.0312
Method 4.2 (with off-line optimization (4.59) included)	0.7488
Volume minimization	7.8469

The estimation results will be further used within a control law. First the unstable magnetic levitation system is controlled using the open-loop Model Predictive Control based on the zonotopic set membership estimation. The weighting matrices in the cost function (5.2) are chosen as $Q = R = I_2$. Thus the simulation of the controlled systems is illustrated in Figures 6.5, 6.6, 6.7, 6.8. Figure 6.5 shows the evolution of the guaranteed state estimation, i.e. the evolution of the position and the speed of the pendulum. The figures 6.6, 6.7, 6.8 show that the constraints on the state and the control signal are fulfilled ($|u| \leq 5$, $x_1 \in [-0.5; 0.5]$, $x_2 \in [-10; 10]$). Due to the effect of the disturbance and the measurement noise, the position of the pendulum can only converge around the origin, as shown in Figure 6.7.

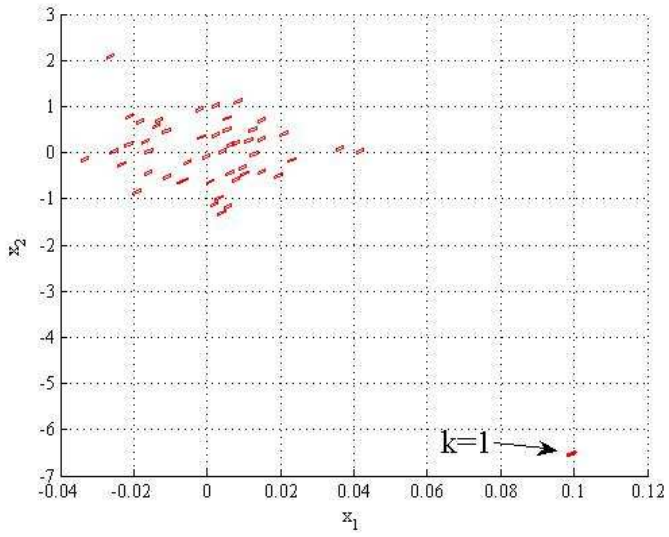

Figure 6.5: Evolution of the guaranteed state estimation of the magnetic levitation system

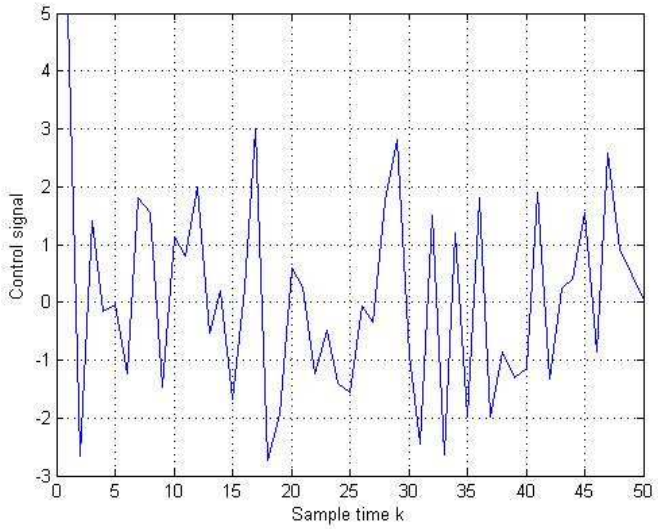

Figure 6.6: Control signal of the closed-loop magnetic levitation system

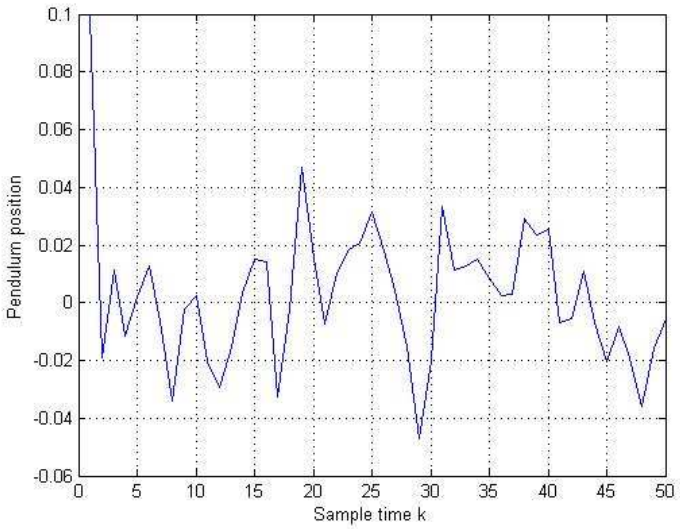

Figure 6.7: Pendulum position obtained by the open-loop MPC

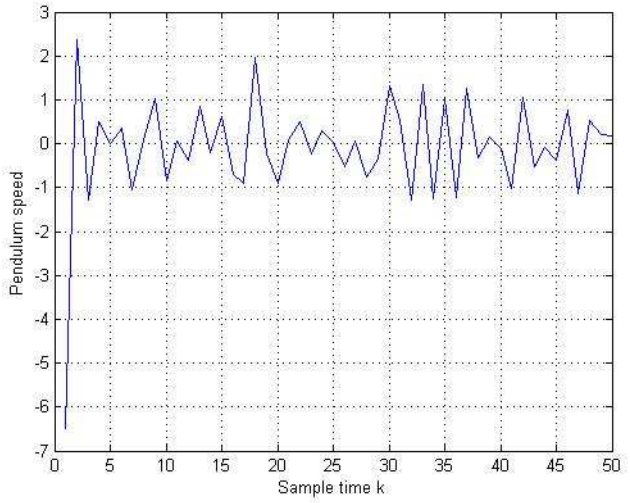

Figure 6.8: Pendulum speed obtained by the open-loop MPC

Second, the TMPC based on zonotopic set-membership estimation is used to stabilize this system as follows. The weighting matrices in the cost function (5.22) are chosen as identity matrices $Q = R = I_2$. The terminal cost $V_f(\underline{x})$ is the value function $\underline{x}^T P_f \underline{x}$ for the unconstrained optimal control problem for the nominal system $\underline{x}_{k+1} = A\underline{x}_k + B\underline{u}_k$ and $\underline{u}_k = K\underline{x}_k$ is the associated Linear Quadratic Regulator (LQR). The initial sets S_0^e (the guaranteed state estimation at time instant $k = 0$), S_0^{co} (the set contains the error between the estimation state and the nominal state at time instant $k = 0$) are computed using the result in [119] as presented in the last chapter. The initial state belongs to the zonotope $Z(\begin{bmatrix} 0.1 \\ -6.5 \end{bmatrix}, S_0^e)$. The prediction horizon is chosen $N = 3$ such that the optimization is feasible at the initial time instant. The terminal constraint set $\underline{X}_f$ (the black set depicted in Figure 6.9) is the maximal positive invariant set for the system $\underline{x}_{k+1} = (A+BK)\underline{x}_k$ under the tighter constraints $\underline{X}_N = X \ominus S_N$ and $\underline{U}_N = U \ominus KS_N^{co}$ with $K = \begin{bmatrix} -47.5680 & -1.4807 \end{bmatrix}$ being the associated LQR, $S_N = S_N^{co} \oplus S_N^e$.

Figure 6.9 and its associated zoom in Figure 6.10 illustrate the tube section which bound the uncertain trajectory of the system. As the real system enters to the terminal set after 2 instants, here only some tube sections can be seen because after the time instant $k = 2$ these tubes section coincide. The red zonotope is the set $\underline{x}^*(\hat{x}_k, k) \oplus S_k$, which is in fact the tube bounding the real system. The smaller zonotope (green) is the set $\underline{x}^*(\hat{x}_k, k) \oplus S_k^{co}$, which bounds the error between the estimation state and the nominal state. The smallest (blue) is the guaranteed state estimation set $\hat{x}_k \oplus S_k^e$, which is computed based on Method 4.2 in Subsection 4.3.1. The initial guaranteed state estimation is small because the robust invariant condition on this set must be satisfied.

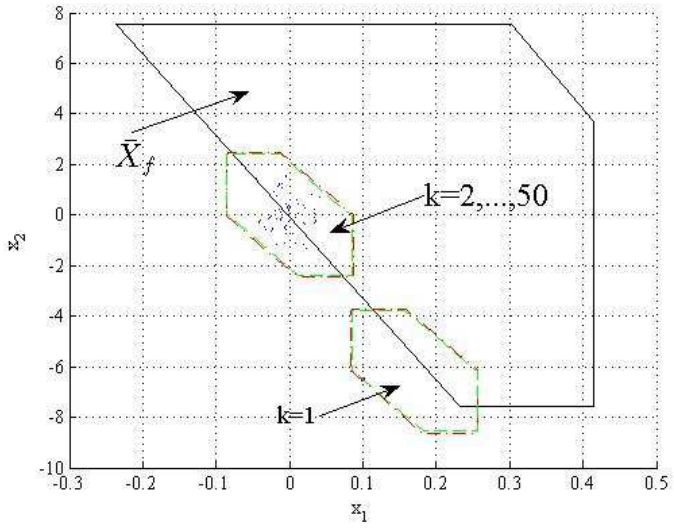

Figure 6.9: Tube trajectory of the controlled magnetic levitation system

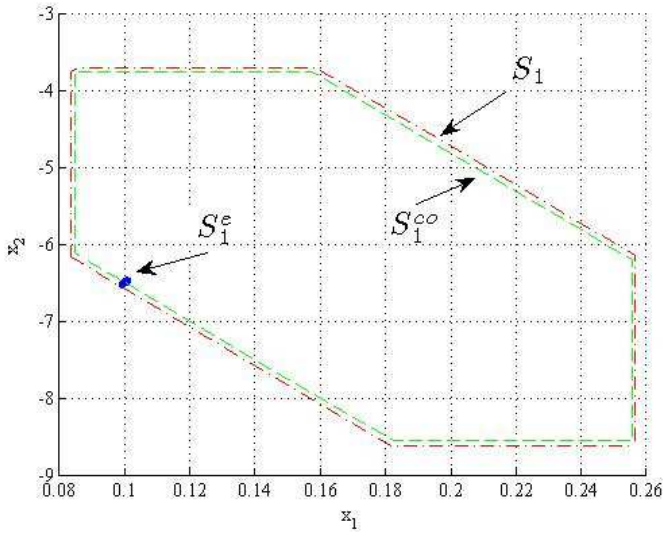

Figure 6.10: Tube section bounding the system trajectory at the initial instant time $k = 1$

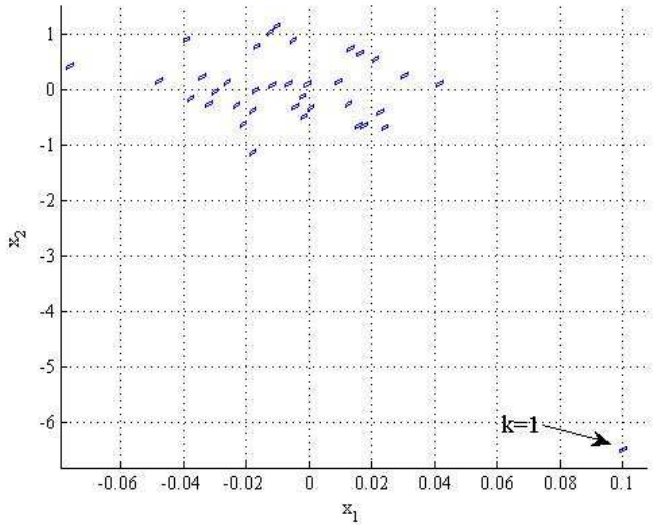

Figure 6.11: Evolution of the guaranteed state estimation using the TMPC

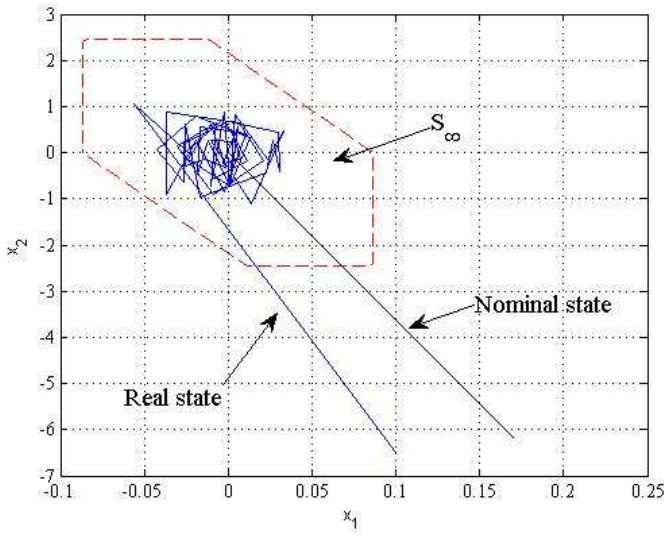

Figure 6.12: Real state and nominal state of the closed-loop pendulum system

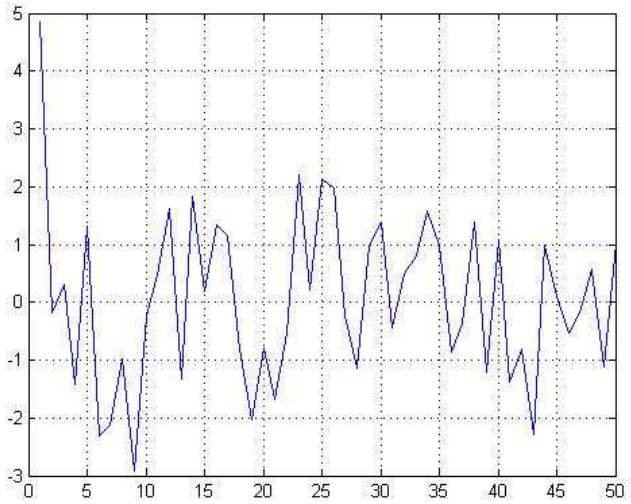

Figure 6.13: Control signal of the closed-loop magnetic levitation system computed by the TMPC

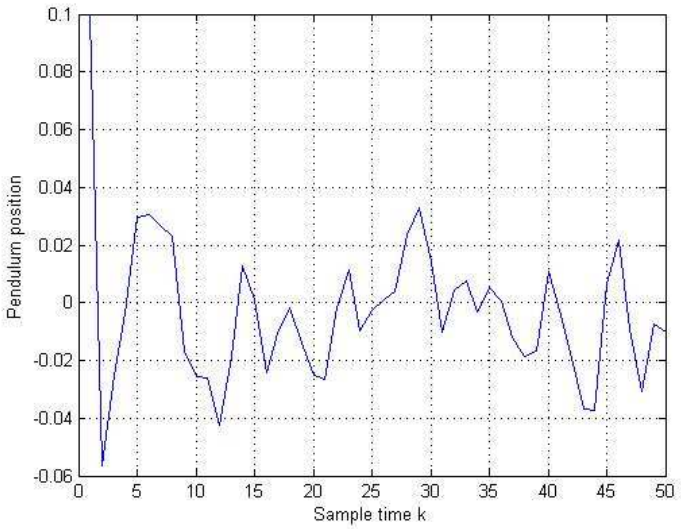

Figure 6.14: Pendulum position controlled by the TMPC

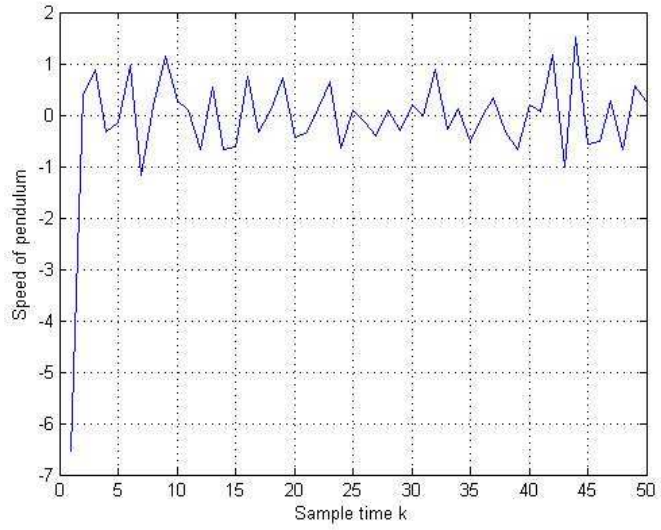

Figure 6.15: Pendulum speed controlled by the TMPC

The evolution of the guaranteed state estimation (blue zonotope $\hat{x}_k \oplus S_k^e$) is illustrated in Figure 6.11.

Figure 6.12 shows the stability of this output feedback system respecting the constraints ($X = \{x \in \mathbb{R}^2 : x_1 \in [-0,5; 0,5](m), x_2 \in [-10, 10](m/s)\}$). Figure 6.13 illustrates the control signal computed by the TMPC. This figure shows that the control signal respects the control constraint $u \in \mathbb{R} : |u| \leq 5(A)$. The pendulum position (Figure 6.14) and the pendulum speed (Figure 6.15) also respect the imposed constraints. It can be noticed that the nominal state (represented in black) reaches the origin as in the stability proof of the TMPC technique. Due to the bounded disturbances and measurement noises, the system state does not converge to the origin but it converges to a set containing the origin (S_∞ in Figure 6.12).

6.4 Conclusion

This chapter proposes an application of the open-loop Model Predicitve Control and the Tube-based Model Predictive control based on the zonotopic set membership estimation presented in this thesis for a magnetic levitation system. The model of the magnetic levitation system is simplified in order to obtain a system of 2 states which facilitate the visualization in 2D. The zonotopic set-membership estimation problem for this system is solved using Method 4.2 proposed in Chapter 4. The estimation result obtained by this method is compared with the volume minimization method and the segment minimization method. In order to illustrate

its properties, the P-radius based estimation method is used for control purposes. The control law is implemented using the open-loop Model Predictive Control and the Tube-based Model Predictive Control. The simulation results show that the control problem is solved (the system is stabilized, the constraints are respected). The next chapter which is the last chapter of this PhD thesis presents some conclusions, the contributions of this thesis and some future directions both on theory and practical applications.

Chapter 7

Conclusion and future works

7.1 Contribution

This thesis proposes a robust predictive control technique for uncertain systems subject to constraints in the presence of bounded disturbances and measurement noises. The contributions of this thesis are divided into two main parts:

- The first part consists in developing a zonotopic set-membership estimation for systems with interval parametric uncertainties in the presence of disturbances and measurement noises.
- The second part is based on the association of the proposed state estimation with a Model Predictive Control law in order to robustly control the considered system subject to state and input constraints.

In the first part, using the deterministic approach, disturbances and measurement noises are assumed to be unknown but bounded by some zonotopes. Then a zonotopic set containing all the possible system states that are consistent with the uncertainties, the disturbances and the noises is computed at each time instant using a set-membership estimation algorithm. One originality of this thesis is to present a new optimization criterion to compute the zonotopic guaranteed state estimation based on the minimization of the P-radius of the zonotopic estimation set offering a good accuracy of the estimation with a reasonable complexity of the computation. Using the P-radius based criterion in an original way leads to off-line solve a Bilinear Matrix Inequality optimization problem [82]. To solve this problem, the *Penbmi* solver [74] can be used. To overcome the use of Bilinear Matrix Inequality solvers, in this thesis the contractiveness speed of the zonotopic state estimation set is optimized leading to a Linear Matrix Inequality optimization problem which can be easily solved [85]. This method is first developed for linear time invariant systems subject to disturbances and measurement noises, then it is extended to the case of systems with interval parametric uncertainties using the maximum principle [83]. Another contribution of this thesis consists in proposing

different strategies for the case of Multi-Output systems that have been presented in [88] and [87] or submitted to [84]. The first proposed solution is based on the direct extension of the adopted solution for the case of Single-Output systems. This solution is shown to be conservative due to neglect the coupling effect of Multi-Output systems. When the coupling effect is taken into account, the optimization problem becomes a Polynomial Matrix Inequality problem which is non convex and thus difficult to solve. In consequence, the proposed solution is to use a relaxation technique [62] to transform this Polynomial Matrix Inequality problem into a Linear Matrix Inequality problem which can be solved using Linear Matrix Inequality solvers. This results have been published in [88]. But this relaxation technique leads to an important increase of the number of scalar decision variables, and, thus, limits the application of the proposed approach to large scale systems. Moreover, the simulation result shows a poor estimation performance due to the used of this relaxation technique. In order to improve the overall performance for Multi-Output systems,, the next contribution of this thesis considers the zonotopic outer approximation of the intersection between a zonotope and a polytope [87]. Using this result and the P-radius based optimization criterion leads to a significant improvement both on the estimation performance and the complexity of the computation in comparison with the previous proposed methods (the direct extension of Single-Output case and the Polynomial Matrix Inequality based method). The comparative results are analyzed in different examples along the thesis.

The second part deals with the problem of robust control for constrained uncertain system in the predictive control context. First, an simple solution based on the open-loop predictive control is proposed. The proposed control law leads to solve a quadratic optimization problem subject to constraints at each sample time. Even if the simulation shows a good result, this solution does not have the guarantees of stability and feasibility. A second solution is to use the Tube based Model Predictive Control for systems with bounded disturbances and measurement noises which build a tube trajectory of the real system around the nominal model. This control technique permits to guarantee the stability of the controlled system. When the system state is not available, the Tube-based Model Predictive Control is usually associated to the Luenberger observer to obtain a state estimation [100]. The next contribution consist in using the Tube based Model Predictive Control in the context of the zonotopic set-membership estimation [85], which permits to improve the estimation performance and thus the performance of the controlled system. To deal with the interval parametric uncertainties presence in the system model, a modification of the cost function in the presented open-loop control is proposed. The solution of the Tube-based Model Predictive Control associated to the set-membership estimation is still an open problem. Finally, the application of the proposed Tube-based Model Predictive Control to the magnetic levitation system shows the effectiveness of the developed technique [86].

7.2 Future works

Several directions are proposed for future developments of this thesis.

As presented in Subsection 4.3.3.4 applying the P-radius based zonotopic set-membership estimation for Multi-Output linear discrete-time systems (with parameter uncertainties or not) subject to bounded disturbances and measurement noises leads to solve a Polynomial Matrix Inequality optimization problem. Due to the poor performance obtained by the relaxation Linear Matrix Inequality technique [62] (outer approximation of the solution of the PMI optimization problem) applied in this thesis, the first perspective consists in comparing the results obtained with the relaxation procedure [62] with other existing techniques [64], [72], [31] or the most recent work [63] which offers an inner approximation of the solution of the PMI optimization problem. If the reader is interested by these results, another direction to explore consists in developing new relaxation techniques that will lead to other sub-optimal solutions of the initial Polynomial Matrix Inequality problem in order to obtain a better performance of the estimation.

An interesting idea to pursue is the extension of the zonotopic set-membership estimation for systems with time-delay and especially for systems with variable time-delay [93]. If the delay can be taken into account in the mathematical model as an interval parametric uncertainty [136], then the extension of this estimation technique should not be too complicated.

In the case of Multi-Output systems, the set-membership estimation is obtained using a multisensor system. Thus, a natural way to explore further is the fault diagnosis problem of the multisensor system [138], [114] [142]. This problem can be considered using the proposed zonotopic outer approximation of the intersection between a zonotope and a polytope. If this intersection is zero it means that a fault is detected. Then a continuing study which can be considered is the fault tolerant control [139], [130], [150].

A different perspective is to build an efficient output feedback control law (offering stability guarantees) which permits to control the system with interval parametric uncertainties in the presence of disturbances, measurement noises and constraints.

Finally, the application of the proposed work on a more complex system with the experimental validation can be also considered.

Bibliography

[1] M. Alamir. Nonlinear moving horizon observers: Theory and real-time implementation. *Lecture Notes in Control and Information Sciences*, 363:139–179, 2007.

[2] T. Alamo, J. M. Bravo, and E. F. Camacho. Guaranteed state estimation by zonotopes. *Automatica*, 41:1035–1043, 2005.

[3] T. Alamo, J. M. Bravo, M. J. Redondo, and E. F. Camacho. A set-membership state estimation algorithm based on dc programming. *Automatica*, 44(1):216–224, 2008.

[4] T. Alamo, D. R. Ramirez, D. Muñoz de la Peña, and E. F. Camacho. Minmax mpc using a tractable qp problem. *Automatica*, 43:693–700, 2007.

[5] T. Alamo, R. Tempo, D. R. Ramírez, and E. F. Camacho. A new vertex result for robustness problems with interval matrix uncertainty. *Systems and Control Letters*, 57:474–481, 2008.

[6] J. C. Allwright. *Advances in Model-based predictive control*. Oxford University Press, 1994.

[7] M. Althoff, O. Stursberg, and M. Buss. Reachability analysis of linear systems with uncertain parameters and inputs. In *Proc. of the 46th IEEE Conference on Decision and Control*, volume 41, pages 726–732, 2007. New Orleans, LA, USA.

[8] M. Althoff, O. Stursberg, and M. Buss. Computing reachable sets of hybrid systems using a combination of zonotopes and polytopes. *Nonlinear Analysis: Hybrid Systems*, 4(2):233–249, 2010.

[9] J. M. Aughenbaugh and C. J. J. Paredis. Why are intervals and imprecision important in engineering design? In *Proc. of the Reliable Engineering Computing Workshop*, 2006. Savannah, USA.

[10] B. M. Ayyub and G. J. Klir. *Uncertainty modeling and analysis in engineering and the sciences*. Chapman and Hall/CRC, 2006.

[11] G. Barequet and S. Har-Peled. Efficiently approximating the minimum-volume bounding box of a point set in three dimensions. *Journal of Algorithms*, 38:91–109, 1999.

[12] A. A. Batabyal. *Dynamic and stochastic approaches to the environment and economic development*. World Scientific Publishing Company, 2008.

[13] Y. Becis-Aubry, D. Aubry, and N. Ramdani. Multisensor set-membership state estimation of nonlinear models with potentially failing measurements. In *Proc. of the 18th World Congress IFAC*, pages 12030–12035, Milan, Italy, 2011.

[14] Y. Becis-Aubry, M. Boutayebb, and M. Darouach. State estimation in the presence of bounded disturbances. *Automatica*, 44(7):1867–1873, 2008.

[15] Y. Becis-Aubry and N. Ramdani. State-bounding estimation for nonlinear models with multiple measurements. In *Proc. of the 2012 American Control Conference ACC*, pages 1883–1888, Montréal, Canada, 2012.

[16] A. Bemporad. Reducing conservativeness in predictive control of constrained systems with disturbances. In *Proc. of the 37th IEEE Conference on Decision and Control*, pages 1384–1391, Tampa, USA, 1998.

[17] A. Bemporad and A. Garulli. Output feedback predictive control of constrained linear systems via set-membership state estimation. *International Journal of Control*, 73(8):655–665, 2000.

[18] A. Bemporad and M. Morari. Robust Model Predictive Control: A Survey. *Robustness in Identification and Control*, 245:207–226, 1999.

[19] D. P. Bertsekas, A. Nedíc, and A. E. Ozdaglar. *Convex analysis and optimization*. Athena Scientific, 2003.

[20] D. P. Bertsekas and I. B. Rhodes. Recursive state estimation for a set-membership description of uncertainty. *IEEE Transactions on Automatic Control*, 16(2):117–128, 1971.

[21] R. Bhattacharya, G. J. Balas, M. A. Kaya, and A. Packard. Nonlinear receding horizon control of an f-16 aircraft. *Journal Guidance Control and Dynamics*, 25(5):924–931, 2002.

[22] F. Blanchini. Set invariance in control. *Automatica*, 35(11):1747–1767, 1999.

[23] F. Blanchini and S. Miani. *Set-theoretic methods in control*. Birkhauser, Boston, 2007.

[24] S. Boyd, L. El Ghaoui, E. Feron, and V. Balakrishnan. *Linear matrix inequalities in system and control theory*. SIAM, Philadelphia, 1994.

[25] J. M. Bravo, T. Alamo, and E. F. Camacho. Bounded error identification of systems with time-varying parameters. *IEEE Transactions on Automatic Control*, 51(7):1144–1150, 2006.

[26] E. M. Bronstein. Approximation of convex sets by polytopes. *Journal of Mathematical Sciences*, 153(6):727–762, 2008.

[27] R. G. Brown and P. Y. C. Hwang. *Introduction to random signals and applied Kalman Filtering*. John Wiley and Sons, 1997.

[28] R. L. Burden and J. D. Faires. *Numerical analysis*. Brooks Cole, 2000.

[29] E. F. Camacho and C. Bordons. *Model predictive control*. Springer-Verlag, London, 2004.

[30] P. J. Campo and M. Morari. Robust model predictive control. In *Proc. of the American Control Conference*, pages 1021–1026, Minneapolis, USA, 1987.

[31] G. Chesi, A. Garulli, A. Tesi, and A. Vicino. An lmi-based approach for characterizing the solution set of polynomial systems. In *Proc. of the 39th IEEE Conference Decision and Control*, pages 1501–1506, Sydney, Australia, 2000.

[32] L. Chisci, A. Garulli, and G. Zappa. Recursive state bounding by parallelotopes. *Automatica*, 32:1049–1055, 1996.

[33] L. Chisci and G. Zappa. Feasibility in predictive control of constrained linear systems: the output feedback case. *International journal of robust and non linear control*, 12:465–487, 2002.

[34] D. W. Clarke. Application of generalized predictive control to industrial processes. *IEEE Control System Magazine*, 122:49–55, 1988.

[35] D. W. Clarke, C. Mohtadi, and P. S. Tuffs. Generalized predictive control, part i: The basic algorithm; part ii: Extensions and interpretations. *Automatica*, 23(2):137–160, 1987.

[36] D. W. Clarke and R. Scatollini. Constrained receding horizon predictive control. *Proceedings IEE-D*, 138:347–354, 1991.

[37] C. Combastel. A state bounding observer based on zonotopes. In *Proc. of European Control Conference*, Cambridge, UK, 2003.

[38] C. Combastel. Observation de systèmes non linéaires appliquée à un modèle de bioréacteur. une approche ensembliste basée sur les zonotopes. *Journal Européen des Systèmes Automatisés*, 38:933–957, 2004.

[39] C. Combastel. A state bounding observer for uncertain non-linear continuous-time systems based on zonotopes. In *Proc. of the 44th IEEE Conference on Decision and Control, and the European Control Conference*, Sevilla, Spain, 2005.

[40] C. Combastel, Q. Zhang, and A. Lalami. Fault diagnosis based on the enclosure of parameters estimated with an adaptive observer. In *Proc. of the 17th World Congress IFAC*, pages 7314–7319, Seoul, Korea, 2008.

[41] C. R. Cutler and B. C. Ramaker. Dynamic matrix control Ű a computer control algorithm. In *Proc. of the Automatic Control Conference*, San Francisco, USA, 1980.

[42] G. B. Dantzig. Fourier-motzkin elimination and its dual. Technical report, DTIC document, 1972.

[43] R. M. C. de Keyser and A. R. Van Cauwenberghe. Extended prediction selfadapted control. In *IFAC Symposium on Identification and System Parameter Estimation*, pages 1317–1322, York, 1985.

[44] J. Douchet and B. Zwahlen. *Calcul différentiel et intégral*. Presses Polytechniques et Universitaires Romande, 2006.

[45] C. Durieu, E. Walter, and B. Polyak. Multi-input multi-output ellipsoidal state bounding. *Journal of Optimization Theory and Applications*, 111(2):273–303, 2001.

[46] Y. K. Foo and Y. C. Soh. Robust kalman filtering for uncertain discrete-time systems with probabilistic parameters bounded within a polytope. *Systems and Control Letters*, 57(6):482–488, 2008.

[47] K. Fukuda. Cdd/cdd+ reference manual, 1999.

[48] K. Fukuda. From the zonotope construction to the minkowski addition of convex polytopes. *Journal of Symbolic Computation*, 38(4):1261–1272, 2004.

[49] C. E. García, D. M. Prett, and M. Morari. Model predictive control : Theory and practice Ű a survey. *Automatica*, 25(3):335–348, 1989.

[50] A. Garulli and A. Vicino. Set membership localization of mobile robots via angle measurement. *IEEE Transactions on Robotic and Automation*, 17(4):450 – 463, 2001.

[51] L. El Ghaoui and G. Calafiore. Worst-case state prediction under structured uncertainty. In *Proc. of American Control Conference*, pages 3402–3406, San Diego, USA, 1999.

[52] E. G. Gilbert and K. T. Tan. Linear systems with state and control constraints: The theory and application of maximal output admissible sets. *IEEE Transactions on Automatic Control*, 36(9):1008–1020, 1991.

[53] A. Girard. Reachability of uncertain linear systems using zonotopes. In *Hybrid Systems: Computation and Control, March, 2005*, volume 3414 of *Lecture Notes in Computer Science*, pages 291–305. Springer, March 2005.

[54] G. Goodwin, M. M. Seron, and J. A. De Doná. *Constrained Control and Estimation: An Optimisation Approach*. Springer, 2004.

[55] C. Greco, G. Menga, E. Mosca, and G. Zappa. Performance improvement of self-tuning controllers by multistep horizons: The musmar approach. *Automatica*, 20:681–100, 1984.

[56] P. Gritzmann and B. Sturmfels. Minkowski addition of polytopes: Computational complexity and applications to gröbner bases. *SIAM Journal on Discrete Mathematic*, 6(2):246–269, 1993.

[57] J. W. Grizzle and P. E. Moraal. Observer based control of nonlinear discrete-time systems. In *Proc. of the 29th IEEE Conference on Decision and Control*, pages 760–767, Honoluu, USA, 1990.

[58] P. Guerra, V. Puig, and M. Witczak. Robust fault detection with unknown-input interval observers using zonotopes. In *Proc. of the 17th World Congress IFAC*, pages 5557–5562, Seoul, Korea, 2008.

[59] L. J. Guibas, A. Nguyen, and L. Zhang. Zonotopes as bounding volume. In *Proc. of the Symposium on Discrete Algorithm*, pages 803–812, 2005.

[60] E. R. Hansen. Interval arithmetic in matrix computations. *SIAM Journal on Numerical Analysis: Series B*, 2(2):308–320, 1965.

[61] D. Henrion and J. B. Lasserre. Gloptipoly: Global optimization over polynomials with matlab and sedumi. *ACM Transactions on Mathematical Software*, 29:165–194, 2002.

[62] D. Henrion and J. B. Lasserre. Convergent relaxations of polynomial matrix inequalities and static output feedback. *IEEE Transactions on Automatic Control*, 51(2):192 – 202, 2006.

[63] D. Henrion and J. B. Lasserre. Inner approximations for polynomial matrix inequalities and robust stability regions. Technical report, LAAS-report 11210, 2011.

[64] C. W. J. Hol and C. W. Scherer. Sum of squares relaxations for polynomial semidefinite programming. In *Proc. Symp. on Mathematical Theory of Networks and Systems*, Leuven, Belgium, 2004.

[65] D. P. Hunttenlocher, G. A. Klanderman, and W. J. Rucklidge. Comparing images using the hausdorff distance. *IEEE Transactions on Pattern Analysis and Machine Intelligence*, 15(9):850 – 863, 1993.

[66] A. Ingimundarson, J. M. Bravo, V. Puig, T. Alamo, and P. Guerra. Robust fault detection using zonotope-based set-membership consistency. *International journal of adaptive control and signal processing*, 23(4):311–330, 2008.

[67] J. A. De Doná J. B. Mare. Moving horizon estimation of constrained nonlinear systems by carleman approximations. In *Proc. of the 45th IEEE Conference on Decision and Control*, pages 2147–2152, San Diego, USA, 2006.

[68] L. Jaulin, M. Kieffer, O. Didrit, and E. Walter. *Interval analysis*. Springer, 2001.

[69] R. E. Kalman. A new approach to linear filtering and prediction problems. *Transactions of the ASME–Journal of Basic Engineering*, 82(Series D):35–45, 1960.

[70] S. S. Keerthi and E. G. Gilbert. Optimal infinite-horizon feedback laws for a general class of constrained discrete-time systems: Stability and moving-horizon approximations. *Journal of Optimization Theory and Applications*, 57(2):265–293, 1988.

[71] M. Kieffer, L. Jaulin, and E. Walter. Guaranteed recursive nonlinear state estimation using interval analysis. *International Journal of Adaptative Control and Signal Processing*, 2002.

[72] M. Kojima. Sums of squares relaxations of polynomial semidefinite programs. Technical report, Department of Mathematical and Computing Sciences, Tokyo Institute of Technology, 2003.

[73] M. V. Kothare, V. Balakrishnan, and M. Morari. Robust constrained model predictive control using linear matrix inequalities. *Automatica*, 32(10):1361–1379, 1996.

[74] M. Kočvara and S. Stingl. Pennon a code for convex nonlinear and semidefinite programming. *Optimization Methods and Software*, 18(3):317–333, 2003.

[75] W. Kühn. Rigorously computed orbits of dynamical systems without the wrapping effect. *Computing*, 61:47–67, 1998.

[76] W. Kühn. Toward an optimal control of wrapping effect. In *International Symposium on Scientific Computing, Computer Arithmetic and Validated Numerics*, pages 125–134, 1998.

[77] A. B. Kurzhanski and I. Vályi. *Ellipsoidal calculus for estimation and control*. Birkhaüser Boston, 1996.

[78] A. A. Kurzhanskiy and P. Varaiya. Ellipsoidal toolbox manual, 2006-2007.

[79] M. Kvasnica, P. Grieder, and M. Baotić. Multi-parametric toolbox (mpt), 2004.

[80] W. Langson, I. Chryssochoos, S.V. Raković, and D.Q. Mayne. Robust model predictive control using tubes. *Automatica*, 40(1):125–133, 2004.

[81] S. R. Lay. *Convex sets and their applications*. Wiley, New york, 1982.

[82] V. T. H. Le, T. Alamo, E. F. Camacho, C. Stoica, and D. Dumur. A new approach for guaranteed state estimation by zonotopes. In *Proc. the 18th World Congress IFAC*, pages 9242–9247, Milan, Italy, 2011.

[83] V. T. H. Le, T. Alamo, E. F. Camacho, C. Stoica, and D. Dumur. Zonotopic set-membership estimation for interval dynamic systems. In *Proc of the 2012 American Control Conference ACC*, pages 6787–6792, Montréal, Canada, 2012.

[84] V. T. H. Le, C. Stoica, T. Alamo, D. Dumur, and E. F. Camacho. Guaranteed state estimation by zonotopes for systems with interval uncertainties. In *submitted to Automatica*, 2012.

[85] V. T. H. Le, C. Stoica, D. Dumur, T. Alamo, and E. F. Camacho. Robust tube-based constrained predictive control via zonotopic set-membership estimation. In *Proc. the 50th IEEE Conference on Decision and Control and European Control Conference*, pages 4580–4585, Orlando, USA, 2011.

[86] V. T. H. Le, C. Stoica, D. Dumur, T. Alamo, and E. F. Camacho. Commande prédictive robuste par des techniques d'observateurs basées sur des ensembles zonotopiques. *Journal Européen des Systèmes Automatisés*, 2-3/2012:235–250, 2012.

[87] V. T. H. Le, C. Stoica, D. Dumur, T. Alamo, and E. F. Camacho. Guaranteed state estimation by zonotopes for systems with interval uncertainties. In *2012 Small Workshop on Interval Methods*, Oldenburg, Germany, 2012.

[88] V. T. H. Le, C. Stoica, D. Dumur, T. Alamo, and E. F. Camacho. A polynomial matrix inequality approach for zonotopic set-membership estimation of multivariable systems. In *Proc. of the 20th Mediterranean Conference on Control and Automation*, pages 18–23, Barcelona, Spain, 2012.

[89] J. H. Lee and Z. Yu. Worst-case formulations of model predictive control for systems with bounded parameters. *Automatica*, 33(5):763–781, 1997.

[90] J. M. Lemos and E. Mosca. A multipredictor-based lq self-tuning controller. In *IFAC Symposium on Identification and System Parameter Estimation*, pages 137–141, York, UK, 1985.

[91] D. Limon, T. Alamo, J. M. Bravo, E. F. Camacho, D. R. Ramirez, D. Mu noz de la Peña, I. Alvarado, and M. R. Arahal. Interval arithmetic in robust nonlinear mpc. *Springer-Verlag*, pages 317–326, 2007.

[92] D. Limon, T. Alamo, and E. F. Camacho. Stability analysis of systems with bounded additive uncertainties based on invariant sets: Stability and feasibility of mpc. In *Proc. of American Control Conference*, pages 364–369, Anchorage, USA, 2002.

[93] W. Lombardi, S. Olaru, and S. I. Niculescu. Invariant sets for a class of linear systems with variable time-delay. In *Proc. of the European Control Conference*, Budapest, Hungary, 2009.

[94] D. G. Luenberger. Observing the state of a linear system. *IEEE Transactions on Military Electronics*, 8:74 – 80, 1964.

[95] D. G. Luenberger. Observers for multivariable systems. *IEEE Transactions on Automatic Control*, 11:190 – 197, 1965.

[96] J. M. Maciejowski. *Predictive Control. A unified approach.* Prentice-Hall, 2000.

[97] M. Mansour. Simplified sufficient conditions for the asymptotic stability of interval matrices. *International Journal of Control*, 50(1):443–444, 1989.

[98] W-J. Mao and J. Chu. Quadratic stability and stabilization of dynamic interval systems. *IEEE Transactions on Automatic Control*, 48(6):1007–1012, 2003.

[99] P. S. Maybeck. *Stochastic models, estimation and control.* Academic Press, 1979.

[100] D. Q. Mayne, S. V. Raković, R. Findeisen, and F. Allgöwer. Robust output feedback model predictive control of constrained linear system: Time varying case. *Automatica*, 45:2082–2087, 2009.

[101] D. Q. Mayne, J. B. Rawlings, C. V. Rao, and P. O. M Scokaert. Constrained model predictive control: Stability and optimality. *Automatica*, 36:789–814, 2000.

[102] D. Q. Mayne, M. M. Seron, and S. V. Raković. Robust model predictive control of constrained linear system with bounded disturbances. *Automatica*, 41:219–224, 2005.

[103] N. Meslem, N. Ramdani, and Y. Candau. Using hybrid automata for set-membership state estimation with uncertain nonlinear continuous-time systems. *Journal of Process Control*, 20(4):481–489, 2010.

[104] H. Michalska and D. Q. Mayne. Moving horizon observers. In *Proc. IFAC Symposium Nonlinear Control System Design*, pages 576–581, Bordeaux, France, 1991.

[105] H. Montgomery. Computing the volume of a zonotope. *The American Mathematicals Monthly*, 97:431, 1989.

[106] J. B. Moore and G. F. Ledwich. Minimal order observers for estimating linear functions of a state vector. *IEEE Transactions on Automatic Control*, 20(5):623–632, 1975.

[107] R. E. Moore. *Interval analysis*. Englewood Cliff, New Jersey: Prentice-Hall, 1966.

[108] M. Morari. *Advances in model based predictive control*. Oxford University Press, 1994.

[109] P. Murdoch. Observer design for a linear functional of the state vector. *IEEE Transactions on Automatic Control*, 18(3):308–310, 1973.

[110] K. Ohrn, A. Ahlen, and M. Sternard. A probabilistic approach to multivariable robust filtering and open-loop control. *IEEE Transactions on Automatic Control*, 40(3):405–418, 1995.

[111] S. Olaru. *Contribution à l'étude de la commande prédictive sous contraintes par approache geometrique*. PhD thesis, Université de Paris Sud-Supélec, 2005.

[112] O. Pastravanu and M. Voicu. Necessary and sufficient conditions for componentwise stability of interval matrix systems. *IEEE Transactions on Automatic Control*, 49(6):1016–1021, 2004.

[113] B. T. Polyak, S. A. Nazin, C. Durieu, and E. Walter. Ellipsoidal parameter or state estimation under model uncertainty. *Automatica*, 40:1171–1179, 2004.

[114] V. Puig. Fault diagnosis and fault tolerant control using set-membership approaches: Application to real case studies. *Applied Mathematics and Computer Science*, 20(4):619–635, 2010.

[115] V. Puig, P. Cugueró, and J. Quevedo. Worst-case estimation and simulation of uncertain discrete-time systems using zonotopes. In *Proc. of Europeen Control Conference*, Portugal, 2001.

[116] V. Puig, J. Saludes, and J. Quevedo. Worst-case simulation of discrete linear time-invariant interval dynamic systems. *Reliable Computing*, 9(4):251–290, 2003.

[117] S. J. Qin and T. A. Badgwell. A survey of industrial model predictive control technology. *Control Engineering Practice*, 11:733–764, 2003.

[118] T. Raïssi, N. Ramdani, and Y. Candau. Set membership state and parameter estimation for systems described by nonlinear differential equations. *Automatica*, 40(10):1771–1777, 2004.

[119] S. V. Raković, E. C. Kerrigan, K. I. Kouramas, and D. Q. Mayne. Invariant approximation of the minimal robustly positively invariant set. *IEEE Transactions on Automatic Control*, 50(3):406–410, 2005.

[120] C. V. Rao and J. B. Rawlings. Linear programming and model predictive control. *Journal of Process Control*, 10(2-3):283–289, 2000.

[121] J. Richalet, A. Rault, J. L. Testud, and J. Papon. Model predictive heuristic control : application to industrial processes. *Automatica*, 14(5):413–428, 1978.

[122] R. T. Rockafellar. *Convex analysis*. Princeton University Press, 1970.

[123] J. A. Rossiter. *Model based predictive control. A practical approach*. CRC Press LLC, 2003.

[124] C. S. Scherer and S. Weiland. Linear matrix inequalities in control.

[125] S. Schön and H. Kutterer. Using zonotopes for overestimation-free interval least-squaresŮsome geodetic applications. *Reliable Computing Springer*, 11:137–155, 2005.

[126] F. C. Schweppe. Recursive state estimation: Unknown but bounded errors and system inputs. *IEEE Transactions on Automatic Control*, 13(1):22–28, 1968.

[127] F. Scibilia, S. Olaru, and M. Hovd. On feasible sets for mpc and their approximations. *Automatica*, 47(1):133–139, 2011.

[128] P. O. M. Scokaert, D. Q. Mayne, and J. B. Rawlings. Suboptimal model predictive control (feasibility implies stability). *IEEE Transactions on Automatic Control*, 44(3):648–654, 1999.

[129] P. O. M. Scokaert and J. B. Rawlings. Stability of model predictive control under perturbations. In *Proc. of the IFAC Symposium on nonlinear control systems design*, pages 1317–1322, Lake Tahoe, CA, 1995.

[130] M. M. Seron, J. A. De Doná, and J. Richter. Fault tolerant control using virtual actuators and set-separation detection principles. *International Journal of Robust and Nonlinear Control*, 22:709–742, 2011.

[131] P. Seymour. A note on hyperplane generation. *Journal of Combinatorial Theory, Series B*, 61(1):88–91, 1994.

[132] G. Shephard. Combinatorial properties of associated zonotopes. *Canadian Journal of Mathematics*, 26:302–321, 1974.

[133] R. Soeterboek. *Predictive Control. A unified approach.* Prentice-Hall, 1992.

[134] M. Sternad, K. Ohrn, and A. Ahlen. Robust h_2 filtering for structured uncertainty: The performance of probabilistic and minimax schemes. In *European Control Conference*, pages 87–92, Rome, Italy, 1995.

[135] C. Stoica. *Robustification de lois de commande prédictives multivariables.* PhD thesis, Université de Paris Sud-Supélec, 2008.

[136] C. Stoica, M. R. Arahal, D. E. Rivera, P. Rodriguez-Ayerbe, and D. Dumur. Application of robustified model predictive control to a production-inventory system. In *Proc. the 48th IEEE Conference on Decision and Control and 28th Chinese Control Conference*, pages 3993–3998, Shanghai, China, 2009.

[137] F. Stoican. *Fault tolerant control based on set-theoretic methods.* PhD thesis, Université de Paris Sud-Supélec, 2011.

[138] F. Stoican, S. Olaru, and G. Bitsoris. A fault detection scheme based on controlled invariant sets for multi-sensor systems. In *Proc. of the 2010 Conference on Control and Fault Tolerant Systems*, pages 468–473, Nice, France, 2010.

[139] F. Stoican, S. Olaru, M. M. Seron, and J. A. De Doná. A fault tolerant control scheme based on sensor switching and dwell time. In *Proc. the 49th IEEE Conference on Decision and Control*, pages 756–761, Atlanta, USA, 2010.

[140] G. Strang. *Linear Algebra and Its Applications.* Brooks Cole, 2005.

[141] O. Stursberg and B. Krogh. Efficient representation and computation of reachable sets for hybrid systems. In *Hybrid Systems: Computation and Control*, volume 2623 of *Lecture Notes in Computer Science*, pages 482–497. Springer, 2003.

[142] S. Tornil-Sin, C. Ocampo-Martinez, V. Puig, and T. Escobet. Robust fault detection of non-linear systems using set-membership state estimation based on constraint satisfaction. *Engineering Applications of Artificial Intelligence*, 25(1):1–10, 2012.

[143] M. Ullah and O. Wolkenhauer. *Stochastic approaches for systems biology.* Springer, 2011.

[144] A. Vicino and G. Zappa. Sequential approximation of feasible parameter sets for identification with set-membership uncertainty. *IEEE Transactions on Automatic Control*, 41:774–785, 1996.

[145] E. Walter and H. Piet-Lahanier. Exact recursive polyhedral description of the feasible parameter set for bounded-error models. *IEEE Transactions on Automatic Control*, 34(8):911–915, 1989.

[146] Z. Wan and M. V. Kothare. Robust output feedback model predictive control using off-line linear matrix inequalities. *Journal of Process Control*, 12(7):763–774, 2001.

[147] S. H. Witsenhausen. Sets of possible states of linear systems given perturbed observations. *IEEE Transactions on Automatic Control*, 13:556–558, 1968.

[148] L. Xie, Y. C. Soh, and C. E. de Souza. Robust kalman filtering for uncertain discrete time systems. *IEEE Transactions on Automatic Control*, 39(6):1310–1314, 1994.

[149] B. E. Ydstie. Extended horizon adaptive control. In *Proc. of the 9th World Congress IFAC*, Budapest, Hungary, 1984.

[150] A. Yetendje, J. A. De Doná, and M. M. Seron. Multisensor fusion fault tolerant control. *Automatica*, 47(7):1461–1466, 2011.

[151] G. M. Ziegler. *Lecture on polytopes*. Springer, 1995.

Résumé :

L'objectif de cette thèse est d'apporter des réponses à deux problèmes importants dans le domaine de l'automatique : l'estimation d'état et la commande prédictive robuste sous contraintes pour des systèmes incertains, en se basant sur des méthodes ensemblistes, plus précisément liées aux ensembles zonotopiques. Les incertitudes agissant sur le système sont modélisées de façon déterministe, elles sont donc inconnues mais bornées par des ensembles connus.

Dans ce contexte, la première partie de la thèse développe une méthode d'estimation afin d'élaborer à chaque instant un ensemble zonotopique contenant l'état du système malgré la présence de perturbations, de bruits de mesure et d'incertitudes paramétriques définies par intervalle. Cette méthode est fondée sur la minimisation du P-rayon d'un zonotope, critère original permettant de caractériser la taille de l'ensemble zonotopique et réalisant un bon compromis entre la complexité et la précision de l'estimation. Cette approche est tout d'abord développée pour les systèmes mono-sortie, puis étendue au cas des systèmes multi-sorties, dans un premier temps par des extensions directes de la solution mono-sortie (le système multi-sorties est considéré comme plusieurs systèmes mono-sortie). Une autre solution est ensuite proposée, qui conduit à résoudre un problème d'optimisation de type Inégalités Matricielles Polynomiales en utilisant une méthode de relaxation. Les approches précédentes n'étant que des extensions de la solution à une seule sortie, et malgré leurs bons résultats obtenus en simulation, une démarche originale, dédiée aux systèmes multi-sorties, fondée sur l'intersection entre un polytope et un zonotope, est finalement développée et validée.

La deuxième partie de la thèse aborde la problématique de la commande robuste par retour de sortie pour des systèmes incertains. La commande prédictive est retenue du fait de son utilisation dans de nombreux domaines, de sa facilité de mise en œuvre et de sa capacité à traiter des contraintes. Parmi les démarches issues de la littérature, l'implantation de techniques robustes fondées sur des tubes de trajectoire est développée plus spécifiquement. Le recours à un observateur ensembliste à base de zonotopes permet d'améliorer la qualité de l'estimation, ainsi que la performance de la commande, dans le cas de systèmes soumis à des perturbations et des bruits de mesure inconnus, mais bornés.

Dans une dernière partie, cette combinaison de l'estimation ensembliste et de la commande prédictive robuste est testée en simulation sur un système de suspension magnétique. Les résultats de simulation traduisent un comportement tout à fait satisfaisant validant les structures théoriques élaborées.

Abstract:

The aim of this thesis is answering to two significant problems in the field of automatic control: the state estimation and the robust model predictive control for uncertain systems in the presence of input and state constraints, based on the set-membership approach, more precisely related to zonotopic sets. Uncertainties acting on the system are modeled via the deterministic approach, and thus they are unknown but bounded by a known set.

In this context, the first part of the thesis proposes an estimation method to compute a zonotope containing the real states of the system, which are consistent with the disturbances, the measurement noise and the interval parametric uncertainties. This method is based on the minimization of the P-radius of a zonotope, which is an original criterion to characterize the size of the zonotope, in order to obtain a good trade-off between the complexity and the precision of the estimation. This approach is first developed for single-output systems, and then extended to the case of multi-output systems. The first solution for multi-output systems is a direct extension of the solution for single-output systems (the multi-output system being considered as several single-output systems). Another solution is then proposed, leading to solve a Polynomial Matrix Inequality optimization problem using a relaxation technique. Due to the fact that the previous approaches are just extensions of the solution for a single-output system, and despite their good performance results obtained in simulation, a novel approach dedicated to multi-output systems based on the intersection of a polytope and a zonotope is finally developed and validated.

The second part of the thesis deals with the problem of robust output feedback control for uncertain systems. Model predictive control is chosen due to its use in many areas, its ability to deal with constraints and uncertainties. Among the approaches from the literature, the implementation of robust predictive techniques based on tubes of trajectories is developed. The use of a zonotopic set-membership estimation improves the quality of the estimation, as well as the performance of the control, for systems subject to unknown, but bounded disturbances and measurement noise.

In the last part, the combination of zonotopic set-membership estimation and robust model predictive control is tested in simulation on a magnetic levitation system. The simulation results reflect a satisfactory behavior validating the developed theoretical techniques.